ScuDo

Scuola di Dottorato ~ Doctoral School

WHAT YOU ARE, TAKES YOU FAR

Doctoral Dissertation

Doctoral Program in Environmental Engineering (XXXI cycle)

Spatial and temporal patterns of global freshwater use for food production and trade

By

Irene Soligno

******

Supervisor(s):

Prof. Francesco Laio, Supervisor

Prof. Luca Ridolfi, Co-Supervisor

Doctoral Examination Committee:

Prof. Marco Bagliani, Università degli Studi di Torino.

Prof. Maria Cristina Rulli, Referee, Politecnico di Milano.

Prof. Stefano Schiavo, Referee, Università di Trento.

Prof. Stefania Tamea, Politecnico di Torino.

Prof. Giulia Vico, Swedish University of Agricultural Sciences.

Politecnico di Torino

2019

Declaration

I hereby declare that, the contents and organization of this dissertation constitute my own original work and does not compromise in any way the rights of third parties, including those relating to the security of personal data.

Irene Soligno
2019

* This dissertation is presented in partial fulfillment of the requirements for **Ph.D. degree** in the Graduate School of Politecnico di Torino (ScuDo).

Abstract

In the past century, global water consumption increased nearly 8 times and over the last decades the rate of demand for water has exceeded twice the rate of population growth. Nowadays, the agriculture sector is by far the largest freshwater-consuming human activity on Earth accounting for nearly 70% of the total withdrawal and around 90% of the total water consumption. Moreover, the agriculture's "thirst" is expected to persistently rise in the next years, due to the growth of the world population, the rising of living standards and climate changes. This pressing human demand for water is causing remarkable environmental impacts, in particular on surface water resources that globally contribute about 60% of the total water used for irrigation. Today, freshwaters are recognized has the most extensively altered ecosystems on Earth by the human intervention. Therefore, fulfilling the competing water requirements of ecosystems and societies is a key global environmental challenge for our time. Globally, about a quarter of the food produced for human consumption is traded internationally and several countries significantly depend on imported commodities. It follows that an important part of the world population relies on external water resources and impacts external freshwater ecosystems. In this context, the concept of "virtual water" has played an essential role in shedding light on the links between the food consumption geography and the water resources exploited. However, virtual water assessments typically aggregate and compare water volumes without taking into account the place where water has been actually withdrawn (e.g., without differentiating between water-abundant and water scarce regions). As a matter of fact, the uneven distribution of surface water resources implies that the withdrawal of a same volume of water can have very different environmental consequences in different riverine ecosystems.

In this context the Thesis aims (i) to develop an approach able to support

the interpretation of the volumetric measure of surface water withdrawal by adopting an impact-oriented perspective, thus considering the environmental aspects of the freshwater ecosystem where the withdrawal actually occurs; (ii) to quantify the environmental impact of food consumption on local and foreign water resources and to understand the role of the food globalization on world's rivers; (iii) to identify the major socio-economic determinants behind the growing use of foreign (and domestic) freshwater resources.
In order to address the first aim, this Thesis defines a novel indicator – named Environmental Cost index - to assess the environmental impact of a withdrawal from a generic river section. The index depends on (i) the environmental relevance of the impacted fluvial ecosystem (e.g., bed-load transport capacity, width of the riparian belt, biodiversity richness) and (ii) the downstream river network affected by the water withdrawal. The index is referred to a potential reference withdrawal that can occur in any river section of the world's hydrographic network. Being referred to a potential unitary withdrawal that can occur in any river section worldwide, the results can be suitably arranged for describing any scenario of surface water consumption (i.e., as the superposition of the actual pattern of withdrawals). Our results highlights the river regions where water withdrawals can cause higher environmental costs. In addition, the approach defined in this Thesis is an easy-to-apply tool to identify the most impacting water consumption patterns on the hydrographic network.
Building on the aforementioned definition of Environmental Cost, we quantify the environmental value of the riverine water (EVRW) embedded in food products. Through this measure we explore the role of food production and trade on the world's riverine ecosystems unveiling a novel facet of the food-water nexus. In this Thesis, we describe the geography of country (or individual) responsibility on the environmental changes of world's rivers. We show globalization drives an international trade of environmental value of surface water and local threats to fluvial ecosystems are induced by the food demands across the globe. Hotspots of food-related river-environment degradation are found in Australia, Pakistan, South Africa, and Spain. Globally, between 1986 and 2013 food consumption has more than doubled its impact on foreign riverine environments, but still the international trade reduces the pressure of food consumption on global river system by 11%, as compared to an ideal situation where all food is produced locally.

As mentioned, the recent intensification of international trade has led to a growing disconnection between the consumers demand for goods and services and the water resources that support them. However, despite the important role of the consumers demands on the exploitation of distant freshwater resources is widely recognized, the different socio-economic drivers behind the trends in domestic and foreign freshwater use remain poorly quantified. In this Thesis, the main mechanisms governing the exploitation of domestic and foreign water resources are quantified by undertaking a structural decomposition analysis over the 1994 – 2010 period in 186 countries. Results show that the affluence growth has been the main determinant of rising water consumption trends worldwide. Consumers in developed countries tend to increase their affluence by intensifying the use of foreign freshwater resources; conversely, the affluence growth in developing regions mostly relies on the exploitation of local water resources revealing a significant imbalance among economies. The affluence and the demographic growth have been only partially offset by improvements in the blue water efficiency of producers and, to a lesser extent, by changes in production technology.

Contents

Nomenclature

Acronyms

BWF Blue Water Footprint

CDF Cumulative distribution function

EC Environmental Cost

EVRW Environmental value of the riverine water

FAO Food and Agricultural Organization of the United Nations

GDP Gross domestic product

GMIA Global Map of Irrigation Areas

GRDC Global Runoff Data Centre

HDI Human Development Index

IO Input-Output

MENA Middle East and North Africa

MRIO Multi-Regional Input-Output

PCC Pearson Correlation Coefficient

SDA Structural Decomposition Analysis

STN-30p Simulated Topological Network

VWC Virtual water content

WBM Water Balance Model

WF Water Footprint

Greek symbols

α Parameter of the Environmental Cost index

$\Delta EVRW_{i,j}$ EVRW efficiency of the trade flow from country i to j

Δs_j Distance between two consecutive river sections $(j-1)$ and j

μ_Q Global average of the natural river discharge

τ_b Bed-shear stress

θ Effective Shields parameter

θ_c Critical Shields parameter

Latin symbols

$\overline{\overline{EC}}_{w,c}$ The weighted average environmental cost at country scale using the undisturbed river discharge as the weight

$\overline{EC}_{w,c}$ The weighted average environmental cost at country scale

$\overline{Y}_{c,1996-2005}$ Average crop yield over the period 1996-2005

$\mathbf{T}_{A,B}$ Transactions from country A to country B intermediate demand in the MRIO framework

$\mathbf{Y}_A$ Final Demand in country A in the Input-Output model

a Affluence term in the Input-Output model

CV Coefficient of variation

ec_w Environmental cost per unit length

ec_{max} Maximum Environmental cost per unit length

EC_{world} Global environmental value of the whole world's water resources

EC_w The environmental cost of a water withdrawal W

$F^p_{i,j}$ Tonnes of the product p traded from country i to j

fp Product fraction (i.e., the weight of a derived product obtained per ton of root product)

fv Value fraction (i.e., the market value of the crop-derived product divided by the aggregated market value of all crop products resulting from one primary input crop)

i_b Bed slope

$k(\alpha)$ Proportionality constant of the Environmental Cost index

Ker Kernel probability distribution

L_w Length of the world river network

$P_{i,j}$ Basket of food products exported from country i to j

Q River discharge

Q_s Sediment volumetric discharge

R Hydraulic radius

Rb Percentage of blue water of the total amount of (blue and green) water

Rs Percentage of surface water of the total amount of blue water

s Curvilinear abscissa of the river

S_W River mouth section

S_W River section where water is withdrawn

U Mean stream velocity

$VWC_{c,t}$ Product-specific virtual water content in country c and year t

W Surface water withdrawal

W_c Channel width

Y Crop yield

p	Population term in the Input-Output model
1	Summation vector operator
A	Matrix of technical coefficients of the Input-Output model
F	Final demand matrix of the Input-Output model
I	Identity matrix
L	Leontief inverse matrix
Q	Matrix of the satellite account in the Input-Output model
q	Blue water intensities vector in the Input-Output model (i.e., m^3 per monetary unit)
T	Intermediate demand matrix of the Input-Output model
u	Final demand composition in the Input-Output model
v	Final demand destination term in the Input-Output model
x	Total output of the Input-Output model
y	Total final demand vector of the Input-Output model
DW	Domestic water spatial decomposition in the MRIO framework
GW	Global water spatial decomposition in the MRIO framework
OW	Outsourced water spatial decomposition in the MRIO framework

Chapter 1

Introduction

1.1 General Overview

Freshwater resources are essential for sustaining societal and economic activities and are vital to both aquatic and terrestrial ecosystems. Since the dawn of civilization, human societies have been inextricably linked and reliant on the use of freshwater resources for several activities, including agriculture, industrial production, and urban water supply.

During the past century, global water consumption has increased nearly 8 times - from 500 km^3yr^{-1} in 1900 to 4000 km^3yr^{-1} in 2000 (Wada and Bierkens, 2014) - and over the last decades the rate of demand for water has exceeded twice the rate of population growth (UN-Water, 2015). This increasing human pressure on water resources has considerably impacted most freshwater systems of the world with respect to their habitat, water quality, morphology and spatio-temporal availability (Dudgeon et al., 2006; Haddeland et al., 2014; Hanasaki et al., 2013; Vörösmarty et al., 2000b; Wada et al., 2013). Nowadays, surface-waters are among the most extensively altered ecosystems on Earth by the human intervention (Carpenter et al., 2011; Vörösmarty et al., 2010).

Currently, more than 1.7 billion people live in river basins where water consumption exceeds natural recharge (UN-Water, 2015). Furthermore, a number of rivers are so intensively exploited that they no longer reach the sea (e.g., the Colorado River and the Rio Grande) (Richter, 2014). Meanwhile, several world's lakes are shrinking at alarming rates in response of water

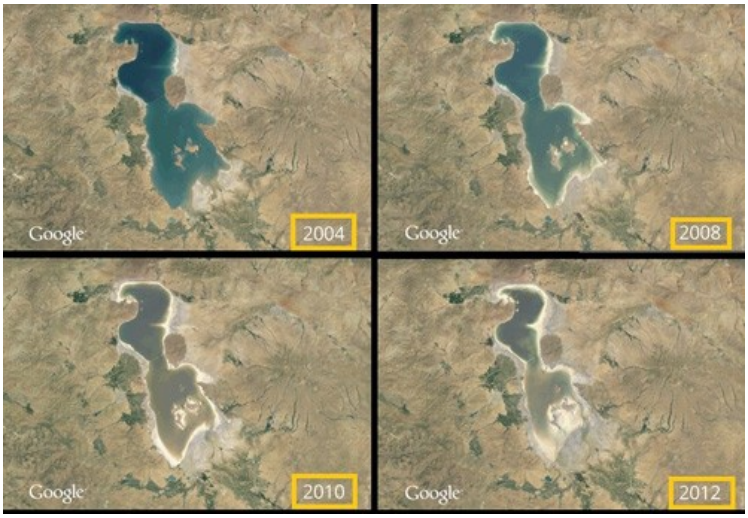

Fig. 1.1 Satellite snapshots of the Urmia Lake (Iran) in four different years.

withdrawals and water diversion to meet irrigation needs, such as the Aral Sea, Lake Chad and the Lake Urmia (see Fig.1.1) (Wurtsbaugh et al., 2017). Globally, water exploitation is one of the main mechanisms that exacerbates the intensity and frequency of hydrological droughts (Wada et al., 2013) and, in numerous regions, growing water withdrawals are expected to have more consequences on surface-water systems than climate change (Alcamo et al., 2007; Haddeland et al., 2014; Hanasaki et al., 2013; Wurtsbaugh et al., 2017).

As a matter of fact, despite water being a renewable resource, the impact of water depletion on freshwater habitats could be irreversible. Excessive water withdrawals from river systems have destroyed aquatic habitats and have been a major cause of species loss (Naiman et al., 2010; Xenopoulos et al., 2005). The Millennium Ecosystem Assessment (2005) points out that between 1970 and 2000 freshwater ecosystems have been deteriorating significantly and at a faster rate than other ecosystems: the freshwater species (included in the Living Planet Index) declined on average by 50%, compared to an average decline of 30% for both terrestrial and marine species over the same period. Moreover, aquatic habitats associated with 65% of global river discharge are under moderate to high threat (Vörösmarty et al., 2010). This picture highlights that fulfilling the competing water requirements of freshwater ecosystems and societies is a key global environmental challenge for both scientists and governments (Dudgeon et al., 2006).

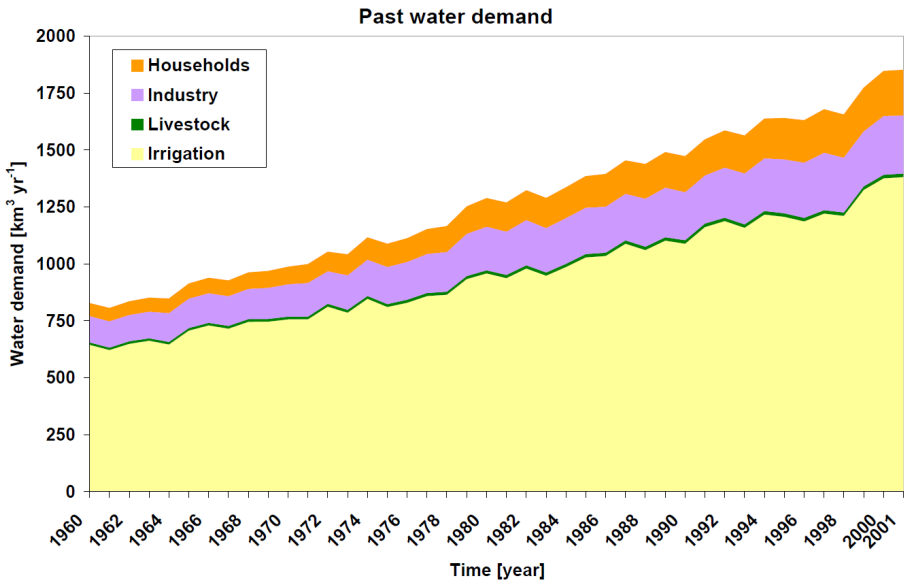

Fig. 1.2 Net water demand from 1960 to 2001 in km^3yr^{-1} estimated by Wada et al. (2011). The net water demand corresponds to the consumptive water use (i.e., water loss to the atmosphere by evapotranspiration), which is less than the actual volumes withdrawn from freshwater resources.

Today, the agriculture sector is by far the largest freshwater-consuming human activity on Earth (e.g., Fig.1.2). Around 90% of the total anthropogenic consumptive water use (i.e., water loss to the atmosphere by evapotranspiration) (Hoekstra and Mekonnen, 2012) and around 70% of the total freshwater withdrawals (FAO, 2011) concern agriculture. Irrigation – which supplies 40% of the world's crop production (Siebert and Döll, 2010) - involves around 2600 km^3 of freshwater withdrawals each year, which roughly corresponds to 2% of the global annual precipitation over land (Sacks et al., 2009). Despite water being a renewable resource that is conserved in the Earth system, irrigated agriculture is recognized as a critical human disturbance of the water cycle, because it strongly increases vapour water flows (also identified as "green water" flows) back to the atmosphere at the expense of the liquid water (temporally) stored in surface-water bodies and aquifers (also known as "blue water") (D'Odorico et al., 2018; Falkenmark and Rockström, 2006; Jägermeyr et al., 2016).

Since the 1960s the demand of water for irrigation have been growing rapidly; for example, as shown in Fig.1.2 over the 1960–2000 period it globally increased more than two-folds (Wada et al., 2011). In addition, the agriculture's

"thirst" is projected to increase further due to i) the rising standard of living, ii) the changes in diet preferences toward an higher consumption of water-intensive commodities (e.g., meat and processed food), iii) the intensification of bioenergy use and iv) the growth of the world population (FAO, 2009; Foley et al., 2011; Vörösmarty et al., 2000b). The latter is currently growing at the rate of 83 million people per year and is projected to continue to rise to reach 9.8 billion people by 2050 (UN-DESA, 2017). To meet the projected demands of the future human population, the agriculture sector must face the enormous challenge to roughly double food supplies in the next few decades (Foley et al., 2011). Climate change will further complicate this future projections, since it is expected to arise major transformations in freshwater availability and productive capacity of soils (Carnicer et al., 2011), as well as to increase the frequency and severity of extreme events (IPCC, 2018).

A strong nexus, thus, exists between agriculture production and freshwater resources (D'Odorico et al., 2018). As the agriculture sector is highly water-demanding, for a society water shortage can be an extremely limiting factor of producing food. Ideally, in order to overcome this limitation, water scarce countries could offset their food needs through food imports. Starting from the emblematic case of the Middle East region – which compensates its shortage of water resources by strongly relying on food imports – Allan (1997) developed the concept of Virtual Water Trade, which denotes the hidden flow of water from one place to another if food commodities are traded. Thus, international trade of agricultural goods leads to a global redistribution of freshwater resources, because the water volumes that are physically used in the country of production are "virtually" transferred to the country of consumption (Hoekstra and Chapagain, 2008). This has led to the so-called globalization of water resources (Allan, 1997; Hoekstra and Chapagain, 2008).

In order to define a framework able to examine the linkage between consumer demand geography and the global water resources exploited, Hoekstra and Hung (2002) introduced the notion of Water Footprint (WF): a comprehensive indicator of direct and indirect freshwater appropriation. The WF quantifies the use of freshwater resources for the production of goods and services along the whole supply chain, differentiating between green water (i.e., soil moisture from precipitation), blue water (i.e., surface and ground water resources), and the non-consumptive use of grey water (as an indicator of

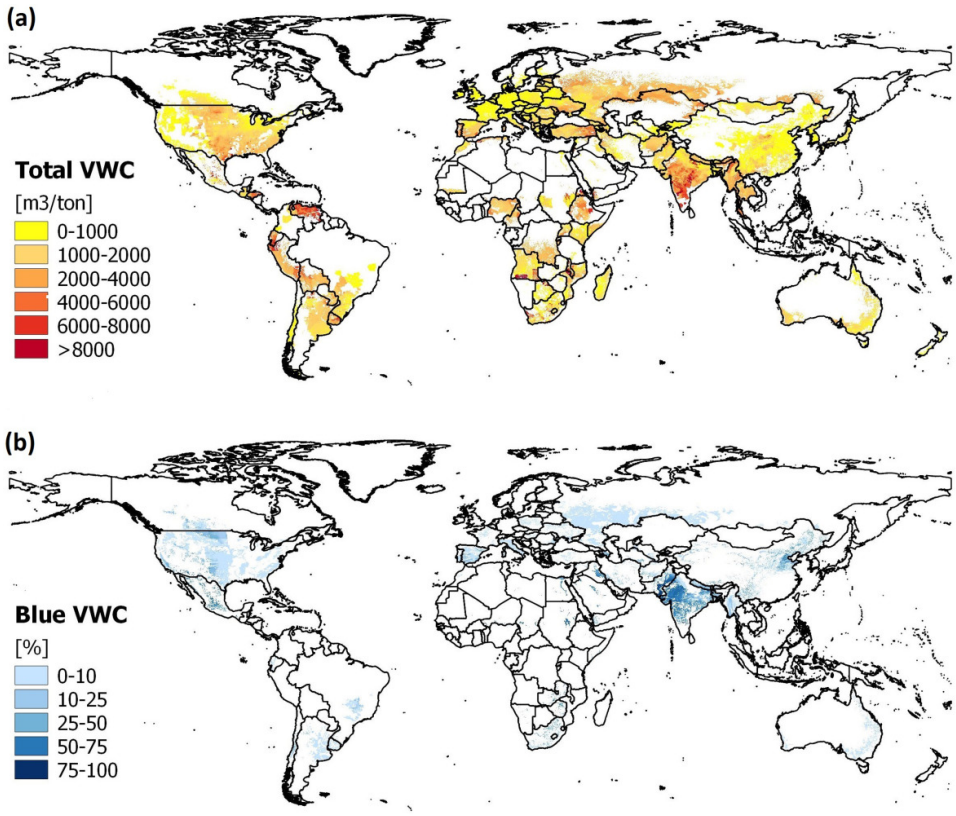

Fig. 1.3 Spatial distribution of the WF of wheat averaged over the period 1996–2005: (a) total crop water footprint, expressed in $m^3 ton^{-1}$ and (b) blue WF, expressed as percentage of the total crop water footprint (Tuninetti et al., 2015).

water pollution). Since the introduction of the WF framework an increasing number of studies have quantified the amount of water consumed (or polluted) to produce different agriculture commodities (e.g., Hanasaki et al., 2010; Liu and Yang, 2010; Mekonnen and Hoekstra, 2011; Rost et al., 2008; Siebert and Döll, 2010; Tuninetti et al., 2015). This have allowed to unveil the significant spatio-temporal heterogeneity of agriculture production. For example in 2000, depending on the agriculture practices and climatic conditions of the considered area, a ton of wheat could need from 400 to 8000 cubic meter of water (Fig.1.3a), this spatial heterogeneity is even further if the blue and the green water components are examined separately (see Fig.1.3b) (Tuninetti et al., 2015). Moreover, also from year to year the WF of each crop can significantly fluctuate in response of agricultural yield variations (Tuninetti et al., 2017a).

Therefore, through the WF framework it is possible to study the linkage between the consumption of any commodity and the volumes of water used to produce it. In the last few decades, the global agri-food system has exhibited a progressive geographical decoupling between food production and consumption (Fader et al., 2013), as testified by the fact that about one quarter of the food produced for human consumption is currently traded internationally (D'Odorico et al., 2014). In recent years, the virtual water network related to internationally-traded food commodities has been investigated to understand its patterns and temporal trends. It has been widely acknowledged that international trade patterns are predominately driven by socioeconomic factors rather than water resources endowments (D'Odorico et al., 2010; Fracasso et al., 2015; Tamea et al., 2014; Yang, 2008), since the commodities prices – which consistently influence trade relationships - rarely reflects water inputs (Gallagher, 2008). Moreover, it has been recognized that (i) water resources are becoming increasingly globalized (Carr et al., 2013; Dalin et al., 2012; D'Odorico et al., 2014), (ii) food demand of several countries heavily rely on foreign water resources (Hoekstra and Mekonnen, 2012), and (iii) exported goods contribute to the water exploitation and degradation of environments far away from the consumers (Dalin and Rodríguez-Iturbe, 2016; Dalin et al., 2017; D'Odorico et al., 2010; Lenzen et al., 2012; Marston et al., 2015).

However, a critique that has been made to the virtual water trade assessments is that they typically aggregate and compare water volumes without taking into account the place where water has been withdrawn (Berger and Finkbeiner, 2013; Lenzen et al., 2013b; Ridoutt and Pfister, 2009; Yano et al., 2016). In fact, the accounting of the water volumes alone to quantify the human pressure on global water resources can be misleading without additional impact-oriented interpretations (Berger and Finkbeiner, 2013; Ridoutt and Pfister, 2009; Yano et al., 2015). In fact, due to the uneven spatiotemporal distribution of freshwater resources, a same volume of depleted water does not have the same environmental impact in different times or places. Since the WF aggregates in a single measure volumes coming from extremely different freshwater environments, it measures water use itself and not the potential environmental impact of water exploitation. The case of river environments is emblematic: the withdrawal of, say, 1000 m^3 of water a day can be completely

negligible in a fluvial region rich in water, while it can be devastating in a semi-arid area.

In order to quantitatively evaluate the average pressure on water resources by human activities, various indicators have been developed comparing the amount of water use to the actual water resources exploited. Despite very recent indices of green water scarcity (Schyns et al., 2015) and of economic water scarcity (Molden, 2007), a wide number of studies have examined physical blue water scarcity. The latter can be fundamentally divided into two facets: water shortage (i.e., population-driven water scarcity) and water stress (i.e., the ratio water use to water availability) (Kummu et al., 2016). Water shortage refers to a condition of low water availability per capita; therefore, in "crowded" regions the capacity of the resource might become insufficient to offset the water-demand of the population, even though the per capita water-demand is relatively low. Differently, blue water stress can be considered as a demand-driven scarcity, since it measures the ratio of water use to water availability. Hence, a region can be classified as under severe water stress even when it is not densely populated, for instance because of large water-use for producing commodities for foreign regions (Kummu et al., 2016; Wada and Bierkens, 2014).

A frequently used measure of water shortage is the water crowding index, which was proposed by Falkenmark (1989). By referring to threshold values, Falkenmark (1989) defined different degrees of water shortage at the country scale ranging from no water scarcity (over 1.700 m^3yr^{-1} per capita) to absolute water scarcity (less than 500 m^3yr^{-1} per capita). Few years later, Raskin et al. (1997) introduced a demand-driven blue water scarcity as the ratio of annual water withdrawals to the annual renewable water resources at the country scale. Raskin et al. (1997) suggested that a given country is severely water scarce if the ratio of withdrawal to availability exceeds 40%, water scarce if this ratio lies in the 20–40% interval, moderately water scarce when this ratio varies from 10% to 20%, and lowly water scarce when the ratio is lower than 10%. These ranges were embraced in the UN report "Comprehensive assessment of the freshwater resources of the world" (UN-Water, 1997) and consequently extensively adopted in the scientific literature, e.g. (Arnell, 1999; Oki et al., 2001; Vörösmarty et al., 2000b) as well as by the European Environmental

Agency (Kristensen, 2003) in order to classify the degree of water stress of an area.

Depending on the objective of the study, the water use-to-availability ratio has been assessed adopting i) a water use value measured as either gross (Arnell, 1999) or net (Kummu et al., 2016; Mekonnen and Hoekstra, 2016) water abstraction from blue water resources and ii) a water availability measure usually expressed as the amount of renewable surface and groundwater resources, with (Hoekstra et al., 2012; Mekonnen and Hoekstra, 2016; Wada et al., 2011) or without (Arnell, 1999) including the environmental flow requirements (EFR); the latter indicates the quantity, quality and timing of water flows required to sustain freshwater ecosystems (Acreman and Dunbar, 2004). Recently, also the non-renewable exploitation of groundwater resources was incorporated in a water stress indicator (Wada and Bierkens, 2014; Wada et al., 2011). In September 2015, the water stress indicator expressed as the ratio of gross water use to renewable resources minus the EFR, was adopted in the Target 6.4 of the Sustainable Development Goals (SDGs) (Vanham et al., 2018).

In recent years, also thanks to new global hydrological models (e.g., H08, PCR-GLOBWB, WaterGAP), different studies adopted blue water scarcity indicators with finer spatio−temporal resolution and identified water scarce areas in current, past or future conditions (Alcamo et al., 2007; Hanasaki et al., 2013; Kummu et al., 2016; Mekonnen and Hoekstra, 2016; Wada and Bierkens, 2014; Wada et al., 2011). Overall, all the studies on physical blue water scarcity share the volumetric comparison of local resources and withdrawals (or population needs); withdrawals and water resources vary from region to region, and stress (or water shortage) occurs when withdrawals significantly affect the available water resources. Therefore, the blue water scarcity measures are strictly related to local socio-economic needs: the availability is affected by upstream withdrawals, but if locally there is no water consumption the region is not classified under water stress, even when the local river environment exhibits a strong impact due to upstream withdrawals. Essentially, these indicators only identify the areas where the competition is critical between human needs and water availability, while the most impacting water consumption patterns remain generally hidden or unidentified.

1.2 Motivations behind the study and outline of the Thesis

The Thesis unfolds in three research projects that have different but tightly linked objectives.

In **Chapter 2**, we define the Environmental Cost Index, which quantifies the impact of a surface water withdrawal on riverine systems. Since fluvial ecosystems are complex environments that exhibit a high number of interplaying processes, we design an indicator able to manage such complexity in a parsimonious way. To this aim, the proposed index: (i) quantifies the impacts that the reduction of the river flow causes on specific fluvial characteristics (e.g., transport of sediments and chemicals, riparian belt width, biodiversity richness, etc.), through suitable non-linear relations with discharge, and (ii) considers the whole portion of river network impacted by a withdrawal, that is from the section where water is withdrawn down to the river mouth. Thus, the environmental cost associated to a withdrawal does not depend exclusively on the status of local water resources, but it considers the downstream conditions as well. The downstream propagation of an hydrological stressor (e.g., a water withdrawal) was also accounted by Vörösmarty et al. (2010), who considered a number of drivers of stress (e.g., dam density, water consumption, livestock density) with the objective to study the current environmental status of the global river systems. In the approach presented in Chapter 2, instead of focusing on a specific scenario of water withdrawing, we provide an easy-to-apply tool to investigate the environmental cost of any water consumption pattern. Indeed, a key point of the approach developed is to first consider a potential withdrawal corresponding to a unitary amount of surface water. We assume that this potential withdrawal occurs in a given river section, and we evaluate its degree of impact, which will depend on the specific riverine environment considered. This procedure is repeated for each and every river sections in the world's hydrographic network and the global geography of the environmental cost associated with single unitary withdrawals is described. The environmental cost corresponding to a real pattern of withdrawals (or to possible future scenarios) is finally obtained as the linear spatial combination (i.e., as the superposition) of the environmental costs due to the unitary withdrawals. The index defined

in this Thesis is an easy-to-apply tool to support the interpretation of the volumetric measure of surface water withdrawal with a perspective that takes into account the fluvial system where the withdrawal actually occurs.

In **Chapter 3**, we quantify the impact of food consumption on local and foreign freshwater resources through an indicator of the environmental value of the riverine water (EVRW) embedded in food products. As mentioned, the virtual water concept provided a framework to link food consumers to water resources use. However, a shortcoming of virtual water assessments is that they typically combined and compare water volumes without considering the place where water has been actually withdrawn (Berger and Finkbeiner, 2013; Lenzen et al., 2013b; Ridoutt and Pfister, 2009; Yano et al., 2016). Therefore - by adopting the EC index introduced in Chapter 2 - in Chapter 3 we quantify the effects of food production and trade on the health of surface water ecosystems over the period 1986-2013. The EVRW measure allows us to study the main implications of the market globalization on the status of world's rivers and to investigate the food trade network efficiency under the perspective of fluvial environments.

In **Chapter 4**, we examine six socio-economic drivers of domestic and foreign freshwater use over the period 1994-2010 considering the consumers final demand of products and services. As mentioned, the recent intensification of international trade has led to a growing disconnection between the consumers demand of commodities and the water resources exploited to produce those commodities (Dalin and Rodríguez-Iturbe, 2016; Dalin et al., 2017; D'Odorico et al., 2010; Lenzen et al., 2012; Marston et al., 2015). However, despite it is widely recognized the important role of the consumers demand for products and services on the exploitation of distant freshwater resources, the different socioeconomic drivers behind the trends in domestic and foreign water use are still unquantified. In this Chapter we address this issue by presenting a comprehensive analysis of the socio-economic drivers that govern outsourcing and domestic freshwater use trends. In order to identify and assess the responsibility of consumers for the exploitation of distant water resources, we employed Multi-Regional Input-Output (MRIO) models. These models map the global economy by considering the monetary transactions between sectors and regions (Miller and Blair, 2009). In the MRIO framework, the changes and trends in global water use can be explained through a well-established

technique named structural decomposition analysis (SDA) (Dietzenbacher and Los, 1998b). Basically, SDA breaks down observed changes in a physical variable (i.e., water use) over time, into the changes in its key determinants which can act as accelerators or retardants. The results presented in Chapter 4 describe the main socio-economic mechanisms that accelerate or decelerate the exploitation of freshwater resources worldwide.

Chapter 2

The environmental cost of a reference withdrawal from surface waters

The work described in this chapter has been partially derived from Soligno et al. (2017).

In the past century, global freshwater withdrawals increased approximately sevenfold (Gleick, 2000) with irrigation accounting for around 70% of the total freshwater withdrawals (FAO, 2011). This growing demand for water resources have considerably influenced most rivers of the world with respect to their habitat, water quality, morphology and flow regimes (Dudgeon et al., 2006; Haddeland et al., 2014; Hanasaki et al., 2013; Vörösmarty et al., 2000b; Wada et al., 2013). Over the years, much effort has been devoted to quantify water consumption at the global scale (e.g., Hanasaki et al., 2010; Liu and Yang, 2010; Mekonnen and Hoekstra, 2011; Rost et al., 2008; Siebert and Döll, 2010; Tuninetti et al., 2015); however, comparisons are not simple because the uneven spatiotemporal distribution of surface water resources entails that the same amount of consumed water does not have the same environmental impact in different times or places. In order to account for this spatiotemporal heterogeneity, this Chapter proposes a novel approach to quantify the environmental impact of a water withdrawal from a generic river section by introducing the Environmental Cost (EC) index. The index depends on (i) the environmental relevance of the impacted fluvial ecosystem (e.g., bed-load transport capacity,

width of the riparian belt, biodiversity richness), which is defined through suitable power-law relations with discharge, and (ii) the downstream river network affected by the water withdrawal. Therefore, the index aims to support the interpretation of the volumetric measure of surface water withdrawal with a perspective that takes into account the fluvial system where the withdrawal actually occurs and the responsibilities that it has on downstream freshwater ecosystems. A key point of the EC index is that is assessed in each and every river section worldwide considering a reference withdrawal. Being referred to a unitary reference withdrawal that can occur in any river section worldwide (instead of focusing on a specific scenario of water withdrawing) we propose a general approach that allows one to quantify and compare the environmental impact of any consumption pattern. In fact, the environmental cost corresponding to a specific pattern of withdrawals can be obtained as the linear spatial combination (i.e., as the superposition) of the environmental costs due to the unitary withdrawals and the actual water consumption patterns.
Our work shares some ground with above mentioned indicators (see Chapter 1) of water shortage (i.e., population-driven water scarcity) and of water stress (i.e., the ratio of water use to water availability) (Kummu et al., 2016). Overall, these indicators evaluate the average competition between human needs and water resources availability through the volumetric comparison of local resources and withdrawals (or population requirements). Water scarcity indicators are, thus, intrinsically linked to the (local) human demand for water. Accordingly, if locally there is no water consumption (or population) the region is not classified under water scarcity, even when the local river environment reveals a strong impact due to upstream depletion. Therefore, water scarcity indicators are valuable metric only to identify hot spots of critical mismatch between water demand and availability, while the most impacting water consumption patterns remain generally hidden or unidentified. Differently from the water scarcity indices, the EC index introduced in this Chapter: (i) is designed to consider a reference withdrawal that can occur anywhere in the global hydrographic network; (ii) entirely depends on the impacted river environment and not on human needs; and (iii) does not make a volumetric comparison between available and consumed water, but attempts to express the non-linear relation between water withdrawals and their impacts on riverine systems.

2.1 The index to assess the environmental cost of a surface withdrawal

2.1.1 Definition of the environmental cost per unit length

The health of a river ecosystem depends on multiple and complex biotic and abiotic processes. In this work, we focus on the impact related to water withdrawals in order to estimate their environmental cost. The environmental cost measure strictly depends on the impact that a water withdrawal has on river ecosystems. This work proposes an index which is function of (i) the water withdrawal and (ii) the undisturbed river discharge, that is the discharge existing before the river flow reduction due to water withdrawals.
We assume the environmental cost per unit length (ec_w) of a withdrawal in a generic section of the river network to be proportional to the river discharge reduction caused by the water withdrawal, $W(ec_w)$, in the same section. Thus, the proportion between the environmental cost and water withdrawal is

$$ec_w : W = ec_{max} : Q \qquad \Rightarrow \qquad ec_w = ec_{max} \cdot \frac{W}{Q} \tag{2.1}$$

where ec_w coincides with the impact of a water withdrawal W and ec_{max} is the maximum possible environmental cost per unit length, which occurs when the entire river discharge, Q, in the river section, is withdrawn (clearly, $W \leq Q$); ec_w has the dimension of an environmental cost per unit length. We model a linear proportion between ec_w and W, neglecting non-linear terms in order to keep the number of parameters at a minimum.
Therefore, ec_w estimates a local impact, which does not take into account downstream effects (i.e., ec_w considers only the impact in the river section where W occurs); in section 2.1.4 we will introduce the index that considers the effects of a withdrawal on the whole fluvial system.

2.1.2 Definition of the maximum environmental cost per unit length

From Eq.(2.1), the environmental cost per unit length of a water withdrawal, ec_w, can be assessed once the undisturbed river discharge and the maximum environmental cost per unit length are known; thus, a method has to be defined to determine ec_{max}, which refers to the water depletion of the river section and occurs when the withdrawal equals the undisturbed river discharge.
The maximum environmental cost is strictly related to the relevance of the fluvial environment considered. However, such relevance cannot be reduced to a single number: a fluvial environment is characterized by multiple and interplaying processes and, thus, its environmental relevance is a multidimensional concept as well. It follows that the value of ec_{max} in a river section depends on the specific perspective adopted. A possible choice is to assume that the importance of a fluvial system linearly depends on the discharge of the considered river; other possible choices are to consider the fluvial biodiversity or the sediment transport capacity of the river. Overall, many fluvial characteristics can be related to the river discharge through suitable power-law relations (see sec.2.1.3) that lead to estimate ec_{max} as

$$ec_{max} = k(\alpha) \cdot Q^{\alpha} \tag{2.2}$$

where α is a parameter that typically varies between 0 and 1 (see Section 2.1.3) and $k(\alpha)$ is a proportionality constant, which is the same in all the river sections once the value of the parameter α has been defined.
Specific values of the parameter α correspond to the perspective chosen (e.g., the width of the riparian belt, the habitat richness, the dilution capacity, etc) to evaluate the relevance of a fluvial environment. In Section 2.1.3, some emblematic cases are described and the corresponding values of α fall in the range [0 1].
The two limiting cases $\alpha = 0$ and $\alpha = 1$ embody the range of perspectives wherein ec_{max} moves. When $\alpha = 0$ all fluvial systems have the same environmental relevance everywhere independently of the discharge, namely the depletion of a large river has the same environmental cost as the depletion of a small stream. Conversely, when $\alpha = 1$, ec_{max} turns out to be directly proportional to the discharge flowing in the considered river section; with this

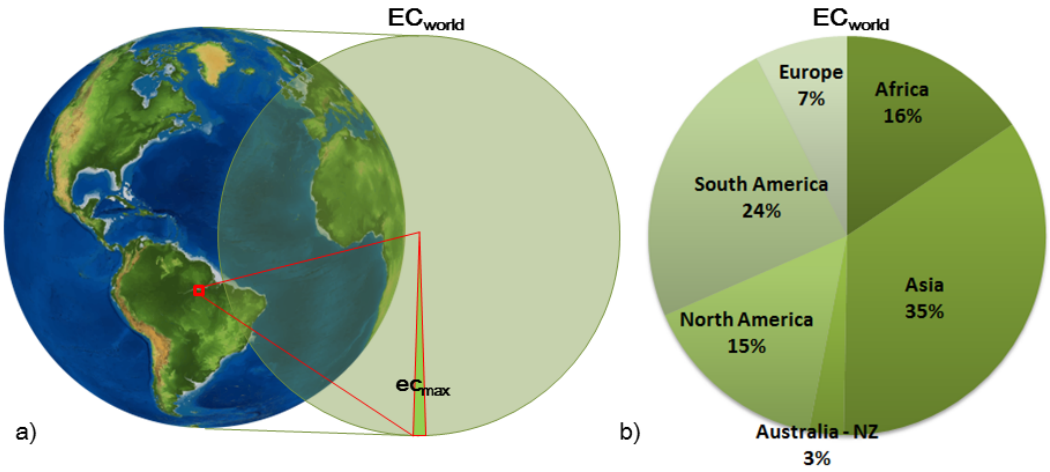

Fig. 2.1 (a) Conceptual presentation of EC_{world}, which is obtained by adding up the different ec_{max} of all the world's river sections. Each river section contributes with a different share to the overall environmental value of the whole world′s water resources; (b) as an example, the pie chart shows the contribution of each continent to the total EC_{world}; which is estimated using the natural river discharge of WaterGAP 2.2c and $\alpha = 0.5$ (see Section 2.2 for detailed information about the application of the index performed in this work).

formulation, the depletion of a large river has more impact than depletion of a small steam. Overall, the formulation of ec_{max} permits a change in the perspective adopted to determine the relevance of a river system, in line with the study targets.

A reasonable constraint is that the environmental cost of withdrawing all the world′s surface water resources is unaffected by α and equal to a constant value, EC_{world}. If all the global surface water resources were consumed, the overall environmental cost EC_{world} would be equal to the summation of the maximum environmental cost per unit length along all river sections worldwide (see Fig.2.1). Using Eq.(2.2), EC_{world} can be evaluated as

$$EC_{world} = L_w \cdot \int_{all\,Q} ec_{max}(Q) \cdot p(Q) \cdot \mathrm{d}Q, \tag{2.3}$$

where $p(Q)$ is the probability density function of the undisturbed river discharge, determined along all river streams in the world, and L_w is the total length of the world river network. Both are evaluated at a detail related to the scale of interest. Thus, EC_{world} is equal to the expected value of the maximum environmental cost per unit length multiplied by L_w. Substituting Eq.(2.2)

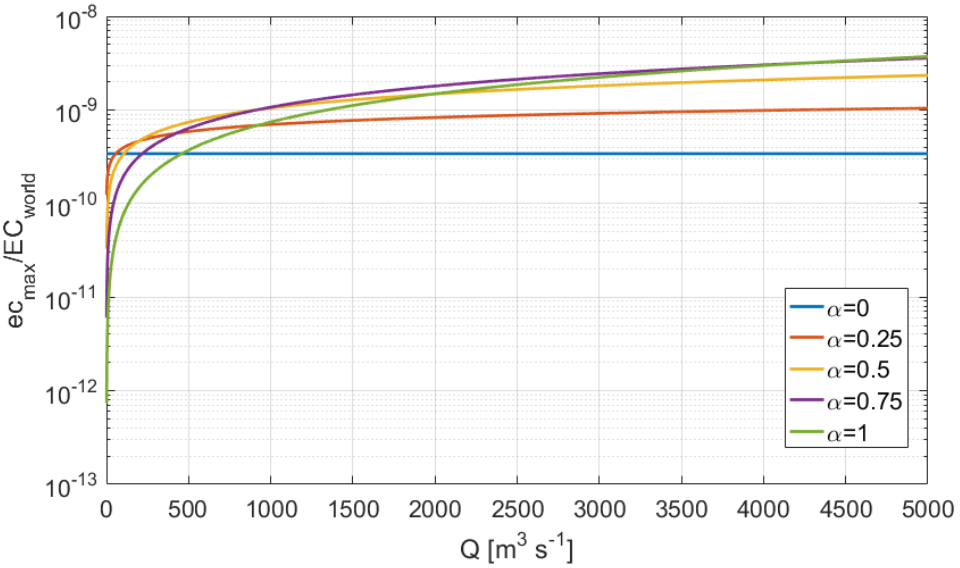

Fig. 2.2 ec_{max}/EC_{world} as a function of the undisturbed river discharge, considering different values of α.

into Eq.(2.3) and exploiting the fact that EC_{world} does not depend on α, $k(\alpha)$ can be assessed as

$$k(\alpha) = \frac{EC_{world}}{L_w \cdot \int_{all\,Q} Q^{\alpha} \cdot p(Q) \cdot \mathrm{d}Q}. \tag{2.4}$$

Therefore, Eq.(2.2) and Eq.(2.4) allow EC_{world} to be subdivided among the different river sections according to the adoption of a specific environmental perspective (i.e., through the designation of the parameter α). Fig.2.2 shows ec_{max} - normalized by EC_{world} - as a function of the undisturbed river discharge considering different values of α. In spite of the environmental value of the whole world′s water resources (EC_{world}) being constant, the environmental significance of a specific river section can significantly change depending on the considered α value; moreover, the dissimilarities in the ec_{max} values among sections having different river discharge rise with α. By introducing Eq.(2.2) into Eq.(2.1), the environmental cost per unit length of a water withdrawal, W, in a generic river section becomes

$$ec_w = k(\alpha) \cdot \frac{W}{Q^{1-\alpha}} \tag{2.5}$$

We note from Eq.(2.5) that there is a power-law relationship among the ec_w values calculated using different values of α. This relation is expressed as

$$ec_w(\alpha_1) = b_1 \cdot ec_w(\alpha_2)^{b_0} \tag{2.6}$$

where $ec_w(\alpha_1)$ and $ec_w(\alpha_2)$ are the environmental cost per unit length values, which are assessed by employing $\alpha = \alpha_1$ and $\alpha = \alpha_2$, respectively; b_0 and b_1 are the power-law coefficients, where $b_0 = (\alpha_1 - 1)/(\alpha_2 - 1)$ and $b_1 = k(\alpha_1) \cdot k(\alpha_2)^{-b_0} \cdot W^{(1-b_0)}$. The relation in Eq.(2.6) implies that if a unitary reference withdrawal is considered in all the river sections, the ranking of the ec_w values among the different river sections is α-independent. However, the choice of α influences the range of variation of the ec_w values, which is minimum when $\alpha = 1$ and maximum when $\alpha = 0$ (as also shown in Fig.2.2).
Finally, notice that the proposed approach to define the environmental cost is able to embed different river characteristics at the same time. E.g., all the possible values of α between 0 and 1 can be considered through a kernel function, $Ker(\alpha)$, to weight them. By integrating Eq.(2.5) between $\alpha = 0$ and $\alpha = 1$ the environmental cost per unit length in this case turns into

$$ec_w = \int_0^1 Ker(\alpha) \cdot k(\alpha) \cdot \frac{W}{Q^{1-\alpha}} \mathrm{d}\alpha. \tag{2.7}$$

This property of the index is exploited in the Chapter in order to consider multiple river characteristics at the same time.

2.1.3 Examples of possible choices of the parameter α

Once the discharge and the water withdrawal in the river section are knows, Eq.(2.5) allows one to evaluate the environmental cost per unit length through the choice of the parameter α, where the designation of α involves establishing the significance of a fluvial system accounting for a specific river characteristic. As aforementioned, when $\alpha = 0$ it follows that $ec_{max} = k(0)$, thus ec_{max} does not depend on the considered river section; under this perspective in any river section the complete loss of the corresponding fluvial system is expressed by a constant value that is equal to EC_{world}/L_w. Differently, when $\alpha = 1$, one

obtains $ec_{max} = k(1) \cdot Q$, and the significance of a fluvial system is directly proportional to the river discharge. In this case, from Eq.(2.4) and Eq.(2.2), $ec_{max} = (EC_{world} \cdot Q)/(L_w \cdot \mu_Q)$, where μ_Q is the global average of the undisturbed river discharge. The case $\alpha = 1$ is reasonable, for example, when one focuses on the river water quality; since it depends on the concentration of nutrients and chemical substances and, then, on the dilution capacity, which is in turn proportional to discharge.

By altering the river discharge, water withdrawals can lead to the impoverishment of riparian ecosystems: there is an intrinsic and significant sensitivity of riparian ecosystem to hydrological modifications (Camporeale et al., 2006; Doulatyari et al., 2014). Riparian areas are the transition zones between terrestrial and aquatic ecosystems and have a significant role in maintaining regional biodiversity; in fact, they have valuable plant communities, fisheries and wildlife (Naiman et al., 1993; Sabater and Tockner, 2009; Shafroth et al., 2002). Therefore, another criterion to estimate α may be to consider the impacted riparian area per unit river length. Such area can be approximately proportional to the channel width. This latter is in turn proportional to a power function of the discharge with an exponent α between 0.4 and 0.5 (Julien and Wargadalam, 1995).

River biodiversity can be another relevant issue: in fact, fish species richness increases as a power law of the river discharge (Oberdoff et al., 1995; Poff et al., 2001; Xenopoulos et al., 2005). Thus, the maximum environmental cost per unit length on river biodiversity can be evaluated considering the species-discharge relationship, where $fish - richness \propto Q^{\alpha}$. Xenopoulos et al. (2005) assumed $\alpha = 0.4$ for rivers between 42°N and 42°S, whereas Oberdoff et al. (1995) conducted a global scale analysis on variations in species richness finding $\alpha = 0.33$. However, the value of α changes depending on the specific site: e.g., Xenopoulos (2006) obtained α in the range 0.1 - 0.2 for two different regions in the United States.

Another point of view about river characteristics is the bed-load transport, which controls the sediment erosion/deposition processes in fluvial systems, as well as the nutrient transport essential for the fluvial habitat health. For steady flows the bed-load transport is commonly represented as $\phi \propto (\theta - {\theta_b}^{\frac{3}{2}})$ (Meyer-Peter and Müller, 1948) where θ and θ_c are the effective and the critical Shields parameters, respectively, which are dimensionless bed-shear stress coefficients

($\theta \propto \tau_b$). Assuming a Chèzy friction law (that is, a steady and turbulent open channel flow) and the alluvial channel geometry relationships by Julien and Wargadalam (1995), the bed-shear stress can be evaluated as

$$\theta_b \propto R \cdot i_b \propto \frac{U^2}{R^{\frac{1}{3}}} \propto Q^{0.33} \tag{2.8}$$

where R is the hydraulic radius (equal to the river depth), i_b is the bed slope, and U is the mean stream velocity. Then, the sediment volumetric discharge can be estimated as

$$Q_s \propto q_s \cdot W_c \propto {\theta_b}^{\frac{3}{2}} \cdot W_c \propto Q^{0.5} \cdot Q^{0.44} = Q^{0.94} \tag{2.9}$$

where W_c is the channel width. Thus, in our framework the environmental cost considering the geomorphologic impact can be assessed employing $\alpha = 0.94$. The examined cases show that typically values of α fall within the interval [0,1]. In any case, as no conceptual reason exists for limiting α within [0,1], values outside this range can be adopted in our framework.

2.1.4 Assessment of the environmental cost including the downstream river network

In the previous sections we assessed the environmental cost per unit length, by focusing only on the specific river section where water is withdrawn. However, the actual environmental cost of a water withdrawal also has to consider the impact on the portion of river network downstream to the point where water is withdrawn. In fact, the subtraction of W will alter the discharge in all the river sections from the section where water is withdrawn down to the river mouth (see Fig.2.3a).

Therefore, the overall environmental cost of a water withdrawal W has to be evaluated as the sum of the environmental cost per unit length from the section where water is withdrawn, S_W, down to the river mouth. The impact per unit length in a generic downstream section, s, is assessed by employing Eq.(2.5) using the value of the undisturbed river discharge in s and a water withdrawal equal to W, since in each downstream section the undisturbed river discharge is reduced by the same amount of water that is withdrawn in S_W, namely W.

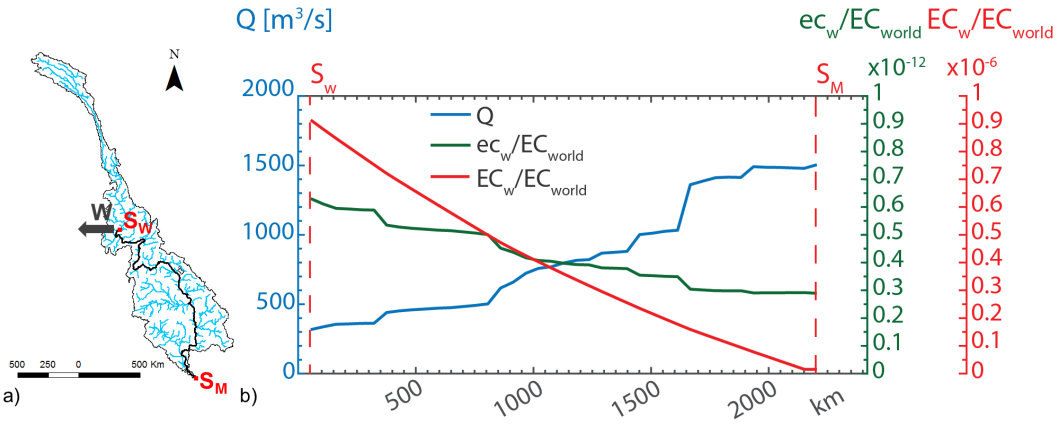

Fig. 2.3 (a) The example shows the main Mekong river network. A water withdrawal, W, located in a river section, S_W, of the river impacts all the downstream sections (marked with the black line) down to the river mouth following the flow direction along the curvilinear abscissa of the river. (b) Panel shows the average annual Mekong river discharge (Q), the environmental cost per unit length of the Mekong′s course (ec_w) and the overall environmental cost in each cell of the Mekong′s course (EC_w) from the section S_w down to the river mouth (S_M); both environmental costs are normalized by EC_{world} and are estimated with $\alpha = 0.5$ and $W = 1\ \mathrm{m^3\,s^{-1}}$.

It follows that we can define the environmental cost, EC_w, of a water withdrawal, W, in a river section S_W of the river network as

$$EC_w = \int_{S_W}^{S_M} ec_w(s)\mathrm{d}s = k(\alpha) \cdot \int_{S_W}^{S_M} \frac{W}{Q(s)^{1-\alpha}}\mathrm{d}s \tag{2.10}$$

where S_M is the river mouth section and the argument of the integral is the environmental cost per unit length (ec_w) of a water withdrawal (W) in the river section s assessed with Eq.(2.5). EC_w and EC_{world} have the same units of measure, namely ec_w multiplied by a length.

In this regard, consider the Mekong river case study illustrated in Fig.2.3a and Fig.2.3b. In Fig.2.3a, water consumption (W) affects the river from the section where water is extracted down to the river mouth section. Actually, in the same river a fixed water withdrawal has a higher environmental cost if this occurs in the upper part of the river (see the red line in Fig.2.3b). This occurs for two reasons: (i) usually river discharge gradually increases from the spring to the river mouth and the same amount of W, thus, represents a very different share of the available water resources (see Eq.(2.5)); (ii) a water withdrawal

impacts all the downstream sections (see Fig.2.3a).
As mentioned in the previous section, instead of estimating the environmental cost per unit length by employing a specific value of α, ec_w can be assessed with Eq.(2.7) and hence in this case the environmental cost of a water withdrawal turns into

$$EC_w = \int_{S_W}^{S_M} \int_0^1 Ker(\alpha) \cdot k(\alpha) \cdot \frac{W}{Q(s)^{1-\alpha}} \mathrm{d}\alpha \mathrm{d}s. \tag{2.11}$$

In this section, the index has been described with the aid of an example related to a specific river segment (see Fig.2.3); more generally, in this work the environmental cost of a surface water withdrawal has been assessed at a global scale as discussed in the following section.

2.2 Application of the EC index at the global scale

The environmental cost of a water withdrawal can be assessed once the river network and the undisturbed river discharge worldwide are known. In this work, EC_w is computed globally with a 0.5° spatial resolution using the global drainage direction map DDM30 (Döll and Lehner, 2002) and the undisturbed river discharges obtained from the pristine scenario of the WaterGAP 2.2c model (Döll et al., 2014; Müller Schmied, 2017; Müller Schmied et al., 2014, 2016). The average annual undisturbed river discharge has been evaluated over the time series 1901 - 2013. In order to assess the environmental cost EC_w of a water withdrawal in a generic river section, a discretization of the river network is needed. The environmental cost of a water withdrawal can be evaluated by discretizing Eq.(2.10) accordingly to the rectangular rule as

$$EC_w = \sum_{j=1}^{N} ec_{w,j} \cdot \Delta s_j \tag{2.12}$$

where $ec_{w,j}$ is the environmental cost per unit length, which is evaluated in the sections where the discharge is known, and Δs_j is the distance between sections $(j-1)$ and j, which are two consecutive sections where the undisturbed river discharge is known (i.e., where $ec_{w,j}$ can be defined). N is the number of

sections between the river section where the water withdrawal occurs and the river mouth. In the present study the index has been assessed at a global scale using an average yearly value of the undisturbed river discharge; Δs_j has been estimated as the square root of the area of the cell. The environmental cost in each cell is $ec_{w,j} \cdot \Delta s_j$, where ec_w has been estimated employing the undisturbed river discharge (Q) at the outlet of the cell, since the within-cell variations of Q are unknown. The discretization adopted in this work is suitable for the data used here (e.g., integration by trapezoidal rule does not change our results), but more refined discretizations can be adopted if more detailed data are available. In order to evaluate the environmental value of a reference amount of surface water equal to W, the EC index is assessed considering everywhere a fixed value of W. Since the environmental cost per unit length is estimated for $W \leq Q$, setting W implies establishing a threshold of Q below which the environmental cost is not estimated. The reference water withdrawal has been fixed at 1 $m^3\,s^{-1}$, which can be considered a very small discharge in a cell of 30 by 30 arc min ($\sim$ 55 x 55 km at the equator).

2.2.1 An example of application of the environmental cost index: the Danube River

An example of the evaluation of the proposed index is given in Fig.2.4, which refers to the Danube river′s undisturbed discharge behaviour from the spring to the river mouth. The trend of the environmental cost per unit length, ec_w, is strictly related to the undisturbed river discharge, although the relation between the two is non-linear (see Eq.(2.5)). The overall environmental cost, EC_w, is assessed applying Eq.(2.12) in each cell of the Danube′s course. Since the Danube discharge increases along the flow direction and EC_w takes into account the discharge-depletion effects on the downstream cells, EC_w gradually decreases from the spring to the river mouth of the Danube river. The cumulative effect accounted in EC_w is highlighted as well observing the dissimilarities between the profiles of ec_w (green line) and EC_w (red line): (i) in the sections where Q sharply increases ec_w promptly decreases, conversely EC_w has a much more smoothed trend than ec_w, as expected by introducing an integral operator; (ii) the range between the maximum and the minimum values of the two

impact measures is very different: $6.8 \cdot 10^{-12}$ for ec_w/EC_{world} and $2.2 \cdot 10^{-6}$ for EC_w/EC_{world}.

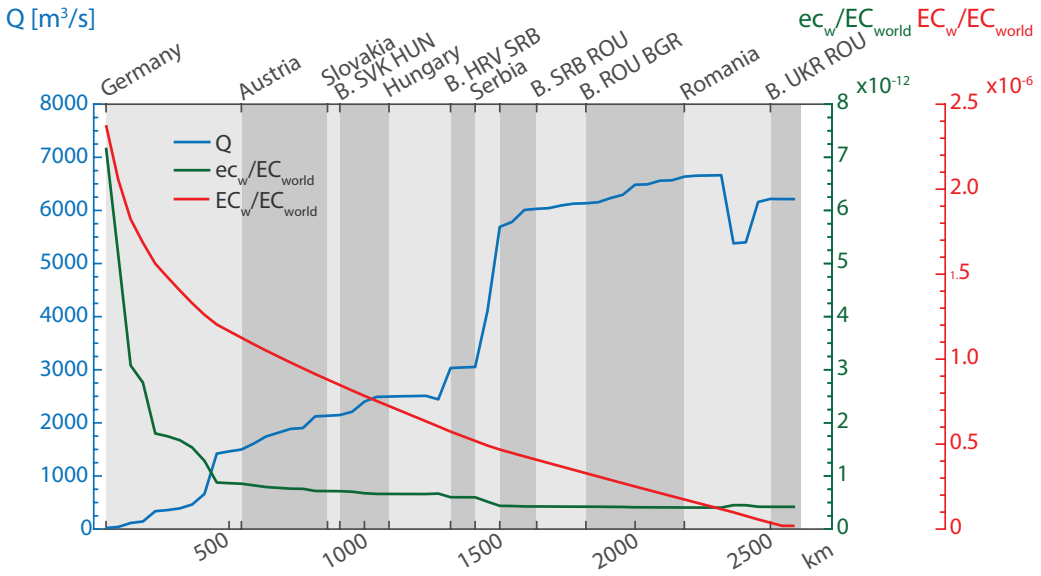

Fig. 2.4 The average annual discharge (Q) of the Danube river, the environmental cost per unit length (ec_w) at the closing section of each cell of the Danube's course, and the overall environmental cost (EC_w) in each cell of the Danube's course; both impacts are normalized by EC_{world} and estimated with $\alpha = 0.5$ and $W = 1$ m^3 s^{-1}. The cells span 30 x 30 arc min (approximately 45 x 45 km at these latitudes). Abscissa reports the distance from the spring of the Danube river. In the top of the figure the countries crossed by the river are shown (the letter $B.$ means that the river flows on the boundary between two countries). Close to the river mouth the discharge has a drop due to the Bala-Old Danube bifurcation.

2.2.2 The geography of EC_w worldwide

Clearly, the environmental cost can be analysed not only focusing on a specific river, but also examining ec_w and EC_w at a global scale, as illustrated in Fig.2.5a and Fig.2.5b, respectively. Both maps are obtained with $\alpha = 0.5$ and $W = 1$ m^3 s^{-1} (see from Fig.A.1 to Fig.A.4 in SectionA.1 of the Appendix for EC_w estimated considering further α values and Fig.A.6 for ec_w and EC_w assessed by a $Ker(\alpha)$). The environmental cost per unit length (ec_w), which varies between 0 and $k(\alpha)$, expresses the local environmental cost of a water withdrawal without accounting for the impact on the downstream sections. It follows that the map in Fig.2.5a is strictly related to the undisturbed river

discharge geography. Since it is not admissible withdrawing more than the available water, in the river sections where $Q < W$, ec_w is not estimated (see grey areas in the maps). Worldwide, the cells having an average yearly undisturbed discharge equal or lower than 1 $m^3 s^{-1}$ are approximately 7.5% (grey cells in Fig.2.5a), which together involve around 0.007% of the total global discharge; these cells belong to deserts or hyperarid areas. In contrast, most of the cells with ec_w under the 5th percentile (namely the areas that at a global scale have the lowest environmental costs per unit length) are located in the world′s largest rivers.

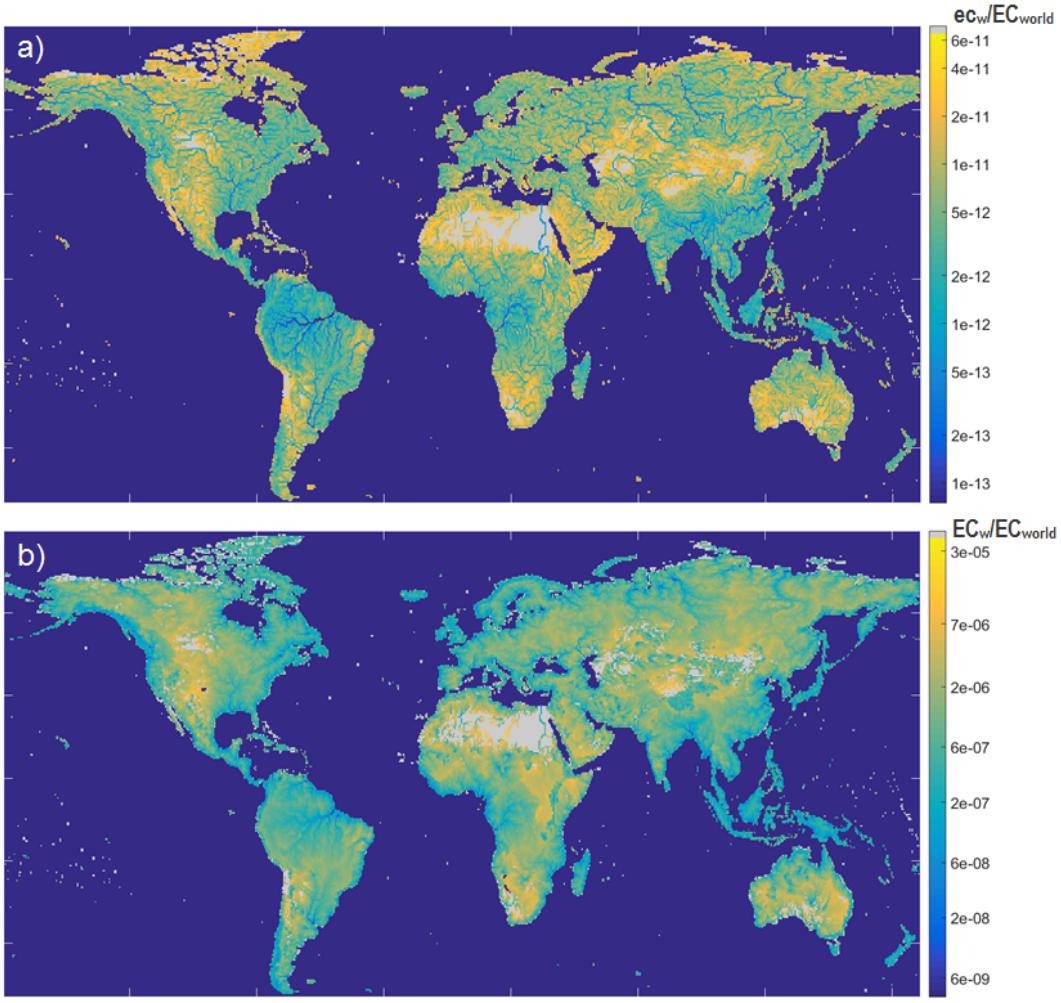

Fig. 2.5 (a) The environmental cost per unit length, ec_w; (b) the overall environmental cost, EC_w. Both maps are estimated with $\alpha = 0.5$ and $W = 1$ m^3 s^{-1} in cells of 30 x 30 arc min and the environmental costs are normalized by EC_{world}. The colour bars are in log scale. Grey areas have $Q < 1$ m^3 s^{-1}, therefore in those areas the environmental cost is not computed.

Changing perspective from the local environmental cost (ec_w) to the overall environmental cost (EC_w) and, thus, accounting for the downstream propagation effect of a water withdrawal on fluvial systems, the environmental value of 1 m^3 s^{-1} assumes worldwide the values shows in Fig.2.5b. In this case, a water withdrawal in a cell having an high value of EC_w implies a significant impact on the overall downstream river course. Generally, the higher EC_w values are located far from the coastline in arid or semi-arid regions because of the combined effect of surface water scarcity and distance from the river

mouth. Most of the cells with EC_w under the 5th percentile are located along the world′s coastline and in the Amazon River; these are thus the areas that have the lowest environmental cost of withdrawing 1 $m^3\,s^{-1}$ of surface water. The average environmental cost of withdrawing 1 $m^3\,s^{-1}$ of surface water in each country can be estimated (see Fig.2.6a) by assessing the average environmental cost at a country level ($\overline{EC}_{w,c}$) as

$$\overline{EC}_{w,c} = \frac{1}{N_c} \cdot \sum_{j=1}^{N_c} EC_{w,j} \tag{2.13}$$

where $EC_{w,j}$ is the overall environmental cost in the cell $j-th$ within the considered country, and N_c is the number of cells in the country. The average environmental cost in Egypt might not be totally representative since this country has only the 21% of the cells with $Q \geq 1$ $m^3\,s^{-1}$.

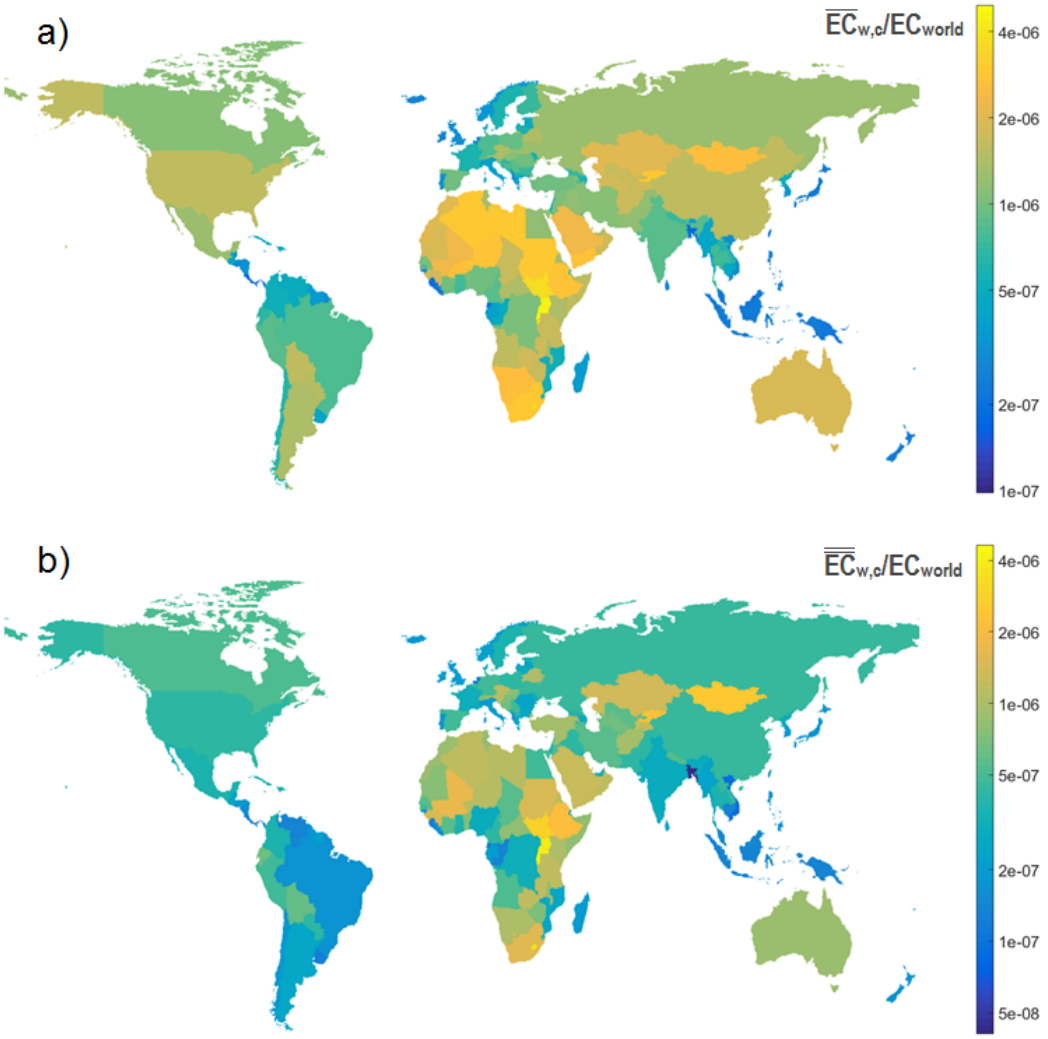

Fig. 2.6 (a) The average environmental cost at country scale ($\overline{EC}_{w,c}$) normalized by EC_{world}; (b) the weighted average environmental cost at country scale using the undisturbed river discharge as the weight ($\overline{\overline{EC}}_{w,c}$) normalized by EC_{world}. Both maps are obtained using $\alpha = 0.5$ and $W = 1$ m^3 s^{-1} in cells of 30 x 30 arc min. The colour bars are in log scale.

Taking the average as in Eq.(2.13) implies that a potential water withdrawal can occur everywhere with the same probability within the country, without considering the fact that water is usually withdrawn where it is more abundant; as a consequence, a different approach to averaging can be considered: the environmental cost at the country scale can be assessed as a weighted average

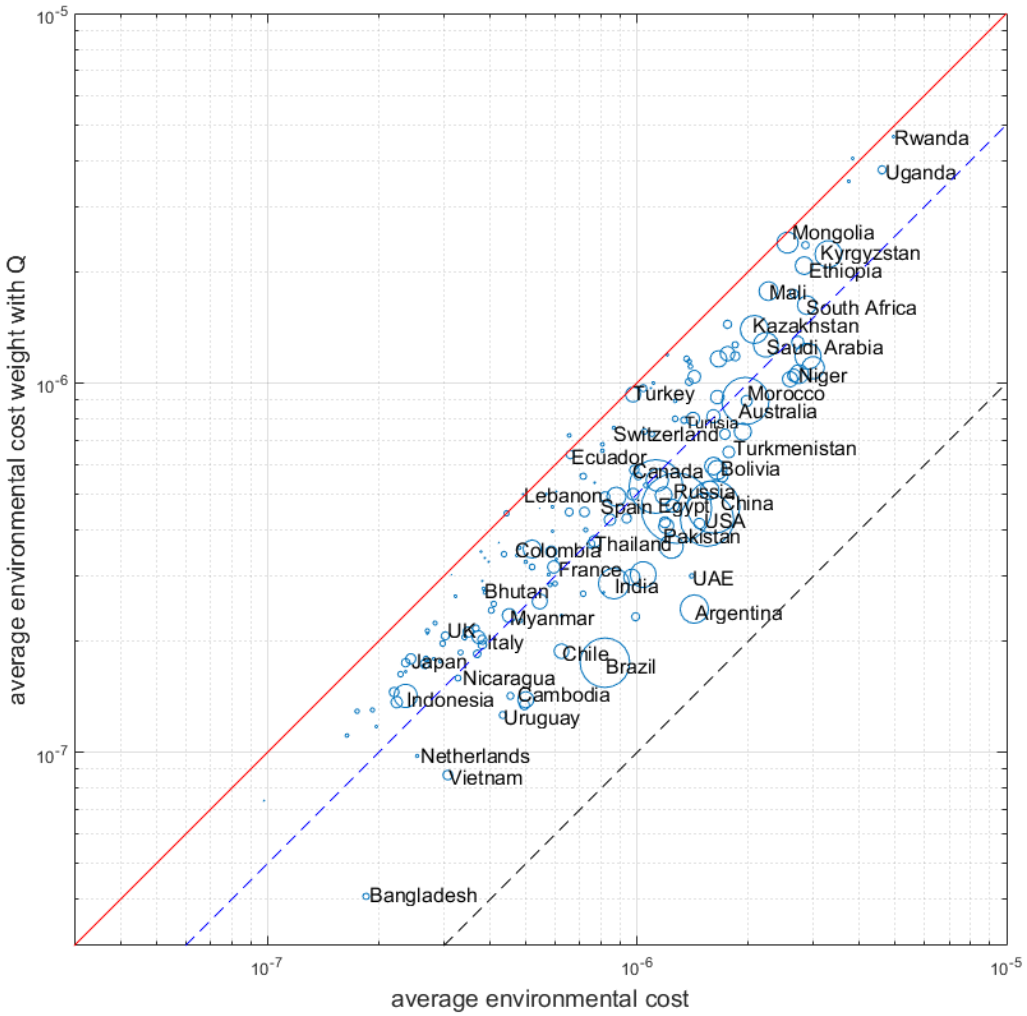

Fig. 2.7 The country average environmental cost ($\overline{EC}_{w,c}$) and the country weighted average environmental cost using the undisturbed river discharge as the weight ($\overline{\overline{EC}}_{w,c}$). The circle size is proportional to the country area. Countries where $\overline{EC}_{w,c} = \overline{\overline{EC}}_{w,c}$ are on the red line; under the dashed blue line there are the countries where $\overline{EC}_{w,c} > 2\overline{\overline{EC}}_{w,c}$; under the dashed black line there are the countries where $\overline{EC}_{w,c} > 10\overline{\overline{EC}}_{w,c}$. Environmental cost values are assessed employing $\alpha = 0.5$ and $W = 1\ \mathrm{m^3\,s^{-1}}$.

using the undisturbed river discharge as the weight

$$\overline{\overline{EC}}_{w,c} = \frac{\sum_{j=1}^{N_c} EC_{w,j} \cdot Q_j}{\sum_{j=1}^{N_c} Q_j}. \tag{2.14}$$

Adopting the weighted average according to Eq.(2.14) (see Fig.2.6b) instead of the average index given by Eq.(2.13) entails that: (i) overall, the environmental cost at the country scale will be reduced, because in a river section the greater is Q the lower is ec_w (see Eq.(2.5)); (ii) countries having arid or semi-arid areas, but also crossed by significant rivers (e.g., Egypt and Pakistan) or, in alternative, large countries having both humid and arid regions (e.g., Argentina and China), will have significantly lower values of EC_w at the country scale than with the unweighted average. Therefore, at the national scale for any α chosen, $\overline{EC}_{w,c} > \overline{\overline{EC}}_{w,c}$. In light of this Fig.2.7 compares $\overline{EC}_{w,c}$ and $\overline{\overline{EC}}_{w,c}$ using $\alpha = 0.5$. In general, the more heterogeneous a country is in terms of undisturbed river discharge, the farther is from the red line, which indicates the countries where $\overline{EC}_{w,c} = \overline{\overline{EC}}_{w,c}$.

2.2.3 The downstream effect: a case study on the Nile River

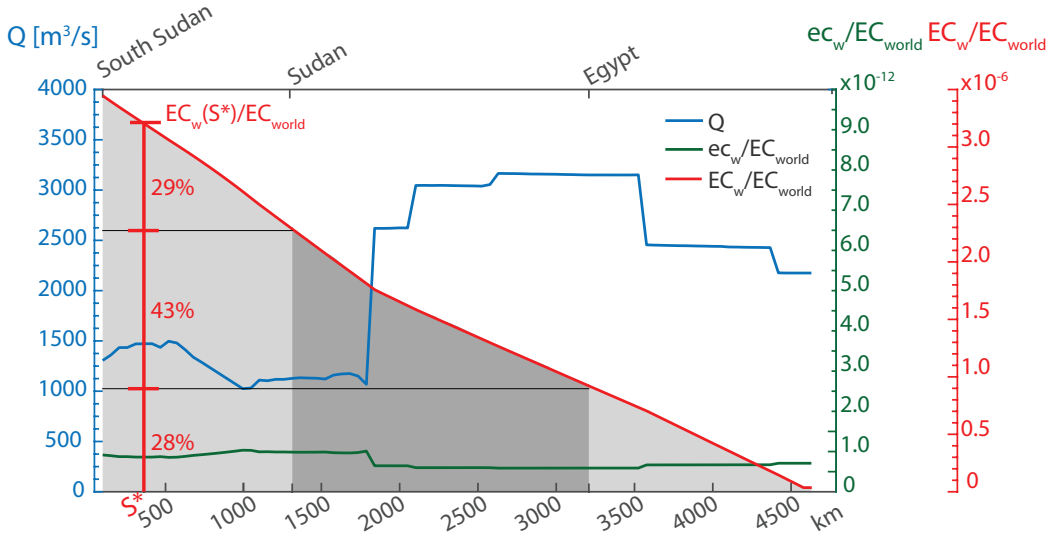

Fig. 2.8 The average annual Nile undisturbed river discharge, the environmental cost per unit length (ec_w) at the closing section of each cell of the Nile′s course and the overall environmental cost (EC_w) in each cell of the Nile′s course. Both environmental costs are normalized by EC_{world} and estimated with $\alpha = 0.5$ and $W = 1\ \mathrm{m^3\,s^{-1}}$. The environmental cost of a water withdrawal that occurs in a generic river section S^* (i.e., $EC_w(S^*)/EC_{world}$) can be divided among the downstream countries affected. In the example, $EC_w(S^*)/EC_{world}$ is divided between: South Sudan (29%), Sudan (43%), and Egypt (28%). The cells span 30 x 30 arc min. Along the abscissa the distance from the Nile section at the border between Uganda and South Sudan is reported. In the top of the figure the countries crossed by the river are shown. In the range [800,1000] km, the WaterGap river discharge exhibits a quite irrealistic peak. Likely, it is due to the complex local hydrography (i.e., wide wetlands) that is very difficult to model. For this reason, the peak has been considered spurious and neglected.

Table 2.1 The average percentage subdivision of the environmental cost of a water withdrawal EC_w on the Nile river course shown in Fig.2.8 among the impacted countries. The first column reports the location of the potential water withdrawal, while the corresponding row indicates the percentage subdivision of EC_w among the downstream countries. On the diagonal, the percentage of EC_w that has consequences within the country where the water withdrawal occurs is shown.

Location	**Percentage of impacted countries**		
water withdrawal	South Sudan	Sudan	Egypt
South Sudan	**23**	46	31
Sudan		**42**	58
Egypt			**100**

Assessing the surface water value of each country through the index proposed in this work implies taking into account the transboundary flows and, thus, the interdependency among countries: e.g., withdrawing 1 $m^3\,s^{-1}$ of water in Sudan from the Nile will impact the Nile′s course in Egypt too; as a consequence, the surface water value of that amount of water cannot be assessed considering exclusively the surface water resources of Sudan. Fig.2.8 describes the Nile river′s trends of the undisturbed discharge and of the two environmental cost measures down to the river mouth. The plot highlights the importance to take into account the downstream consequences of a water withdrawal. For example, even if the environmental costs per unit length after the 2000th kilometer are approximately constant, the values of EC_w are very different depending on the downstream river course impacted.

In Fig.2.8 an example is also proposed of a hypothetical withdrawal that occurs in a Nile′s river section S^* within South Sudan. The resulting overall environmental cost is divided in three portions, in correspondence of the country borders, which are the shares of $EC_w(S^*)/EC_{world}$ that affect South Sudan ($0.29 \cdot EC_w(S^*)/EC_{world}$), Sudan ($0.43 \cdot EC_w(S^*)/EC_{world}$), and Egypt ($0.28 \cdot EC_w(S^*)/EC_{world}$). Overall, this procedure can be extended by considering all the area under the curve EC_w/EC_{world}, which is divided according to the country borders (dark grey and bight grey areas). Therefore, comparing the areas under the curve of EC_w/EC_{world}, one can estimate the average percentage subdivision of the environmental cost of a generic potential withdrawal that can occur anywhere in the considered country, along the Nile river. The case study of the Nile′s river network (see Table 2.1) underlines that the average

environmental cost of a reference amount of surface water withdrawn can be considerably higher if the overall freshwater network is considered.

2.2.4 Estimation and comparison of EC_w using different input data

In order to evaluate the robustness of the index to different river discharge patterns, the environmental cost of the reference water withdrawal, 1 $m^3\,s^{-1}$, has been also estimated using an alternative average annual undisturbed river discharge. This discharge has been obtained at a 30 by 30 arc minute spatial resolution using the flow direction grid and the runoff data of the UNH/GRDC Composite Runoff V1.0 database (Fekete et al., 2002). The Composite Runoff database provides the runoff generated at each cell combining observed river discharge information with a climate-driven water balance model and it is consistent with long-term mean annual observed discharges. The GRDC database provides three types of runoff data: (i) the Observed Runoff, which is uniformly distributed in the inter-station areas (the area identified between gauging stations) and is equal to the ratio of the mean annual observed inter-station discharge to the inter-station area; (ii) the simulated runoff, which is developed applying the Water Balance Model (WBM) of *Fekete et al.*(Fekete et al., 2002), and (iii) the Composite Runoff, which is obtained applying to the simulated runoff a correction coefficient, namely the ratio of the yearly Observed Runoff to the yearly simulated runoff in the inter-station areas. Generally, we have used the Composite Runoff; however, in the inter-basins having a negative Observed Runoff − they are the inter-basins where the discharge decreases from the upstream gauging station to the downstream gauging station − and/or a negative average simulated runoff, the correction coefficient has not been applied to the simulated runoff (Fekete et al., 2002). Therefore, in those regions the annual Observed Runoff has been used in order to obtain everywhere values consistent with the long-term mean annual observed discharges.
The average annual volume of surface water generated at each cell has been estimated multiplying the runoff of each grid cell, which is expressed in millimetres per year, by the cell area. The latter decreases from the equator to the poles. Then, the average annual undisturbed river discharge has been assessed by summing up the discharge generated in each grid cell draining toward the

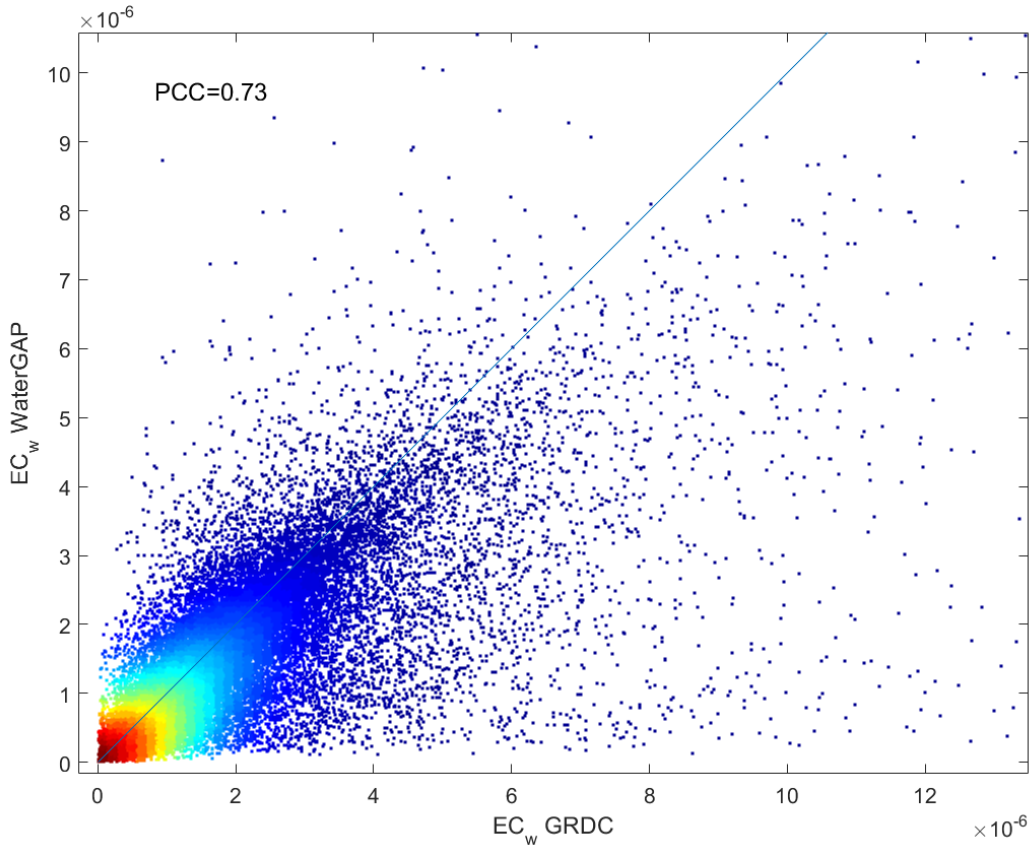

Fig. 2.9 Density scatter plot of the overall environmental cost values (EC_w) estimated using two different input database: the GRDC database (abscissa) and the WaterGAP 2.2c model (ordinate). Both values are normalized by EC_{world} and estimated with $\alpha = 0.5$ and $W = 1\ \mathrm{m^3\,s^{-1}}$. Also the Pearson Correlation Coefficient (PCC) of the two estimation is shown.

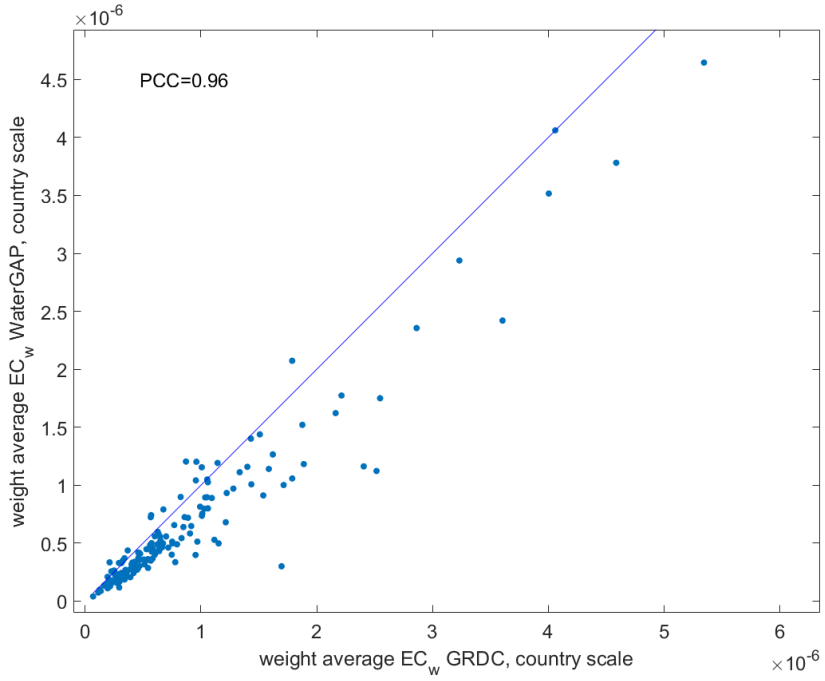

Fig. 2.10 Scatter plot of the country weighted average environmental cost values ($\overline{\overline{EC}}_{w,c}$) estimated using the GRDC database (abscissa) and the WaterGAP 2.2c model (ordinate). Both values are normalized by EC_{world} and estimated with $\alpha = 0.5$ and $W = 1\ \mathrm{m^3\,s^{-1}}$. Also the Pearson Correlation Coefficient (PCC) of the two estimation is shown.

considered one, using the global Simulated Topological Network (STN-30p) to define the flow directions (Vörösmarty et al., 2000a).
The environmental cost values obtained using the UNH/GRDC database are compared to the EC_w values derived from the WaterGAP 2.2c model as shown in Fig.2.9 and Fig.2.10. Only cells with $Q \geq 1$ m^3 s^{-1} in both databases were considered in the estimation of EC_w in order to consistently compare the two environmental cost values. Clearly, the index maintains its robustness employing a different distribution of Q, even though the EC_w estimated using the GRDC database tends to be slightly higher; this is partly due to the fact that the distribution of the Q derived by the GRDC leads to a proportionality constant, $k(\alpha)$, slightly greater than the $k(\alpha)$ evaluated with the discharges of WaterGAP (see Eq.(2.4)).

2.3 Discussion and concluding remark

The index proposed in this Thesis, EC_w, aims to attribute an environmental cost of a reference withdrawal of water accounting for the impact that it would cause on river ecosystems. In order to develop an easy-to-apply tool to interpret any geography of the withdrawals, the index is referred to an unitary potential withdrawal. The effort in this work was devoted to design an index able to interpret, with a feasible level of complexity, the interaction between water consumption and its effects on fluvial ecosystems (i.e., taking into account the downstream effect of a water withdrawal and considering the non-linear relation between discharge and environmental significance of a river ecosystem). In an attempt to design a parsimonious index we introduced only one parameter, α, and kept at a minimum the number of variables employed, namely the river discharge and the river network, which are the main factors that influence the fluvial ecosystem equilibrium. Due to the small amount of data needed, the index can be consistently applied at a global scale. Depending on the available data and on the target of the application, other withdrawal scenarios and river discharge patterns can be used; in fact, the proposed method is general. As an example of this, the index was tested applying it to a different distribution of river discharges demonstrating consistent results compared to those shown in this work (as described in Section 2.2.4).

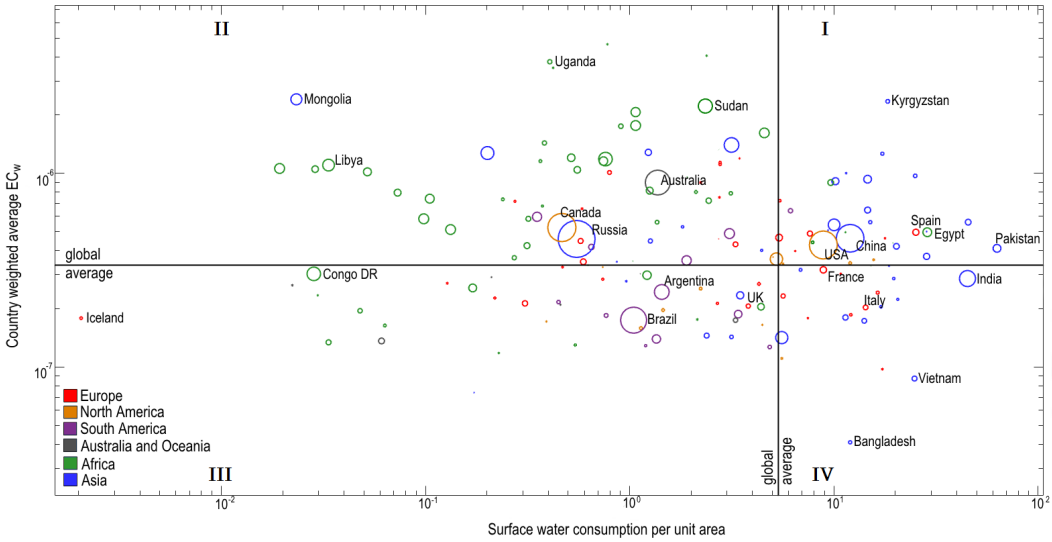

Fig. 2.11 Scatter plot of the yearly national surface water consumption per unit area (in mm yr^{-1}) and the average country impact index, $\overline{\overline{EC}}_{w,c}$, weighted in accordance to Q. The scatter plot is divided in 4 quadrants by two black lines. The horizontal line is the world weighted average of EC_w weighed in accordance to Q, and the vertical line is the world average surface water consumption per unit area. The circle size is proportional to the country area, while the color refers to the continent.

The index can provide a further interpretation to the volumetric measure of surface water consumption, by evaluating the environmental cost of a potential water withdrawal on fluvial ecosystems. An example of application is shown in Fig.2.11: the weighted average environmental cost at the country scale (shown in Fig.2.6b) is compared with the yearly national surface water consumption per unit area. The latter is assessed employing the annual blue water footprint (BWF) of national production (Mekonnen and Hoekstra, 2011) divided by the country area (Food and of the United Nations, 2017) (thus mm/year). Since the BWF considers both surface and groundwater consumption, this value is multiplied by the average country percentage of surface water withdrawal in order to consider only the surface water component of the BWF. This percentage is evaluated at the country scale as the ratio of the surface water withdrawal to the total freshwater withdrawal (Food and of the United Nations, 2017); a percentage equal to 64% is employed in countries where these data were not provided, which is the weighted world average percentage of surface water withdrawal (where the BWF of national production is the weight). The value 64% is consistent with the results given by *Döll et al.* (Döll et al., 2012) who

estimated that 35% of the water withdrawn worldwide is groundwater.
Fig.2.11 is divided into four quadrants by two black lines, which are: the global discharge-weighted average of the environmental cost, $\overline{\overline{EC}}_w$, and the global average of surface water consumption per unit area. Therefore, in the first quadrant one finds those countries that, despite the high environmental cost of withdrawing surface water (i.e., high $\overline{\overline{EC}}_{w,c}$ values), have an yearly surface water consumption per unit area higher than the global average (e.g., Kyrgyzstan, Egypt, Spain and Pakistan). Conversely, countries as Bangladesh and Vietnam, which fall in the fourth quadrant, have a high value of yearly surface water consumption per unit area, but their freshwater ecosystems are comparatively less impacted by water withdrawals than those in other countries. From a global point of view, a system that aims exclusively to minimize the impact on surface water resources, ideally, would require countries of the first quadrant to move toward the second one by reducing the volumes of surface water withdrawn. Those volumes could be compensated by moving the third quadrant countries toward the fourth quadrant, since these countries are characterized by low $\overline{\overline{EC}}_{w,c}$ and (currently) comparatively lower surface water consumption per unit area.
The application of the index highlights regions and countries more environmentally vulnerable to surface water exploitation. Since the index systematically assesses the environmental cost by accounting for the downstream propagation effect of a water withdrawal on the fluvial ecosystem, it aims to support decision-making in transboundary river basins as well, with the challenge to support water management strategies overcoming administrative borders. Moreover, as widely discussed in the next Chapter, the index is a novel tool to analyse the food trade network with an impact-oriented approach, evaluating the environmental cost of the surface water volumes consumed to produce a good by accounting for the freshwater ecosystems from which the volumes are removed.

Chapter 3

The globalization of riverine environmental resources through the food trade

The work described in this chapter has been partially derived from Soligno et al. (2018).

Food production is the largest form of societal water consumption (Falkenmark and Rockström, 2004; Wada and Bierkens, 2014) and agriculture's "thirst" is expected to further increase in the next years, due to the growth of the world population, the rising of living standards, and climate change (Foley et al., 2011; Vörösmarty et al., 2000b; Wada and Bierkens, 2014). This pressing water demand is causing remarkable environmental impacts (Dudgeon et al., 2006; Vörösmarty et al., 2010; Wada et al., 2013) that are growing to an unprecedented extent (Alcamo et al., 2007; Haddeland et al., 2014; Hanasaki et al., 2013), in particular on freshwater ecosystems (Assessment, 2005) that globally contribute about 60% of the total water used for irrigation (Döll et al., 2012).

In the last few decades, globalization has increased the geographical distance between food producers and consumers (D'odorico and Rulli, 2013; Fader et al., 2013). Today, about one quarter of the food produced for human consumption is currently traded internationally (D'Odorico et al., 2014). The concept of virtual water has played a key role in shedding light on the links between

the food consumption geography and the water resources (over)exploitated. However, a critique that has been made to the virtual water trade assessments is that they typically aggregate and compare water volumes without considering the place where water has been withdrawn, i.e. without differentiating among water-abundant and water scarce regions (Berger and Finkbeiner, 2013; Lenzen et al., 2013b; Ridoutt and Pfister, 2009; Yano et al., 2016). Some recent exceptions are the works by Lenzen et al. (2013b) an Yano et al. (2016). In order to focus on scarce-water trade flows, Lenzen et al. (2013b) weighted the virtual water network adopting a country-specific water scarcity indicator. Recently, Yano et al. (2016) proposed to scale the virtual water volumes by a factor expressing local water unavailability, which is calculated in each cell as the land area required to collect a reference amount of water. In spite of these studies investigate the virtual water network considering the availability (or unavailability) of the exploited resource, however they neglect: (i) the relevance of the impacted environment (e.g., its biodiversity richness, bio-geomorphologic characteristics, and habitat health) and (ii) the downstream propagation effect of an hydrological stressor.

Our work aims to overcome these limitations, focusing on the fluvial ecosystems. These are among the most precious, important and sensitive environments on Earth (Allan and Castillo, 2007); on the other hand, rivers are also the major water sources for irrigation and many of them show high stress levels due to local food consumption and trade (Wang and Zimmerman, 2016). For these reasons, it is urgent to disclose the environmental significance of the water extracted from river ecosystems. To this aim, we quantify the "environmental value of the riverine water" (EVRW) embedded in food product. Building on the concept of Environmental Cost (EC) index introduced in the previous Chapter, we quantify the impact of food consumption on local and foreign water resources taking into account both the local environmental relevance of the fluvial area where water is withdrawn (biodiversity richness, riparian vegetation, sediment transport, etc.) and the downstream effects of water withdrawals. By this approach, we obtain the global picture of the EVRW involved in the food production and the corresponding network of the traded riverine resources. This allows us to unveil the main implications of the globalization of water resources on the health of surface water systems and to investigate the EVRW network efficiency over the period 1986-2013.

3.1 Method

3.1.1 Assessment of the surface virtual water trade network

From the FAOSTAT database, we collected twenty-eight years (1986 - 2013) of food production and bilateral trade data for 270 food and agricultural commodities, including crops, crop-derived goods, and animal products (the detailed list is reported in Tab.B.1 in Appendix B). For each year, trade data were stored in (non-symmetrical) product-specific matrices, whose (i, j) element corresponds to the export of the product from country i to country j. The matrix size equals the number of countries and changes from year to year, according to political-administrative arrangements (e.g., the collapse of the USSR in 1990-91). In the FAOSTAT database, the trade from i to j is sometimes reported by country i and country j with discordant values; in these cases, we adopted a reconciliation method that takes into account the degree of reliability of each reporting country (see Distefano et al. (2018a)). Further details about the matrix construction and country arrangements are given by Carr et al. (2013) and Tamea et al. (2014).

We adopted the approach validated by Tuninetti et al. (2017a) in order to take into account the temporal variations of the water footprint per crop unit due to yield trends. Accordingly, the yearly country-specific virtual water content (VWC) for each primary crop was assessed as

$$VWC_{c,t} = \frac{\overline{VWC}_{c,1996-2005} \cdot \overline{Y}_{c,1996-2005}}{Y_{c,t}} \quad \left[\frac{m^3}{ton}\right] \tag{3.1}$$

where subscripts c and t refer to the country and year considered, respectively, $\overline{VWC}_{c,1996-2005}$ is the average virtual water content (over the period 1996 - 2005) given by Mekonnen and Hoekstra (2010b), $\overline{Y}_{c,1996-2005}$ is the corresponding average yield, and $Y_{c,t}$ is the country yield in the year t. Yield time-series at the country scale for each primary crop are provided by the FAOSTAT database.

The evaluation of the virtual water content of crop-derived products required a number of steps. Firstly, we collected (i) the VWC of the primary input crops adjusted with the product fraction (i.e., ton of crop-derived product obtained

per ton of primary input crop) and (ii) the value fraction (i.e., the market value of the crop-derived product divided by the aggregated market value of all crop products resulting from one primary input crop). Both fractions are provided by Mekonnen and Hoekstra (2010b). Secondly, a crop-derived product is often obtained from both local and imported primary crops that have different VWCs, due to different yields and climatic conditions. To take these differences into account, we assessed the VWC of the primary input crop (at the national and yearly scale) as the weighted average of the VWC related to the domestic production and the VWCs of the imports, where the weights are the tons of the domestic production (minus exports) and the imported tons. Thirdly, some crop-derived products are obtained through successive process steps; in these cases, starting from the primary crops we estimated the VWC of the increasingly complex products at each step, considering the weighted average between domestic production and imports for each intermediate product. An example of the estimation of the VWC for a crop-derived product is reported in the next section.

Differently from the primary and crop-derived commodities - where the temporal variability of the virtual water content was considered - for animal products we used the time-averaged VWC given by Mekonnen and Hoekstra (2010a). This choice is due to a lack of reliable data about the country-specific composition of feed for each animal type. Moreover, fish products were not included in our analysis as there are no country-specific data about their blue VWC.

Once food trade and production data of each commodity were converted into virtual water values, the blue virtual water component was estimated using the country-specific ratio (herein called Rb) of the average blue VWC to the overall VWC, both given by Mekonnen and Hoekstra (2010b) for each food commodity. The blue water component includes both groundwater and surface water resources. To estimate the surface water contribution, we used the "Global Map of Irrigation Areas" (version 5.0) dataset (Siebert et al., 2013); considering the percentage of the area equipped for irrigation served by surface water resources (herein called Rs).

Since the input products used to produce a crop-derived good usually have different geographical origins, the amount of surface blue water of each crop-

derived product was assessed (at the national and yearly scale) as the weighted average of the surface blue water content related to domestic production and the surface blue water content of the imported input products, using the blue water volumes as the weights.

Once all the food commodities were converted into surface virtual water values, they were added together to obtain (i) the total yearly surface virtual water transferred between pairs of trading partners and (ii) the total yearly amount of surface water used within each country to produce food. The trade pattern was reconstructed considering all the food commodities, while the total amount of surface water used for food production was estimated without considering secondary products (e.g., bread) in order to avoid double accounting issues. For further details about this topic, see D'Odorico et al. (2014).

3.1.2 Assessment of the network of the riverine environmental value related to food products

Surface water resources exhibit very heterogeneous characteristics and, thus, a same volume of withdrawn water does not have the same environmental value in different places worldwide. Therefore, in order to quantify the share of responsibility that each country (or individual) has on the overall degradation of world rivers through the consumption, production and trade of food commodities, we multiply the amount of surface water used to produce food goods by the Environmental Cost (EC) index proposed in Chapter 2 and in Soligno et al. (2017). Accordingly, in a given river section the environmental cost per unit length (ec_w) of a unitary water withdrawal W is defined to be proportional to the river discharge reduction caused by the withdrawal. Namely, $ec_w = ec_{max} \cdot W/Q$, where ec_{max} is the maximum environmental cost per unit length, which occurs when the entire river discharge (Q) is depleted. The value of ec_{max} is related to the relevance of the river environment considered and is evaluated by considering fluvial site-specific characteristics (e.g., width of the riparian belt, biodiversity richness, transport of sediments and chemicals) related through power laws to the river discharge. Since the subtraction of W alters the discharge from the section where water is withdrawn (S_W) down to the river mouth (S_M), the overall environmental cost, EC_w, is evaluated as

the sum of the environmental cost per unit length generated downstream by the withdrawal. Accordingly, $EC_w = \int_{S_W}^{S_M} ec_w(s)\mathrm{d}s$, where s is the curvilinear abscissa along the river.

As the present study aims to describe the comprehensive impact on world rivers and not the impact related to a specific fluvial characteristic (i.e., a specific value of α), we employed a formulation of EC_w able to embed different features of the river environment at the same time. Therefore, different α values in the interval [0 1] are considered, and weighted through a triangular kernel. A sensitivity analysis (see Section 3.1.3) shows that the main results of this work do not change by using different peak positions in the triangular kernel. For this reason, reported results refer to a symmetric kernel with peak at $\alpha = 0.5$. The environmental cost of a water withdrawal is thus

$$EC_w = \int_{S_W}^{S_M} \int_0^1 Ker(\alpha) \cdot k(\alpha) \cdot \frac{W}{Q(s)^{1-\alpha}} \mathrm{d}\alpha \mathrm{d}s, \tag{3.2}$$

where $Ker(\alpha) = 4\alpha$ when $\alpha \leq 0.5$, and $Ker(\alpha) = 4 - 4\alpha$ when $\alpha > 0.5$.

We computed the EC_w value related to a unitary surface water withdrawal with a 0.5° spatial resolution, adopting the global drainage direction map DDM30 (Döll and Lehner, 2002) and the annual average river discharges obtained from the pristine scenario of the WaterGAP 2.2c model (Döll et al., 2014; Müller Schmied, 2017; Müller Schmied et al., 2014, 2016). The pristine river discharges were averaged over the period 1901-2013. The EC_w computation was obtained for each fluvial section of the world river network and is shown in Fig.A.6. In order to evaluate the environmental value enclosed in the surface virtual water network (see previous section), we adopted a country-specific $EC_{w,c}$ value. No global data are available about the specific river sections where water is withdrawn for irrigation; however, it is reasonable to assume that water is generally withdrawn in river sections where it is more abundant. Therefore, we assessed the country-specific $EC_{w,c}$ as the weighted average of the EC_w of each cell within the considered country using the river discharge of each cell as the weight (see Eq.(2.14)). Finally, surface water trade links were multiplied by the $EC_{w,c}$ value of the exporting countries, while the volumes of surface water related to national food production were multiplied by the $EC_{w,c}$ of the corresponding country. In this way, we obtained the dataset (at

the country and yearly scale) of the productions, exports and imports of the environmental value of riverine waters.

Conveyance and distribution losses in the irrigation system increase the water withdrawal with respect to the surface water volumes consumed by each agricultural item (i.e., surface water loss to the atmosphere by evapotranspiration); since we considered the latter volumes, we likely underestimated the real withdrawal from the river system.

3.1.3 A sensitivity analysis of the average environmental cost of a water withdrawal at the country scale

In the previous, we described the approach followed in this work to quantify the environmental value of the riverine water involved in the production and trade of food commodities. To this aim, we adopted the Environmental Cost (EC) index and used a formulation of EC_w able to concurrently consider different river characteristics (i.e., we did not focus on a specific value of α). Therefore, all the values of α within the range [0 1] were considered and weighted through a triangular kernel with the lower vertexes in $\alpha = 0$ and $\alpha = 1$, and the peak in $\alpha = 0.5$ (see Eq.3.2). Finally, the country-specific $EC_{w,c}$ was assessed as the weighted average of the EC_w of each cell within the considered country, using the river discharge in the cell as the weight.

Fig.3.1 compares (at the country scale) the $EC_{w,c}$ values adopted in this work (i.e., assessed with the peak of the triangular kernel in $\alpha = 0.5$) with those obtained considering different positions of the peak (i.e., in $\alpha = 0, 0.25, 0.75,$ and 1; the case of a uniform kernel is also considered). The scatter plots in Fig.3.1 show that $EC_{w,c}$ values are quite insensitive to the exact shape of the kernel.

Notice that when α tends to 1 the natural river discharge has a limited (or null) effect on ec_w (see Eq.2.5). As a consequence, when high values of α are adopted, the length of the downstream river network turns out to be the main factor that influences the environmental cost of a surface water withdrawal. Hence, for countries such as Brazil and Canada – which are characterized by long river networks – the more the peak of the distribution approaches

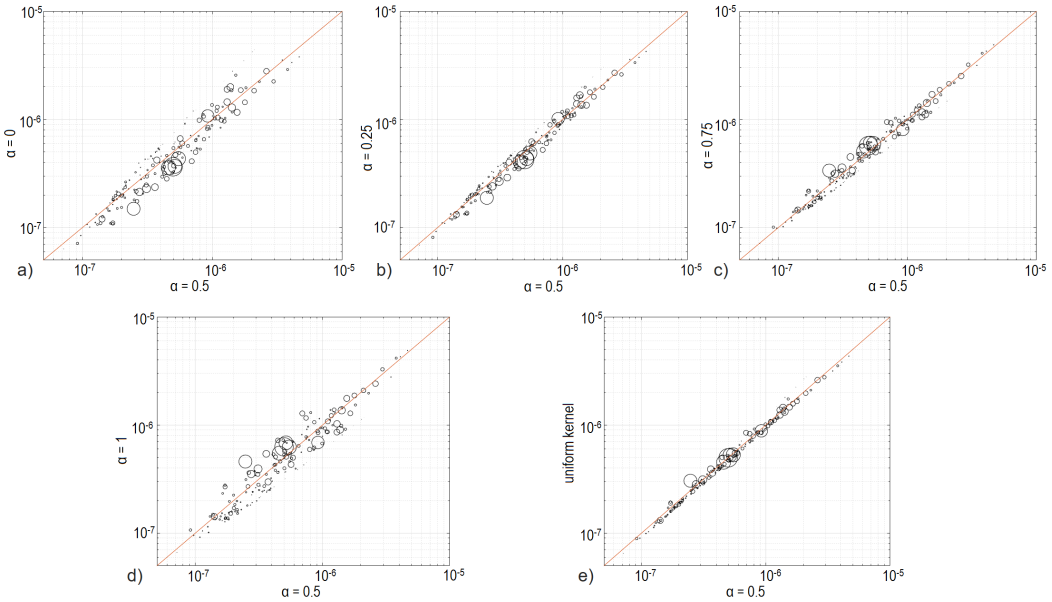

Fig. 3.1 Influence of the peak position of the triangular kernel on the evaluation of the country-specific weighted average environmental cost, $EC_{w,c}$. The case with the peak in $\alpha = 0.5$ (adopted in the main text) is compared with kernels with peak in $\alpha = 0$ (a), $\alpha = 0.25$ (b), $\alpha = 0.75$ (c), and $\alpha = 1$ (d). Panel (e) compares the weighted average environmental costs estimated using a triangular kernel (peak in $\alpha = 0.5$) and a uniform kernel within the interval [0 1]. Circle sizes are proportional to the country area; axis are in log-scale.

$\alpha = 1$, the more the country-specific $EC_{w,c}$ increases. The opposite occurs for countries such as South Africa and Spain.

3.1.4 Assessment of the EVRW efficiency of the food trade network

We assessed the EVRW efficiency by comparing the business as usual trade network (see Fig.3.2) with a scenario in which countries are self-reliant. This latter scenario assumes that all food is produced and consumed within the same country instead of being imported from foreign regions. The difference between these two scenarios provides a measure of the efficiency (or inefficiency) of each trade flow. The global EVRW efficiency of the food trade network is obtained by summing up the contributions of all the trade links.

Consider the export of a basket of food products $P_{i,j}$ from country i to country j. The difference between the EVRW for the production of the products in the importer country j (i.e., the self-reliant scenario) and in the exporter country i (i.e., the business as usual scenario) defines the EVRW efficiency of the trade flow, $\Delta EVRW_{i,j}$. It can be assessed as

$$\begin{aligned}\Delta EVRW_{i,j} = \sum\nolimits_{p \in P_{i,j}} (F^p_{i,j} \cdot VWC^p_j \cdot Rb^p_j \cdot Rs_j \cdot EC_{w,j} - \\ - F^p_{i,j} \cdot VWC^p_i \cdot Rb^p_i \cdot Rs_i \cdot EC_{w,i})\end{aligned} \tag{3.3}$$

where the superscript p refers to the considered product, which belongs to the product basket $P_{i,j}$; $F^p_{i,j}$ are the tons of the product p that currently flow from i to j; $VWC^p \cdot Rb^p$ denotes the blue virtual water content of product p; and Rs is the ratio of surface water to the total blue water consumed within the considered country. Finally, EC_w stands for the environmental value per unit of surface water used. When $\Delta EVRW_{i,j} > 0$, the trade relationship reduces the environmental value of the riverine water embedded in food products (i.e., the considered trade flow leads to save EVRW).

Eq.(3.3) enables to distinguish the different contributions to $\Delta EVRW_{i,j}$. For each product, VWC^p_j and VWC^p_i influence the EVRW efficiency through the difference in the virtual water productivity between i and j. This contribution

reduces the efficiency of the trade connection when the importer country requires less water per ton of p than the exporter (i.e., when $VWC_j^p < VWC_i^p$). The blue water share depends on the water supply system adopted to produce p in the considered country; it can range from fully irrigated ($Rb = 1$) to fully rain-fed ($Rb = 0$). Therefore, the efficiency value improves when the exporter (importer) country reduces (increases) the irrigation water use. Rs_j and Rs_i focus on the different country-specific exploitation rate of surface water in agriculture. Finally, the EC_w typical of each country depends on the sensitivity of domestic rivers to water withdrawals and it is the only term in Eq.(3.3) unrelated to agricultural practices.

Since there are imported-goods that cannot be offset by domestic production (e.g., tropical fruits imported by Northern European countries), in the generic link from i to j the efficiency was calculated considering only the imported-goods that could be conceivably produced in j. To this end, for each trade flow we included only the products with known $\overline{VWC}^p_{1996-2005}$ in both countries (for the crop-derived commodities the $\overline{VWC}_{1996-2005}$ value of their input products was considered). Therefore, in Eq.(3.3) $P_{i,j}$ is a subset of the products actually exported from i to j.

In order to identify the main differences between exporters and importers that influence the overall efficiency value, the EVRW efficiency was assessed in four steps by considering an increasing number of disparities between i and j. Firstly, only the dissimilarities in terms of EC_w were considered, while the other differences among importers and exporters were neglected (see green line in Fig.3.8); in this case, the business as usual scenario was compared to a scenario where country j consumes the same amount of surface water of country i to produce any commodity, thus

$$\Delta EVRW_{i,j}^{step_1} = \sum\nolimits_{p \in P_{i,j}} (F_{i,j}^p \cdot VWC_i^p \cdot Rb_i^p \cdot Rs_i) \cdot (EC_{w,j} - EC_{w,i}). \quad (3.4)$$

Thereafter, also the dissimilarities on the VWCs typical of each pair of countries were taken into account, while the impact on the EVRW efficiency of both Rb and Rs were still neglected, thus $Rb_j^p = Rb_i^p$ and $Rs_j = Rs_i$ (see blue line in Fig.3.8). The third step was performed including also the effect of the different product-specific blue water shares of importers and exporters (see purple line in Fig.3.8). Ultimately, the EVRW efficiency was estimated as in Eq.(3.3),

where $EC_{w,j} \neq EC_{w,i}$, $VWC_j^p \neq VWC_i^p$, $Rb_j^p \neq Rb_i^p$, $Rs_j \neq Rs_i$ (see red line in Fig.3.8).

Finally, our efficiency measure focuses exclusively on the impact of food production on riverine systems and it does not take into account any social, economic or resource limitations (e.g., the availability of agricultural land).

3.2 Results and Discussions

3.2.1 Food trade activates a global network of riverine value

In each nation, the riverine resources embedded in the food consumed has two components: one concerns food goods produced and consumed within the country (i.e., exploiting domestic rivers), the other concerns imported food commodities (i.e., exploiting foreign fluvial systems). We will call these the "local" and the "non-local", component respectively. Our results show that, globally, the EVRW involved in food consumption increased by 40% during the considered period, while the non-local EVRW embodied in trade has more than doubled since 1986. Therefore, threats to fluvial ecosystems are increasingly driven by consumer demand across the globe.

The global network of riverine resources (see Fig.3.2) highlights the unexpected links by which final food consumers may impact rivers very far away from consumption places. A snapshot of the multiple routes in the network of Fig.3.2 is shown in Fig.3.3, where the non-local EVRW consumed by Italy and the environmental value of Thailand's surface resources "eaten" by consumers abroad are depicted. Italy imports many food goods and is the eighth largest world EVRW importer; it follows that Italian consumers significantly affect several out-of-Italy river systems. *Vice versa*, a lot of the environmental value of the Thai riverine waters used for irrigation is exported through food trade, making Thailand the sixth largest world exporter of riverine resources.

Overall, the EVRW trade network in Fig.3.2 can be interpreted as a network of responsibility of countries for the consumption of riverine resources beyond their national borders. In the case shown in Fig.3.3a Italy is responsible for

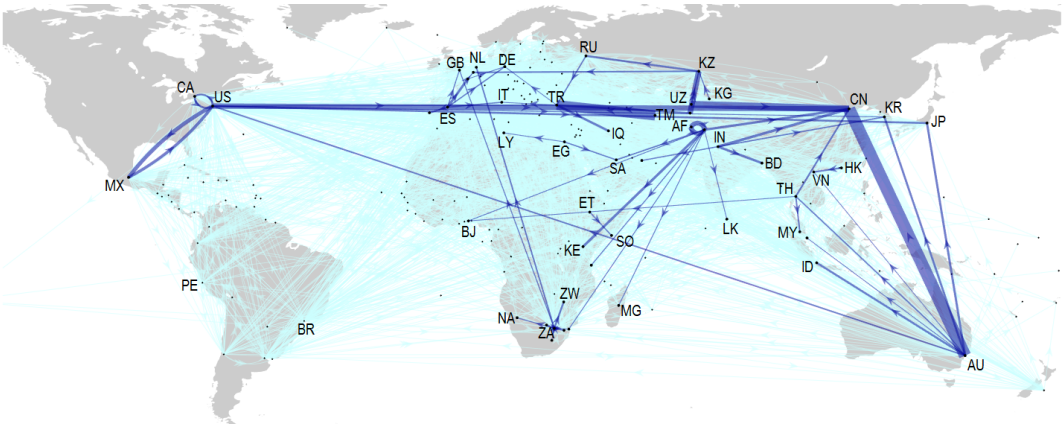

Fig. 3.2 the EVRW world network in 2013. Blue and light blue links refer to EVRW flows higher than 0.25% and 0.001% of the total EVRW internationally traded in 2013, respectively. The line widths are proportional to the embedded EVRW. The network nodes correspond to the barycentre of the population distribution within each country (available at http://www.cepii.fr). Country names are in ISO 3166-1.

2.2% of the overall riverine resources embedded in the world food trade and the largest share of its externalized pressure on surface waters concerns Spanish and Turkish rivers. Instead, China and Malaysia are among the main foreign countries that drain environmental value from Thai fluvial systems. Overall, China is the biggest importer of EVRW in the world with a share of 12% of the total EVRW traded internationally; in particular, the trade link from Australia to China is the highest recorded EVRW flow, involving a share around 4%.

The key point of looking at the environmental value of surface waters is that a same volume of surface water does not have the same environmental value in different countries. It follows that the amount of riverine resources imported by a country depends on the specific characteristics of the river environments of its trading partners. For example, the flow from Turkey to Italy conveys about $3 \cdot 10^5$ m^3 of surface virtual water (mostly embedded in shelled hazelnuts), which corresponds to an EVRW share of 0.27%; a smaller EVRW is imported from France (i.e., 0.24%) despite the surface virtual water volume ($8 \cdot 10^5$ m^3) being almost three times larger. This disparity is due to the greater environmental fragility of the Turkish river environments compared to the French ones.

Imports allow a region to satisfy its food needs without exploiting local resources and, thus, externalizing the impact of the national food consumption to foreign river systems. However, when food is imported by countries with

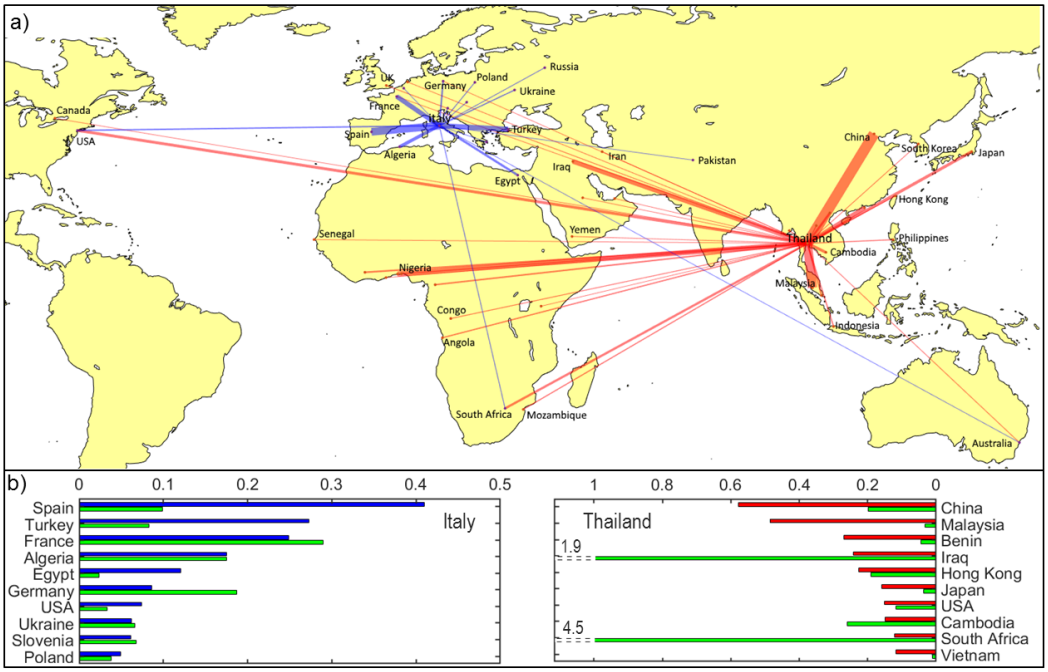

Fig. 3.3 (a) Snapshot of the environmental value of the riverine water network in 2013, where the major import flows to Italy (in blue) and the major export flows from Thailand (in red) are shown. The line width is proportional to the EVRW flow. (b) The top 10 major countries from which Italy imports EVRW (blue bars) and the top 10 countries to which Thailand exports EVRW (red bars). The share of the global traded EVRW is reported. Green bars indicate the EVRW under a self-reliant scenario (i.e., if the same food had been produced locally, rather than imported). When the green bars exceed the others, the business as usual flow trade provides an advantage for the environmental status of global rivers.

a lower surface water productivity (i.e., m^3 of surface water used per unit of product) and a higher environmental value per unit of surface water than the trading partner, then there is a trade-induced global saving of EVRW. In order to highlight the occurrence of EVRW savings, in Fig.3.3b we compare the business as usual trade situation with a scenario in which production and consumption spatially coincide, namely where all food is produced locally. The difference between these two scenarios provides a measure of the efficiency of the considered trade relationship (this approach was detailed in Section 3.1.4).

Regarding Italy, Fig.3.3b shows that significant EVRW inefficiencies occur in the import flows from Spain, Turkey, and Egypt; these inefficiencies depends on both the different sensitivity of rivers to withdrawals and the surface water productivity typical of the exporters. For example, in the case of Egypt, if the same imported-food had been produced in Italy, the impact on riverine systems would have been 5 times lower. This gap is due to a number of factors, where the main ones are (i) the greater environmental value per unit of Egyptian riverine water and (ii) the considerable share of blue water in Egypt. Also Thailand exports exhibit highly negative EVRW unbalances; e.g., flows towards China, Malaysia, Japan, and Vietnam. Conversely, although often the geography of food production and trade neglects the health of riverine ecosystem, there is a number of trade relationships that induce significant savings of EVRW. Two striking cases corresponds to the internationally-traded products that flow from Thailand to Iraq and to South Africa, which enable to cut down the EVRW by 8 and 37 times, respectively.

3.2.2 Importers, exporters, and consumers of riverine value

Our analyses reveal that there is a great spatial heterogeneity in EVRW dynamics (e.g., see Fig.3.4a). For instance, food consumption in Australia, India and South Africa has little impact on foreign river systems; conversely, these countries are among the largest exporters of EVRW in the world and, therefore, there are foreign economies that have strong responsibilities on the river ecosystem health of these regions. “Unpacking" each red bar of Fig.3.4a, the major trade links that drive the degradation of Australian rivers point

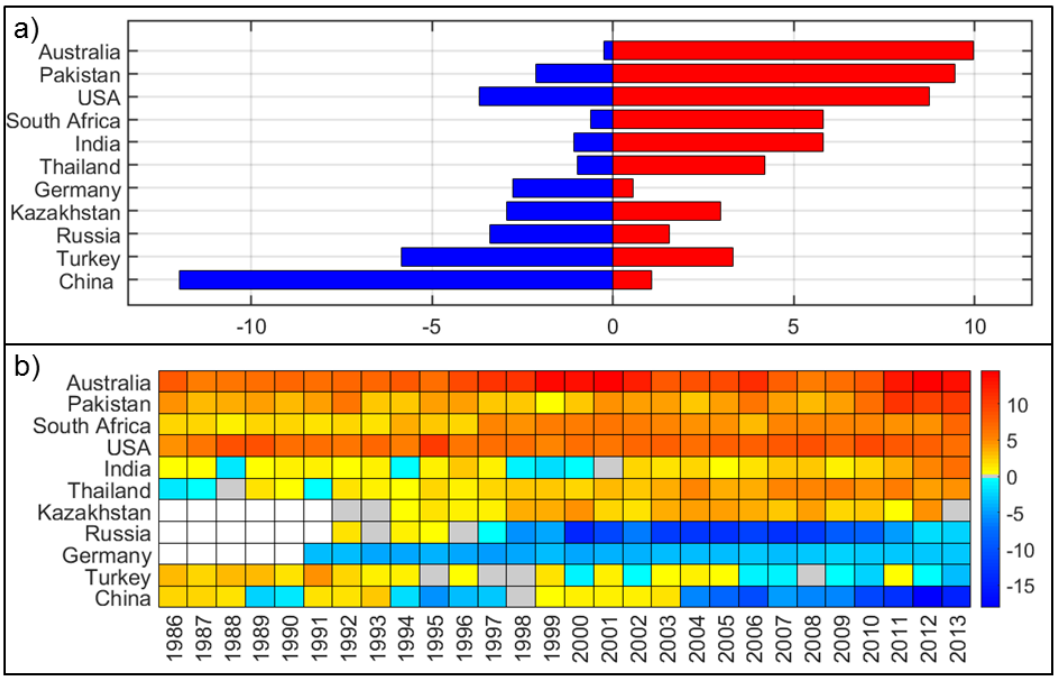

Fig. 3.4 (a) Exports (in red) and imports (in blue) of EVRW for the six world major exporters and the six major importers in 2013 (the USA are both). The abscissa reports the shares of the overall EVRW exchanged during year 2013. (b) Global share of net export flows of EVRW embedded in food products for the same countries from 1986 to 2013. The shares are calculated based on the average EVRW yearly traded in the period 1986-2013.

towards China, Japan, Indonesia, and South Korea, while South Africa's major EVRW exportations go towards Zimbabwe, Botswana, Swaziland, Netherlands, and Namibia. *Vice versa*, China and Turkey are the most important importers of riverine resources, but also Germany emerges as a strong net importer.

The picture shown in Fig.3.4a refers to year 2013 and it is a sample of the temporal dynamics exhibited by the EVRW flow network. Fig.3.4b discloses the temporal pattern of net exporters and importers during the period 1986-2013. Some countries maintain their characteristic of net exporter or net importer throughout the entire period (e.g., Australia, USA, and Germany), while other countries show substantial overturns, both pulsing (e.g., India and Turkey) or showing some persistence (China, at least in the last decades). These shifts are due to changes in both the basket of products imported/exported from each country and in the structure (topology and flows) of the trade partners. In the case of the USSR-Russia, the shift is due to the dissolution of the Soviet Union and the consequent EVRW import by Russia from neighbouring (ex-Soviet) countries characterized by fragile surface water systems (e.g., Kazakhstan and Uzbekistan).

The global EVRW network exhibits remarkable changes over time. In 28 years, the number of yearly active links in the network almost doubled, implying that year after year global food consumption relies on an increasingly interconnected network. A comprehensive description of the major temporal developments of the EVRW network is shown in Fig.3.5, where trade flows are aggregated into nine world macro-regions and flows greater than 1% of the annual EVRW globally traded are displayed. Interestingly, from the year 2004 the number of (macro) links have decreased despite it has grown the total riverine value traded among the macro-regions. Therefore, the backbone of the network has strengthened by relying on a smaller number of (macro) links.

During the 1986-2013 period, East Asia and Europe had have the highest influence on foreign rivers. Over the past three decades, European countries have maintained their strong dependence on the rivers of the Middle East and Africa and, meanwhile, they increased their impact in Central Asia (especially in Kazakhstan and Turkey). The latter region has significantly increased the trade of riverine resources both with neighbouring areas (in particular with Europe and East Asia) and within the region itself. Also the EVRW

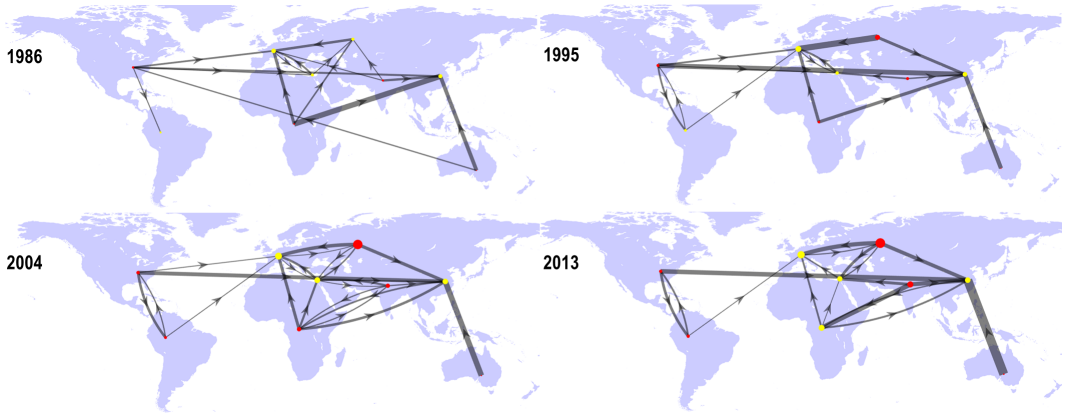

Fig. 3.5 Four snapshots of the network backbone of the environmental value of the riverine water in 1986, 1995, 2004, and 2013. Nine world's macro-region are considered. The link width is proportional to the EVRW flow between macro-regions. The node are proportional to the EVRW flow within each macro-region. Yellow and red nodes indicate net importer and exporter of riverine value, respectively. Fig.B.1 in the Appendix shows the geographical division into the nine macro-region; i.e., North America, Latin America and the Caribbean, Europe, Africa, North Africa and the Middle East, East Europe and Central Asia, South Asia, East Asia, and Oceania. The shares are calculated based on the average EVRW yearly traded in the period 1986-2013 and only the links higher than 1% are reported in the figure. About Africa, notice that the FAOSTAT database suffers of a lack of trade data related to Sudan and South Sudan in 2012-13.

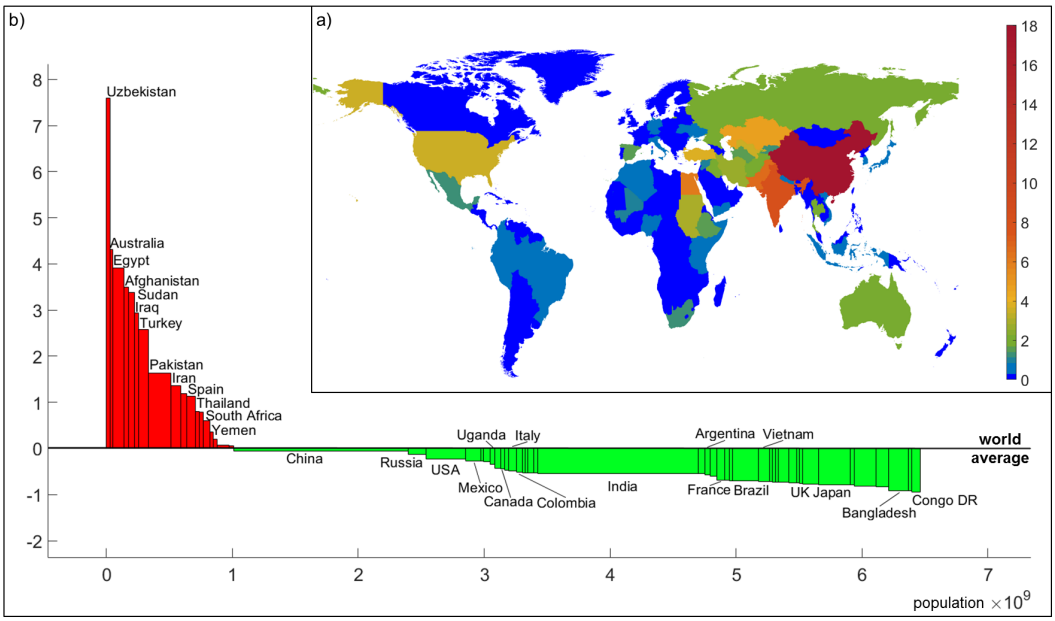

Fig. 3.6 (a) The shares of responsibility of each country on the overall degradation of world river systems through the consumption of food goods in 2013. (b) Per capita impact related to the overall EVRW embedded in food consumption in 2013. The bar height indicates the normalized difference between the country's share and the world average. The normalization factor is again the global average. The width of each bar is equal to the total population of the considered country. Only countries with more than 20 million inhabitants are represented in the bar plot.

trading relationships among European countries have grown considerably since 1986 (threefold increased), despite the number of active trading links slightly decreased. Meanwhile, since 1986 South Asia has incessantly increased its exports of EVRW (e.g., towards India and Pakistan approximately by 8 and 3 times, respectively), becoming the largest world's net exporter. Although the EVRW network is highly dynamic and over time several new links appear (e.g., from the South Asian to the African countries) and other links disappear, overall the network has a global tendency to intensify trade relations between geographically close regions, e.g., see in Fig.3.5 the links between East Asia and Oceania or between North and South America. This confirms that the physical distance between trading partners is one of the major drivers of virtual water flows Tamea et al. (2014).

The fluvial environmental value that we "eat" typically includes both a local component – linked to the domestic food production – and a non-local

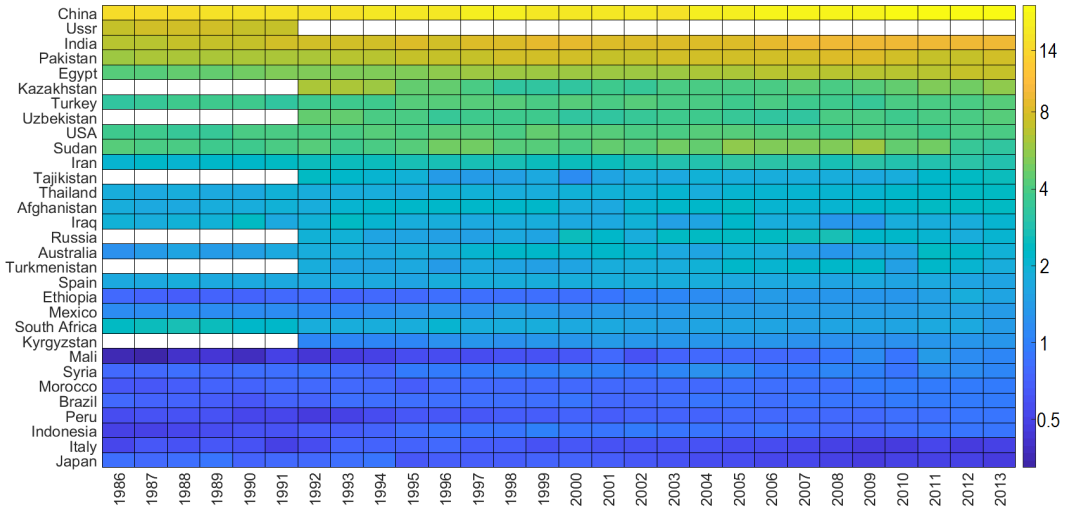

Fig. 3.7 The major consumers of EVRW embedded in food products from 1986 to 2013. The shares in the colorbar are related to the average annual EVRW globally consumed during the considered period; the colorbar is in log-scale.

component, due to the food import. Therefore, to assess the average EVRW related to the overall food consumption of a country (or of an average citizen), one has to consider the balance equation: consumption = (import + production - export), where stock variations are neglected for the sake of simplicity. Fig.3.6a shows the shares of responsibility of each country on the overall degradation of world river systems through the consumption of food goods in 2013, while the time-series of the consumption values is reported in Fig.3.7. The sum of all the EVRW shares equals 100%, which corresponds to the global impact of the world population on the health of surface waters worldwide. The picture is quite heterogeneous and testifies that country shares depend on multiple factors, including the typology of the exploited water sources (e.g., groundwater or surface water resources), the vulnerability of the involved river systems, the partition between local and imported food, and the import pattern. For example, countries like Saudi Arabia and Denmark use almost exclusively blue water from groundwater sources; this explains their low shares of consumption of riverine value. Many tropical countries have low EVRW share as they largely use rain-water for agriculture; a noteworthy exception is Indonesia, where food production mostly uses rainfall water (around 96%), but the share is quite high compared to other tropical countries since Indonesia imports large flows of EVRW from Australia, India, Pakistan, USA and South Africa.

Evidently, country population is one of the main drivers of EVRW consumption. Over time, the rising living standard and the the growth of the world population have led to increase the consumption of water-intensive food goods over time (D'Odorico et al., 2018; Tilman et al., 2011); this fact has clearly influenced the amount of riverine systems impacted by the food sector, as can be seen in Fig.3.7. In order to compare the citizens of different countries, Fig.3.6b shows the per-capita impact. The world average value of the share is assumed as the reference value and citizens from countries in red (or in green) are responsible for a larger (or smaller) pressure on the global rivers. For example, Uzbekistan citizens show a high consumption per capita due (i) to the high vulnerability of the local surface water systems, which makes the local production of food and agricultural goods environmentally "expensive", and (ii) to the significant import flows from Kazakhstan, which has analogous issues. Notice that also large river systems can become environmentally vulnerable when they are overexploited, as in the case of the Indus river. This is one of the largest water resources in the world, but its use to feed wide irrigation systems explains why Pakistan ranks among the largest consumers of riverine resources worldwide (see Fig.3.6b). Finally, it is worth to notice that, despite China and India being in the first positions in the country ranking (see figure Fig.3.6a), an average Indian or Chinese citizen has a lower EVRW consumption than the world average.

3.2.3 The sustainability of the food trade under a riverine perspective

From a riverine water resources point of view, when a trade flow saves EVRW it can be defined as an efficient flow; conversely, when the opposite happens the flow is defined as inefficient. For example, the flows from Turkey and Egypt to Italy in Fig.3.3b are inefficient flows. Through these two flow categories, we can quantify the global efficiency of the EVRW network by evaluating, for each trade link, the difference in the EVRW under two different scenarios: a business as usual scenario and a self-reliant scenario, where all food is produced and consumed locally, at the country scale.

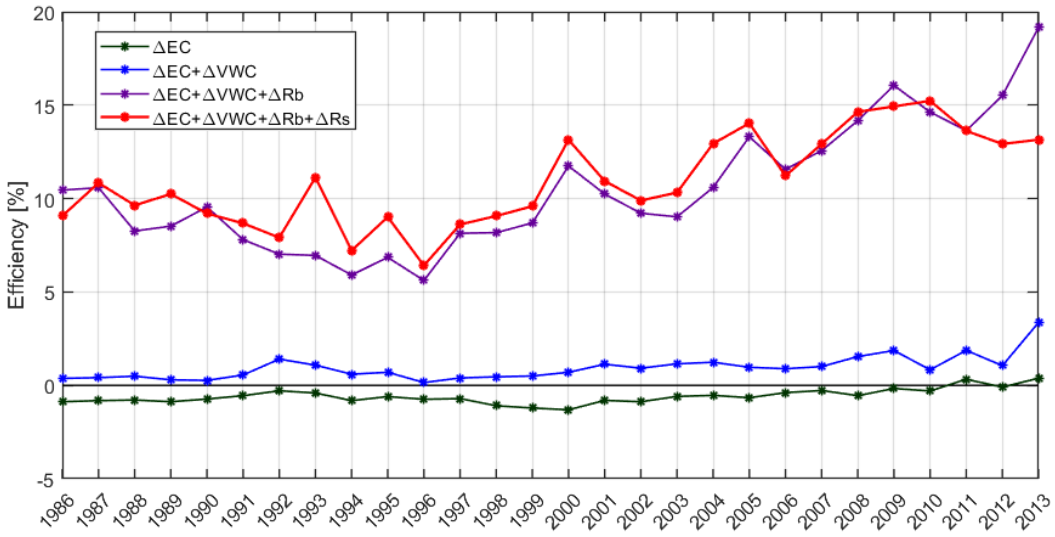

Fig. 3.8 The global yearly efficiency of the EVRW trade network from 1986 to 2013. The ordinate axis reports the relative network efficiency (in percentage), which is the ratio between the global savings (or losses) of EVRW due to food trade divided by the total EVRW yearly embedded in the global food production under the business as usual scenario. The total efficiency (red line) is the result of a combination of disparities between importers and exporters related to: the environmental value per unit of surface water used (ΔEC), the virtual water content of each product (ΔVWC), the percentage of blue water in each product (ΔRb), and the surface water use (ΔRs).

Fig.3.8 reveals (see red line) that the international food trade has increasingly led to save environmental value over the considered period: annually, trade-induced EVRW saving ranged from 6% to 15% . However, despite the significant global EVRW efficiency of the food network, the number of trade efficient and inefficient connections is about the same, with the former being about 48% of the total number of links. The reason of the global EVRW efficiency is shown in Fig.3.9: the higher are the riverine resources involved in the transaction the higher is the percentage of efficient links. Therefore, there is a global tendency to save riverine value when “strong" trade relationships are considered. As a consequence when a high EVRW threshold is focused on, namely the upper tail of the cumulative distribution is considered, only few inefficient links occur (e.g., the products exported from Uzbekistan and Australia to China).

The global efficiency of the EVRW network is driven by a combination of differences between exporters and importers (see Section 3.1.4); it partly depends on the agricultural practices and climatic conditions of the main exporters and importers (i.e., the different amount of riverine water used per unit of product) and partly relies on the uneven distribution of riverine water resources worldwide. For example, the flow from Brazil to Egypt is saving EVRW (see the map in the inset of Fig.3.9) both because Brazil has less vulnerable riverine ecosystems than Egypt and because a significant part of the Brazilian agriculture relies on rainwater rather than blue water.

In order to unveil the main disparities between exporters and importers that influence the overall EVRW efficiency value, Fig.3.8 shows the global efficiency value assessed by progressively considering an increasing number of differences between trading partners. Firstly (see the green line in Fig.3.8), only the different country-specific environmental values per unit of surface water use are considered while other differences among importers and exporters are neglected; in this case, the business as usual scenario is compared to a scenario where the same amount of surface water is consumed in the importer and exporter country for any food product. Under these conditions the global EVRW network is slightly inefficient. Thereafter, also the dissimilarity in the virtual water contents are taken into account (e.g., in 2013 to produce one ton of wheat the amount of water used ranged from 400 to 9000 m^3, depending on the considered country). Finally, also the differences in the percentage of blue water and surface water use are considered (see purple and red lines in Fig.3.8,

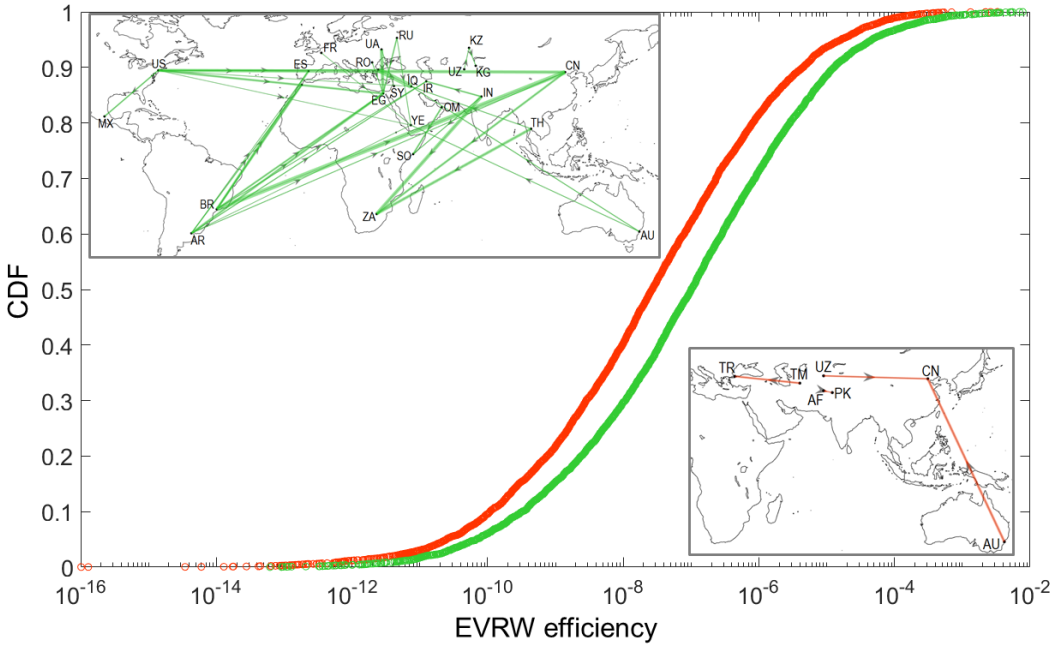

Fig. 3.9 The cumulative distribution functions (CDF) of the EVRW efficiency of the international food trade links in 2013. The green curve refers to the efficient links (about 48% of the total number of links), while the orange curve is the CDF of the inefficient links (about 52%). The abscissa reports the absolute value of the EVRW efficiency (or inefficiency) of each trade link expressed in log scale and as a percentage of the total EVRW embedded in global food production, under the business as usual scenario in 2013. Maps in the insets show the major trade flows related to a global saving (in green) or loss (in orange); all values greater than 10^{-3} (in absolute value) are reported. The link widths are proportional to the efficiency/inefficiency value. Country acronyms are in ISO 3166-1.

respectively). Overall, the fact that exporters tend to exploit lower amounts of blue water than importers (see purple lines) appears to be the most significant factor that improves the global EVRW efficiency. The latter result is in line with the findings of Konar et al. (2012), who investigated the efficiency of the food trade network under a volumetric perspective and found a global saving of 119 x 10^9 m^3 of blue water in 2008 due to the international trade.

3.3 Concluding remarks

In the last decades, globalization of water resources by food trade has dramatically changed the human impact on riverine ecosystems. The quantification of

the volumes of water involved in the production and trade of agricultural goods is an essential tool to investigate food-water-trade nexus issues. However, the volumetric point of view tells only a part of story, because the withdrawal of the same water volume can have very different environmental consequences depending on the particular ecosystem where water is withdrawn. In this Chapter, we investigated this aspect and focused on the environmental value of the water withdrawn from riverine systems.

We have shown that water globalization drives a global trade of environmental value of surface water and local threats to fluvial ecosystems are induced by the food demands across the globe. Through food imports, consumers can affect river environments thousands of kilometres away from them. However, despite the growing geographical gap between food consumption and production, international trade has been increasingly reducing the impact of global food production on riverine systems over time, compared to an ideal situation where all food is produced locally. We find an average annual global saving of riverine environmental value of 11% due to the international food trade. Nevertheless, a large number of trade links is still largely inefficient and several countries rely on vulnerable riverine ecosystems locally or abroad.

Chapter 4

Socio-economic drivers of blue water use trend worldwide

The work described in this chapter has been partially derived from Soligno et al. (2019).

Over the years, globalization has strengthened and expanded connections between socioeconomic systems and the resources they exploit (Dalin et al., 2012): allowing consumer demand in one region to be fulfilled with the resources exploited in another (Marston et al., 2015). It follows that the final consumption of commodities involves the use - along the whole supply chain - of both local and foreign water resources (Lenzen et al., 2013b). The share of non-domestic water embodied in a commodity can be identified as outsourced water use.

In recent years, the virtual water network related to internationally-traded food commodities has been investigated to disclose its temporal patterns and dynamics (Carr et al., 2013; Dalin et al., 2012; Tuninetti et al., 2017b), and it has been recognized that virtual water trade is mainly driven by socioeconomic factors rather than water resources availability (D'Odorico et al., 2010; Tamea et al., 2014; Yang, 2008). A large number of outsourcing patterns of water consumption has been linked to the unsustainable use of freshwater resources worldwide (Dalin et al., 2017; Lenzen et al., 2013b; Marston et al., 2015). Therefore, conservation strategies must consider not only the impacted areas, but also the consumer demand that drives those impacts (Lenzen et al., 2012; Marston et al., 2015).

Over the years, a number of studies has investigated water use issues employing

multi-regional input-output (MRIO) analysis, which allows to identify and assess the responsibility of consumers for the use of water resources along a complex system of international supply chains (Daniels et al., 2011; Lenzen et al., 2013b). By considering the monetary transactions between sectors and regions, MRIO models depict and quantify the sectoral and regional interdependence within the global economic system (Miller and Blair, 2009). Since MRIO models consider the entire industrial supply chains, differently from the bottom-up approaches, they have a comprehensive system boundary avoiding truncation error issues in the allocation of the virtual water flows to the final consumers (Feng et al., 2011).

In this framework, the changes and trends in global water use can be explained through a well-established technique called structural decomposition analysis (SDA) (Dietzenbacher and Los, 1998b). Broadly speaking, structural decomposition analysis breaks down observed changes in a physical variable (e.g., water use) over time, into the changes in its key determinants which can act as accelerators or retardants. SDA has become a widely accepted analytical tool to evaluate the drivers of change for a number of environmental indicators; for instance greenhouse gas emissions (Arto and Dietzenbacher, 2014; Malik and Lan, 2016), energy footprint (Lan et al., 2016), and nitrogen water pollution (Wan et al., 2016).

Furthermore, recent efforts have been devoted to investigate the main determinants of water use trends employing SDA in different socioeconomic systems. Cazcarro et al. (2013) studied the technological, structural and final demand factors that influence water consumption in Spain identifying household demand and the increase of exports as key explicative drivers. Wang and Small (2014) examined the governing factors of water withdrawal trends in the USA between 1997 and 2002. A number of studies have also investigated water use issues in China by undertaking SDA at different spatial scales (Yang et al., 2016; Zhang, 2012; Zhi et al., 2014). In order to investigate water use trends under a wider perspective, Distefano et al. (2018b) applied a SDA to an international MRIO model, recognizing the growth in final demand per capita as the key determinant of rising water consumption trend. However, their finding focused on the major economically important countries cutting out some of the most vulnerable world areas to water withdrawals (e.g., most of the African and Middle East countries).

The global economy is an increasingly interconnected system and it is widely acknowledged that the final consumption of commodities involves both local and foreign resources. However, scant information is available on the different socioeconomic determinants behind the changes in outsourcing and domestic water use trends over time, which are ultimately driven by the consumption of goods and services worldwide. This Chapter tackles this issue by applying, for the first time, a MRIO-based SDA considering 186 individual countries and by presenting a comprehensive analysis of the outsourcing and domestic trends over the period 1994 - 2010 . In this Chapter, we study 6 key socioeconomic drivers of blue water use: blue water efficiency, production recipe, final demand composition, final demand destination, affluence and population. Countries that play a significant role on foreign water resources are highlighted and, in each country, the major driving forces of outsourcing water use trends are quantified. Our results allow us to understand the main mechanisms that accelerate or decelerate the exploitation of global freshwater resources worldwide.

4.1 Materials and Method

4.1.1 The input-output model

The Multi-Region Input-Output (MRIO) model represents the monetary transactions of commodities and services among different sectors of an economic system, within and between different regions.

Trade transactions are recorded in the $n \times n$ intermediate demand matrix, $\mathbf{T}$, where the t_{ij} element of the matrix denotes the monetary transaction from sector i to sector j (see Fig.4.1). In our work $n = 4836$ since we are considering 186 countries and 26 sectors. The final demand of commodities and services is stored in an $n \times m$ matrix $\mathbf{F}$, where are recorded the sales to m purchasers who are exogenous to the industrial sectors (e.g., households and government in Fig.4.1a). The sum of intermediate and final demand transactions equals the total economic output $\mathbf{x} = \mathbf{T}\,\mathbf{1} + \mathbf{F}\,\mathbf{1}$, where $\mathbf{1}$ is the proper summation operator and the $\mathbf{F}\,\mathbf{1}$ term coincides with the total final demand vector $\mathbf{y}$. Accordingly, $\mathbf{x}$ is an $n \times 1$ vector where the x_i element is the total production of sector i and equals the intermediate and the final demands for sector i's

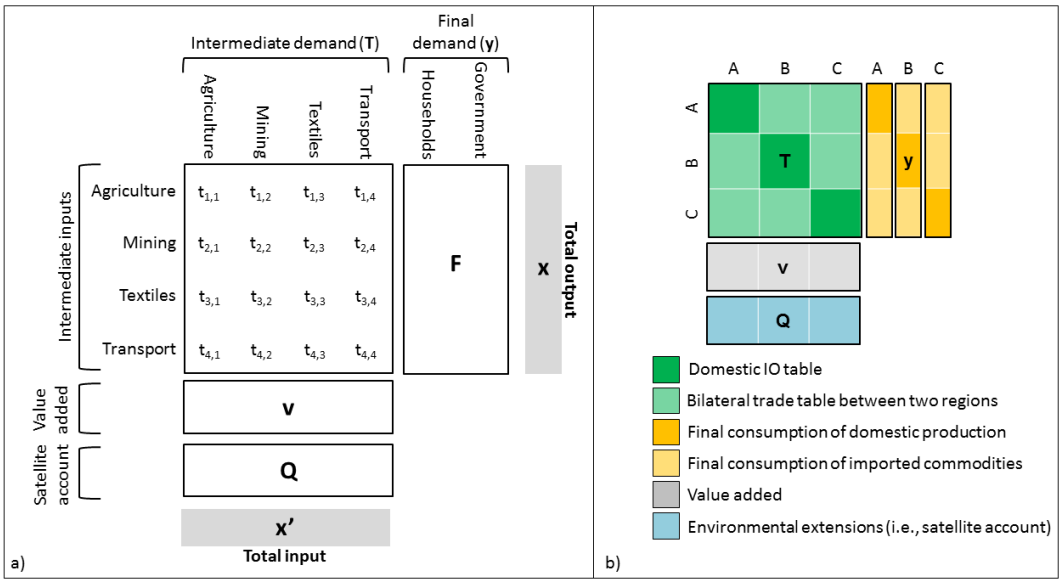

Fig. 4.1 Schematic examples of environmentally extended input-output (IO) tables in (a) a single region and (b) a 3-region system (where the regions are A, B, and C). (a) in the example, $\mathbf{T}$ is a 4×4 matrix, $\mathbf{F}$ is a 4×2 matrix (where $\mathbf{F}\,\mathbf{1} = \mathbf{y}$, which is the 4×1 final demand vector), and $\mathbf{x}$ is the 4×1 total output vector. (b) In the MRIO table are recorded both the transactions within and between regions. In the present work 186 countries and 26 sectors are considered and, thus, $\mathbf{T}$ is a 4836×4836 matrix.

products, namely $x_i = t_{i1} + ... + t_{ij} + ... + t_{in} + y_i$ (see $\mathbf{T}$, $\mathbf{y}$, and $\mathbf{x}$ in the scheme of Fig.4.1a).

The input-output model assumes that in a given period the flow from i to j depends exclusively on the total output of sector j for that same period. The main idea is that if for example the furniture industry, j, increased its total production (x_j), during the same period the wood industry, i, would need to increase the transactions toward the furniture industry (t_{ij}). The ratio of t_{ij} to x_j is called technical coefficient (a_{ij}) and, hence, $t_{ij} = a_{ij}x_j$ (see the numerical example in Fig.4.2). Therefore, the total output of sector i can be rewritten as: $x_i = a_{i1}x_1 + ... + a_{ij}x_j + ... + a_{in}x_n + y_i$; which from the final demand point of view it turns into: $y_i = -a_{i1}x_1 - ... + (1 - a_{ij})x_j - ... - a_{in}x_n$. Considering all the n sectors of an economic system, this formulation can be represented compactly in matrix form as $(\mathbf{I} - \mathbf{A})\ \mathbf{x} = \mathbf{y}$, where $\mathbf{I}$ is the $n \times n$ identity matrix and $\mathbf{A}$ is the $n \times n$ matrix of technical coefficients, which is $\mathbf{A} = \mathbf{T}\,\hat{\mathbf{x}}^{-1}$ (the hat symbol denotes diagonalization of a vector).

Therefore, the total output of an economy $\mathbf{x}$ can be defined as

$$\mathbf{x} = (\mathbf{I} - \mathbf{A})^{-1}\,\mathbf{y}. \tag{4.1}$$

This equation - formulated by the Nobel Prize Laureate Wassily Leontief - represents the input-output demand-pull model of the economy, where the provision of final demand ($\mathbf{y}$) requires total output ($\mathbf{x}$) to be produced along the whole supply chain network. The matrix $(\mathbf{I} - \mathbf{A})^{-1}$ is the Leontief's inverse, $\mathbf{L}$, which includes all the direct and indirect links between industries and countries.

In order to analyse the blue water consumption changes over time, the aforementioned input-output model needs to be extended as

$$\mathbf{Q} = \mathbf{q}\,\mathbf{L}\,\mathbf{y} \tag{4.2}$$

where the $1 \times n$ vector $\mathbf{Q}$ accounts for the blue water consumed (in m^3) by countries and industry sectors during the considered period (see Fig.4.1); $\mathbf{q}$ is a $1 \times n$ vector of blue water intensities and represents the total blue water consumed by each country and industry sector per unit of the total output of the corresponding country and industry sector and, thus, is $\mathbf{q} = \mathbf{Q}\,\hat{\mathbf{x}}^{-1}$ (i.e.,

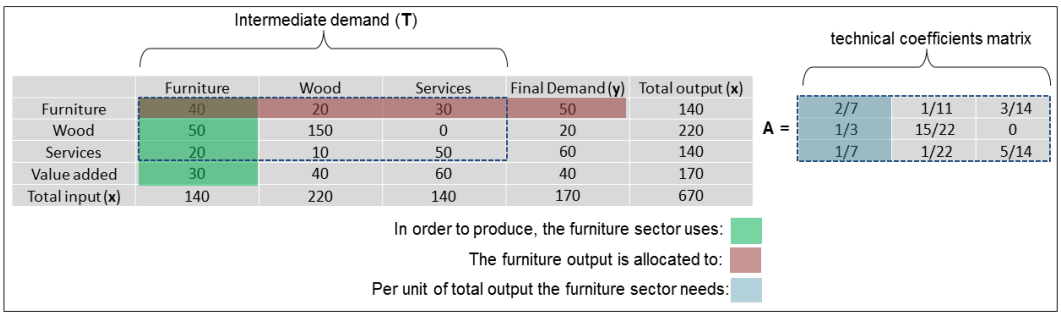

Fig. 4.2 The input-output table of a very simple economy and its corresponding matrix of technical coefficients (**A**). In this example, 1/3 (i.e., 50/140) of input from the wood sector is needed per unit of total output of the furniture industry. In the input-output framework, the interindustry flows from i to j in a given period (say a year) depend exclusively on the total output of sector j for that same time period (namely, **A** does not change). For example, if the furniture industry increased its total production from 140 to 280, during the same period the wood industry would need to increase the transactions toward the furniture industry from 50 to 100.

m^3 per monetary unit). For further information on input-output analysis see Miller and Blair (2009).

4.1.2 Structural decomposition analysis (SDA)

SDA relies on the input-output demand-pull model formulated by Leontief; it is an analytical technique that aims to decompose changes in one variable into a number of mutually exclusive contributions induced by a set of determinant variables (i.e., drivers). In this work, we performed a SDA to break down the total change in blue water consumption into contributions from six key determinants: blue water efficiency, production recipe, final demand composition, final demand destination, affluence and population.

The blue water efficiency is expressed by the **q** term of Eq.(4.2) and indicates the blue water consumed per unit of total production (i.e., m^3/\$); this variable suggests the improvement in the direct use of blue water by the producers. The Leontief's inverse (**L**) encloses the interdependence among sectors of different countries and, thus, it can describe the changes in the input products needed by the different sectors (i.e., the production recipe).

In order to examine the disparate contributions embedded in the final demand, **y** was further decomposed into four drivers: final demand composition

($\mathbf{u}$), final demand destination ($\mathbf{v}$)), affluence (a) and population (p). The changes in the consumption baskets of final consumers over the considered period are expressed by the final demand composition. This term can be derived from the final demand $n \times m$ matrix as $\mathbf{u} = \mathbf{F}\,\hat{\mathbf{g}}^{-1}$, where $\mathbf{g}$ is the $1 \times m$ vector of total final demand by category of final consumer and is obtained by summing up the element of $\mathbf{F}$ along the rows.

The final demand destination considers the changes in the distribution of the final demand among the different ultimate agents (namely, households, governments, investments etc.) and it can be derived as $\mathbf{v} = (\mathbf{g}\,\hat{\mathbf{y}}^{-1})'$ (the prime symbol denotes matrix transposition). Finally, to investigate the influence of both population and affluence variations on blue water consumption trends, the amount of national final consumption, $\sum_{j=1}^{m} \mathbf{g}_j$ (i.e., the total national GDP), was further divided into the population and the per-capita consumption (namely, the affluence) of each country. Notice that since the SDA is performed for each individual country (see Section 4.1.3) a and p are scalar quantities. Therefore, by introducing the above-mentioned terms in Eq.(4.2), the total blue water consumed by the final demand of each country can be evaluated as:

$$\mathbf{Q} = \mathbf{q}\,\mathbf{L}\,\mathbf{u}\,\mathbf{v}\,a\,p. \tag{4.3}$$

Then, suppose the total blue water consumed at time 0 and t are $\mathbf{Q^0}$ and $\mathbf{Q}^t$, respectively; the variation in the total blue water consumed between time 0 and 1, $\Delta\mathbf{Q}$, can be expressed through the following decomposition:

$$\begin{aligned}\Delta\mathbf{Q} = \Delta\mathbf{q}\,\mathbf{L}\,\mathbf{u}\,\mathbf{v}\,a\,p + \mathbf{q}\,\Delta\mathbf{L}\,\mathbf{u}\,\mathbf{v}\,a\,p + \mathbf{q}\,\mathbf{L}\,\Delta\mathbf{u}\,\mathbf{v}\,a\,p + \mathbf{q}\,\mathbf{L}\,\mathbf{u}\,\Delta\mathbf{v}\,a\,p + \\ + \mathbf{q}\,\mathbf{L}\,\mathbf{u}\,\mathbf{v}\,\Delta a\,p + \mathbf{q}\,\mathbf{L}\,\mathbf{u}\,\mathbf{v}\,\mathbf{a}\,\Delta p\end{aligned} \tag{4.4}$$

where $\Delta\mathbf{q}\,\mathbf{L}\,\mathbf{u}\,\mathbf{v}\,a\,p$ measures the water efficiency effect, $\mathbf{q}\,\Delta\mathbf{L}\,\mathbf{u}\,\mathbf{v}\,a\,p$ estimate the changes in the Leontief structure, $\mathbf{q}\,\mathbf{L}\,\Delta\mathbf{u}\,\mathbf{v}\,a\,p$ is the variation in the final demand distribution among industries, $\mathbf{q}\,\mathbf{L}\,\mathbf{u}\,\Delta\mathbf{v}\,a\,p$ is the final demand destination effect, $\mathbf{q}\,\mathbf{L}\,\mathbf{u}\,\mathbf{v}\,\Delta a\,p$ is due to the changes on the level of affluence, and $\mathbf{q}\,\mathbf{L}\,\mathbf{u}\,\mathbf{v}\,a\,\Delta p$ estimate the demographic impact.

Mathematically, there is no unique way to perform a SDA; for the sake of simplicity consider the case of only two determinants, e.g. $\mathbf{x} = \mathbf{L}\,\mathbf{y}$. The change in $\mathbf{x}$ between $time = 0$ and $time = 1$ (i.e. $\Delta\mathbf{x} = \mathbf{L}_1\,\mathbf{y}_1 - \mathbf{L}_0\,\mathbf{y}_0$) can be decomposed as $\Delta\mathbf{x} = \mathbf{L}_1\,\Delta\mathbf{y} + \Delta\mathbf{L}\,\mathbf{y}_0$ or, alternatively, as $\Delta\mathbf{x} = \mathbf{L}_0\,\Delta\mathbf{y} + \Delta\mathbf{L}\,\mathbf{y}_1$. These two decompositions are equivalent and there is no reason why one form should be preferred in favour of the other. In the case of k determinants there are $k!$ different exact decomposition forms and the results may differ significantly across the alternative procedures (Dietzenbacher and Los, 1998a).

To overcome the "non-uniqueness problem", Dietzenbacher and Los (1998a) suggested to use the average of all the $k!$ possible decomposition forms. In the aforementioned example, thus, the effects of $\mathbf{L}$ and of $\mathbf{y}$ on $\mathbf{x}$ changes are quantified as $\mathbf{L}_{eff} = \frac{1}{2}(\Delta\mathbf{L}\,\mathbf{y}_0 + \Delta\mathbf{L}\,\mathbf{y}_1)$ and $\mathbf{y}_{eff} = \frac{1}{2}(\mathbf{L}_0\,\Delta\mathbf{y} + \mathbf{L}_1\,\Delta\mathbf{y})$. Since this approach has been shown to be zero-residual and non-parametrical (Lenzen, 2006), in this study we adopted the Dietzenbacher and Los (1998a) method. Accordingly, we have $6! = 720$ alternative decompositions and the average of all these forms has been employed.

Computationally, in order to increase the speed of calculation, we applied the Dietzenbacher and Los (1998a) method following the approach introduced by Seibel (2003) (for further detail about this approach we refer to Rørmose and Olsen (2005)).

4.1.3 MRIO-based spatial decomposition

Using the MRIO framework, we decomposed changes in the blue water consumed worldwide not only structurally, but also geographically. In Fig.4.3 the three spatial decompositions developed in our work are schematically illustrated by considering an example three-world region (i.e., A, B, and C).

First, we study the global blue water use trend driven by the final demand of each individual region (e.g., $\mathbf{Y}_A$). This spatial decomposition (GW) estimates the influence of the final demand of a specific country on the global water resources; accordingly, in the MRIO model the whole $\mathbf{Q}$ vector and $\mathbf{T}$ matrix are considered (see Fig.4.3a).

To distinguish between the use of domestic and foreign water resources, we split the MRIO framework into a domestic component (Fig.4.3b) and an

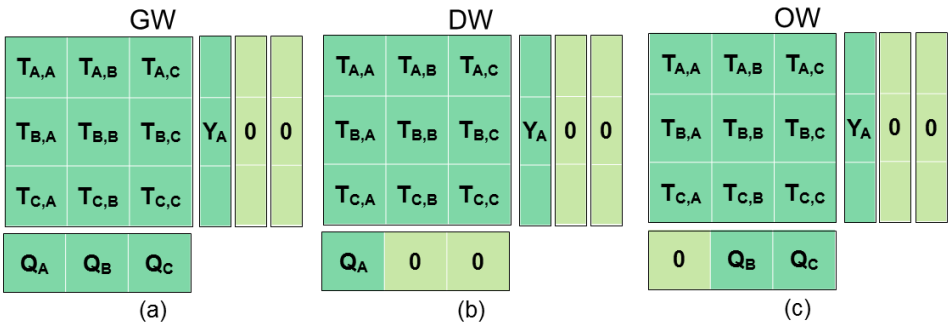

Fig. 4.3 MRIO-based spatial decompositions by considering 3 countries (i.e., A,B, and C as in Fig.4.1b). The general structure of a MRIO table is detailed in Fig.4.2. In the example, the $\mathbf{T}_{A,A}$ matrix records the domestic transactions in country A (i.e., the domestic IO table), $\mathbf{T}_{A,B}$ reports the transactions from country A to country B intermediate demand, $\mathbf{Y}_A$ denotes the final demand in country A, and $\mathbf{Q}_A$ the use of blue water in country A; (a) The GW spatial decomposition considers the global blue water consumed by the final demand in the country considered (i.e., $\mathbf{Y}_A$); (b) the DW decomposition takes into account only domestic water (i.e., $\mathbf{Q}_A$) and (c) the OW decomposition considers the consumption of non-domestic water resources.

outsourcing component (Fig.4.3c) for each individual country. To this end, we performed two complementary spatial decompositions: one (DW) with respect to the part of $\mathbf{Q}$ related to the water resources within the considered country (i.e., $\mathbf{Q}_A$ in Fig.4.3b) and the other (OW) related to the foreign water resources (i.e., $\mathbf{Q}_B$ and $\mathbf{Q}_C$ in Fig.4.3c).

Notice that since we considered the whole $\mathbf{T}$ matrix and not only the part of the intermediate demand related to the transactions within the considered country (i.e., $\mathbf{T}_{A,A}$), we assessed the domestic water resources embodied in the whole international supply chain network. For example, focusing on the water exploitation driven by $\mathbf{Y}_A$, the DW spatial decomposition allows for the evaluation also of the blue water used to grow cotton in A, thereafter exported to C to produce clothes and finally exported and consumed in country A again. Similarly, the entire supply chain is considered in the OW spatial decomposition method, but adding up only the blue water resources initially used in countries other than the one considered. Finally, notice that these two latter spatial decompositions (i.e., DW and OW) are mutually exclusive and together can exhaustively describe the drivers of global water use trend.

By performing SDAs using the DW and the OW frameworks, we can estimate the different determinants underlying the changes in outsourcing and

domestic water use trends over time; In addition, we can highlight the countries that heavily rely on foreign water resources taking into account the whole international supply chain network.

4.1.4 Data

We used the Eora global MRIO database (Lenzen et al., 2013a) which contains comprehensive and harmonized time-series data of trade flows, production, consumption and intermediate use of goods and services aggregated to 26 sectors for 186 countries.

A key requirement to perform SDA is to use constant-price MRIO tables. Using input-output data in current prices rather than constant-prices can seriously bias the results. Suppose, for example, that a given sector in two different years produced exactly the same amount of goods (e.g., in tonnes) by using the same volumes of water (i.e., the water efficiency was stable during the considered period). Using MRIO tables in current prices imply that if the output prices increased over the considered period due to inflation, the water intensity coefficients will wrongly appear to decrease. In order to have constant-price MRIO tables, we used the constant-price MRIO tables constructed by Lan et al. (2016). These constant-price MRIO tables were obtained by applying the "convert-first then deflate" procedure (Fremdling et al., 2007) to the Eora's input-output tables (Lenzen et al., 2013a). In Lan et al. (2016), the conversion from the national currencies to constant US$ was achieved by using the Purchasing Power Parities indexes (PPP) published by the Organization for Economic Co-operation and Development (OECD); while as deflators were adopted the Producer Price Indexes (PPI) published by the U.S. Bureau of Labor Statistics. For further details about this topic, see Appendix A in Lan et al. (2016).

The blue water satellite account (i.e., $\mathbf{Q}$) are provided by the Eora database. In Eora, the satellite data are derived from the water footprints of national production given by Hoekstra and Mekonnen (2012), which are sectoral water consumption values averaged over the period 1996-2005. In Eora, based on the averaged values provided by Hoekstra and Mekonnen (2012), the sectoral blue water consumption time-series were interpolated. In the year 2000 were

adopted the values given by Hoekstra and Mekonnen (2012), then the time-series were reconstructed assuming that the water intensity (i.e., m^3/yr/\$) of each sector remains constant over time; namely assuming that the water consumption of each sector scales according to the economic growth of the considered sector. The water intensity in the industry was assessed based on the annual sectoral gross output, while the water intensity of households was based on the household's total annual final demand.

The aforementioned assumption introduced in Eora to reconstruct a water use time-series is mainly due to the lack of temporal data on the consumption of blue water for most of the industrial sectors. However, in the agriculture sector more detailed analysis can be performed to assess the blue water used over time. In this study, thus, for all sectors except agriculture we employed the blue water consumption satellite account (i.e., Q) provided by Eora, while the annual blue water consumption of agriculture was calculated by adopting the following procedure.

We collected sixteen years (1994 - 2010) of production data from the Food and Agricultural Organization of the United Nations for 235 crops and animal products (the detailed list is reported in Tab.B.1 in Appendix B in the column labelled "in production"). The FAOSTAT database provides for each commodity and year the amounts produced in any given country expressed in tonnes, heads or units, depending on the type of product. These amounts were then multiplied by the corresponding country-specific blue virtual water content (VWC) to estimate the volume of water consumed for the production of each commodity. The virtual water content of each type of product was assessed at the country and yearly scale as described in Section 3.1.1.

Finally, by adding up these volumes the total yearly amount of blue water used in the agriculture sector was calculated for each country. Therefore, the water annually consumed by the agriculture sector depends on (i) the type of water-intensive agricultural goods annually produced in the country, (ii) the tonnes annually produced of each product, and (iii) the country-specific improvements (or decline) in the agricultural yields of each crop (see Section 3.1.1).

Notice that in the SDA carried out in this work the water efficiency term exclusively depends on the agriculture sector, since in the other industries

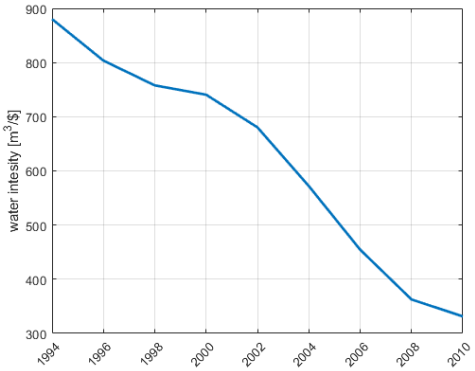

Fig. 4.4 Global average water intensity of the agriculture sector (i.e., blue water use per unit of production [m^3/$]).

the water intensity (i.e., m^3 of blue water used per unit of economic output) was assumed constant over time by the Eora database. This is an acceptable approximation since, from the production-side, agriculture is by far the most water-consuming sector: over the period 1996 - 2005 more than 90% of the global consumptive water use (Hoekstra and Mekonnen, 2012) and 70% of the gross water use (Gleick, 2000) concerned the production of crops and animal products.

4.2 Results and discussion

4.2.1 A global overview of the major drivers of blue water use trends

Between 1994 and 2010, the amount of blue water annually involved in the production of goods and services globally increased by $4.5 \cdot 10^{11}$ m^3/yr (i.e. 37% of the initial amount). Overall, the largest relative increases occurred in developing countries and emerging economies, which in a number of cases more than doubled the direct use of domestic water resources (e.g., in Egypt, Indonesia, Brazil, Peru, Bolivia, the United Arab Emirates, Turkmenistan, Angola, and Myanmar). Meanwhile, the relative increases in most developed countries did not exceed 20%, although noteworthy exceptions occurred in Australia (58%), Canada (38%), and Spain (35%). At the global scale, the

Table 4.1 Structural decomposition analysis of global blue water use at 2-years time step from 1994 to 2010. The overall effect of each driver is reported as a percentage of the total variation in global blue water use between 1994 and 2010. The first column reports the drivers considered: blue water efficiency ($\Delta\mathbf{q}$), production recipe ($\Delta\mathbf{L}$), final demand composition ($\Delta\mathbf{u}$), final demand destination ($\Delta\mathbf{v}$), affluence (Δa) and population (Δp). In a given time-interval, each determinant can act as an accelerator (i.e., positive value) or retardant (i.e., negative value) on blue water use changes.

	1994-1996	1996-1998	1998-2000	2000-2002	2002-2004	2004-2006	2006-2008	2008-2010	1994-2010
$\Delta\mathbf{q}$ [%]	-22.0	-23.9	-6.8	-28.5	-52.2	-84.7	-71.5	-38.5	-328.2
$\Delta\mathbf{L}$ [%]	-12.5	-7.0	-3.9	2.0	-0.5	2.8	3.0	-0.1	-16.1
$\Delta\mathbf{u}$ [%]	-9.1	14.7	-2.6	-0.3	-10.9	10.6	-10.7	1.7	-6.5
$\Delta\mathbf{v}$ [%]	-1.9	2.0	-1.3	0.2	-2.5	1.3	-2.1	-0.9	-5.2
Δa [%]	50.6	10.2	9.3	19.9	77.9	85.6	102.2	39.9	395.7
Δp [%]	7.8	7.7	7.3	7.0	7.0	7.5	8.0	7.9	60.4

agriculture sector experienced the largest increased in the volume of blue water used, which increased by $1.5 \cdot 10^{11}$ m^3/yr. Meanwhile, the economic productivity of the world's agriculture grew faster than the volumes of water used: on average, the volume of blue water per unit of production more than halved during the 1994-2010 interval (see Fig.4.4).

Since the use of natural resources is ultimately driven by the (global) final demand for products and services, through the input-output framework we linked the direct use of blue water resources (the **Q**-side in Fig.4.3) to the final demand of consumers (i.e. the **Y**-side in Fig.4.3); then we quantified the impact of 6 key drivers on global water use trends by performing an SDA at 2-year time step and considering the final demand of 186 countries.

At the global scale, the results of our analyses are reported in Table 4.1, where the effect of each socio-economic driver is expressed as a percentage of the total variation in global blue water use; a negative percentage indicates that the considered determinant acted as a retardant, conversely a positive percentage implies that the considered determinant accelerated the global use of blue water. Worldwide, the affluence growth was the major driver of rising water consumption trends, accounting for +396% of the total variation between 1994 and 2010. At the global scale, the affluence effect was partly offset by remarkable improvements in the blue water efficiency of producers (-328% of the total variation).

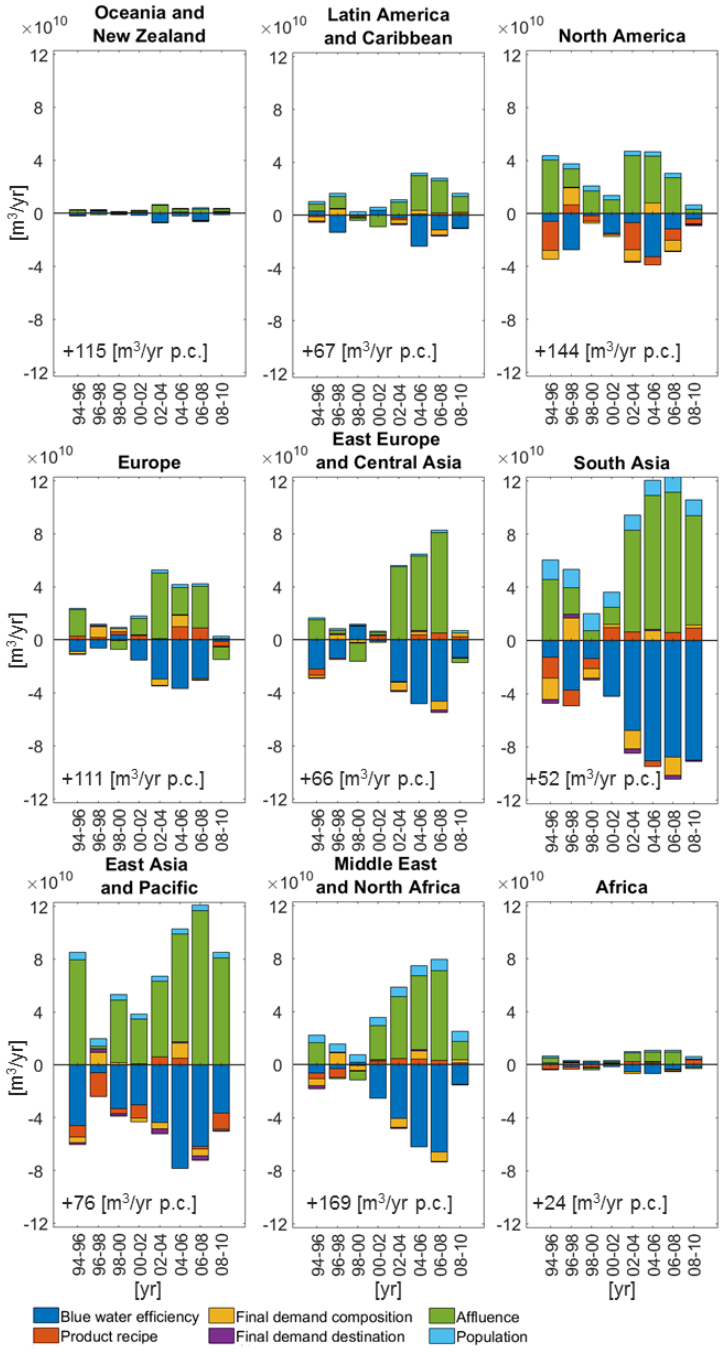

Fig. 4.5 Structural decomposition analysis of global blue water use at 2-years time step from 1994 to 2010. Each panel of the plot shows the drivers of the global blue water use (in m^3/yr) driven by the final demand of different world macro regions (see Fig.B.1 for countries belonging to each world area). Each panel also reports the increase in the blue virtual water consumed per capita (in m^3/yr per capita) by the final demand of each macro region between 1994 and 2010.

A global overview of the main socio-economic effects driven by the final demand of the consumers in 9 world macro regions is displayed in Fig.4.5 (for further results at the regional scale see Section A.3 in the Appendix). The impact of affluence dominates across most countries, except for some African countries afflicted by conflicts and in periods of economic recession. During the economic crisis that primarily hit Europe and North America in 2008, for example, affluence had a decelerating impact on water consumption trends in several developed countries (see the bars labelled “08-10" in Fig.4.5). Meanwhile, the blue water efficiency of producers allowed to globally reduce water consumption; its decelerating effect was increasingly significant in several developing countries (e.g., in India, Egypt, Iran, and Pakistan) and in a number of developed countries, such as Germany and Spain (the latter before the year 2008). Although efficiency improvements caused a remarkable global decelerating effect on water trends, in a number of countries its contribution experienced significant fluctuations, often related to economic crises (e.g., in several European countries during the period 2008-2010) or climatic anomalies. From 2000 to 2001, for example, a severe drought occurred in Central Asia and the Caucasus causing significant losses in agricultural production and involving an overall economic cost of 800 million US$ (FAO, 2017); as a consequence, during the years affected by the drought the blue water efficiency decreased significantly in the drought-stricken regions (see central panel in Fig.4.5).

Geographically, the hot spots of total growth were located in South and East Asia (especially in China and India); while the largest increases of blue water consumption per capita were driven by the final demand of the citizens of the Middle East and North Africa and the North America, where the blue water annually consumed by a person increased on average by 169 and 144 cubic meters, respectively, between 1994 and 2010 (see the per capita values within the plots of Fig.4.5).

At the global scale, as detailed in Table 4.1, population growth had a regular accelerating effect on blue water use variations of approximately +7% every two years (+60% between 1994 and 2010). As shown in Fig.4.5, demographic changes had a considerable impact, especially in South Asia, where the population increased from 1.2 to 1.6 billion people, and in the Middle East and North Africa, which had a demographic increase of 130 million people during the period considered. India experienced the greatest impact related to population

growth, with an overall effect due to demographic changes equal to +15% of the total variation in global blue water use. Meanwhile, in the USA, China and Pakistan the overall population effect was approximately equal to +5% over the 1994 - 2010 interval.

Production recipe changes (i.e., the variations in the interdependence across countries and sectors) had heterogeneous and fluctuating effects on blue water use trends across different countries and years (globally -16% of the total variation between 1994 and 2010), as did the impacts of the final demand composition and the final demand destination (globally -6.5% and -5.5%, respectively). For example, significant improvements related to the production recipe were driven by the final demand of the United States and China (-13% and -11% of the total variation, respectively); conversely in Germany, Japan, and India the production recipe led to rise blue water consumption trends.

4.2.2 Decoupling the drivers of domestic and outsourced blue water use trends

In the previous subsection the results of the SDA were presented without distinguishing between domestic and foreign blue water resources consumed by the final demand considered. Here, we decoupled the drivers of domestic and outsourced blue water use trends by splitting the total blue water consumed by the final demand of each country into contributions from domestic production (DW spatial decomposition) and international imports (OW spatial decomposition), as schematically depicted in Fig.4.3b and Fig.4.3c.

Globally, the (virtual) water volumes imported from non-domestic resources rose steadily from 1994 to 2008, confirming that water resources are increasingly globalized (Dalin et al., 2012; Yang, 2008). Fig.4.6 shows the outsourcing and domestic blue water use patterns by considering countries with diverse levels of development – according to their Human Development Index (HDI) - and different climatic regimes (ranging from semi-arid to tropical conditions).

Fig.4.6 reveals a significant imbalance in the origin of the blue water increasingly consumed by developed and developing economies: over the period considered, consumers in developing countries strongly influenced domestic water use trends; conversely developed economies increasingly drove variations

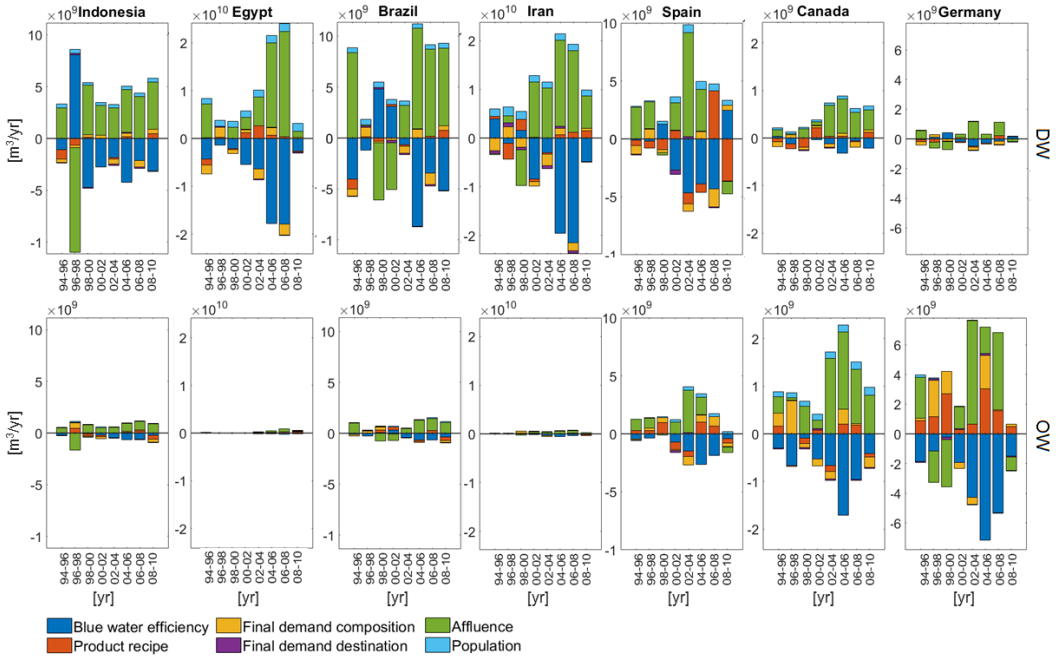

Fig. 4.6 Drivers of domestic (top panels) and outsourced (bottom panels) blue water use (in m^3/yr) at 2-year time step from 1994 to 2010. The DW and the OW spatial decompositions concern the final demand of both developing (Indonesia, Egypt, Brazil, and Iran) and developed (Spain, Canada, and Germany) countries. Countries are sorted according to their Human Development Index (in 2010) and are selected in order to cover different climatic regimes.

in the use of foreign water resources. Moreover, although the virtual water concept was introduced as a potential approach to address water scarcity (Allan, 1997), also in semi-arid regions, such as Egypt and Iran, the final demand for products and services drove changes primarily in domestic resources rather than in foreign water-abundant economies. The imbalance in the volumes imported by developed and developing countries in spite of their climatic regimes is in line with previous studies, which have emphasized the fact that virtual water flows are driven by economic aspects rather than water solidarity (D'Odorico et al., 2010; Tamea et al., 2014).

By performing SDAs using the DW and the OW frameworks, we estimated the different determinants behind the changes in outsourcing and domestic water use variations, in order to study the different dynamics that involve various types of economic systems over time. For example, the 2008 financial crisis impacted domestic and outsourced trends in different economies in different ways: in Germany and Canada the affluence reduction primarily affected outsourced resources, conversely in Iran and Egypt the major consequences of the economic crisis affected domestic resources.

Overall, affluence had a remarkable influence on rising blue water use trends, both in domestic and in outsourced patterns, while blue water efficiency progressively decelerated blue water consumption growth. The most consistent fluctuations with respect to this overall tendency were mainly caused by economic crises or drought events. For example, the severe financial crisis that hit Indonesia in 1999 induced an abrupt inversion in the domestic effects of the blue water efficiency and the affluence (see Fig.4.6). In this case, the inversion in the efficiency effect was due to a significant reduction in the total economic value of production (i.e. in \$), which accordingly caused a sudden growth in the amount of blue water consumed per unit of total production (i.e. m^3/\$). A further example of domestic efficiency shift occurred in Iran, which experienced a severe drought event during the years 1999 and 2000. As a consequence, the Iranian agricultural sector - which uses 93% of Iran's total water consumption (Alizadeh and Keshavarz, 2005) – experienced considerable crop failures (OCHA, 2000).

Worldwide, affluence growth was the socio-economic factor that drove blue water consumption growth the most, however this growth spread differently

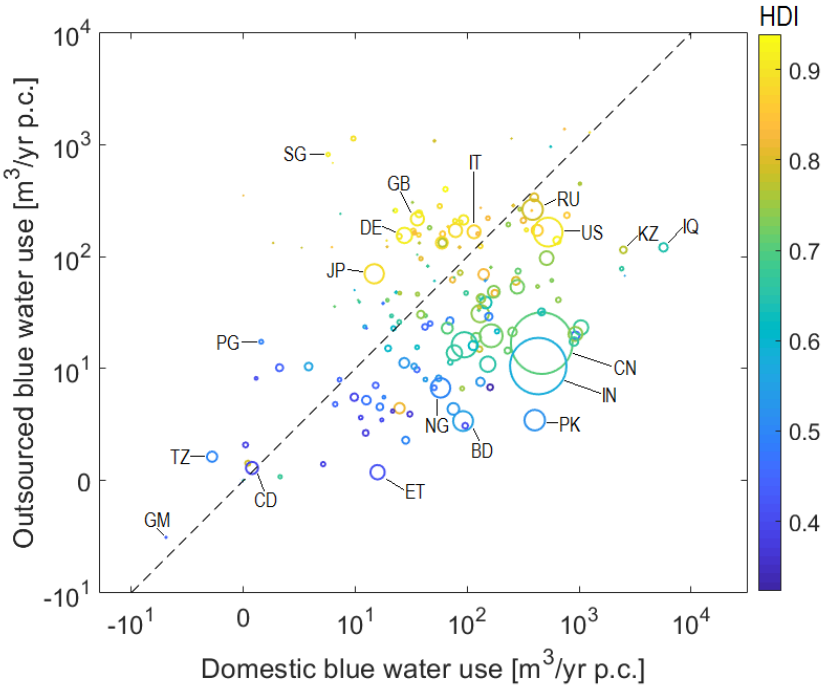

Fig. 4.7 The impact of affluence growth on domestic and foreign water resources use trends (in m^3/yr per capita). The x-axis indicates the per capita use of domestic blue water resources while the y-axis indicates the per capita use of non-domestic blue water resources, both induced by the affluence variation of the final demand of each country. Both axes are in log-scale. Circle sizes are proportional to the population, circle colours indicate the Human Development Index in the year 2010. The SDA was conducted on the interval 1994-2010. Country names are expressed in ISO 3166-1.

among water resources depending on the nationality of the final consumers (as pointed out in Fig.4.6). In Fig.4.7, the affluence effect of each country on the per capita use of domestic blue water resources is compared to the per capita use of non-domestic resources (for each country, the per capita water volume is estimated using a population value averaged over the period 1994-2010). The bisection of the graph in Fig.4.7 (i.e. the dotted line) can be considered as a theoretical boundary between the outsourcers (above the line) and the contractors (below the line). As a result, the citizens living in outsourcer countries tend to increase their affluence by intensifying mainly the use of foreign water resources, *vice versa* the affluence growth in contractor countries mostly leads to rise the use of domestic resources.

Overall - despite some exceptions (such as Iraq and Kazakhstan) - the higher the development level of the country considered, the higher was the increase of the per capita blue water volumes consumed by its citizens over the period 1994-2010 (see the color pattern of the scatter in Fig.4.7). While in a number of African country the affluence effect was negligible or negative on the per capita consumption of blue water, such as Tanzania and the Democratic Republic of Congo.

Often, the affluence variation of a citizen of developed countries induced more changes in the exploitation of foreign rather than local freshwater resources. Indeed, as can be seen from Fig.4.7, most of the outsourcer countries are highly developed, with a number of exceptions mainly concerning island regions (e.g., Papua New Guinea and Jamaica). Interestingly, there is a threshold (approximately, in total, at 800 cubic meters per capita) above which countries become contractors in spite of their HDI rank (e.g., in Russia, Saudi Arabia, and the USA).

Finally, from Fig.4.7 it can be noticed that highly populated countries tend to mostly increase the use of local water resources compared to the increase in the imports, as highlighted for example by the two emblematic cases of China and India, in which about 70% of the affluence effect concerned freshwater resources within their national borders. Japan is an exception to this global pattern; indeed, despite having a large population, it is an outsourcer. This is mainly due to the limited availability of natural resources (e.g., arable land) compared to the country's needs (Oki and Kanae, 2004).

4.3 Concluding remark

In this Chapter, we quantified the major socio-economic factors that drove global blue water use trends over the 1994 - 2010 period. Since the use of freshwater resources is ultimately driven by the (global) final demand for products and services, through the Multi-Regional Input-Output framework, we decomposed changes in the blue water consumed worldwide both structurally and geographically by considering the consumers final demand in 186 individual countries.

Between 1994 and 2010, the demand of blue water rose by 37%, with the hot spots of total growth located in South-East Asia. Worldwide, the affluence growth was the main driver of increasing blue water use trends both for developing and developed economies. Indeed, it is recognized that the affluence growth have allowed households to increase the consumption of water-intensive products, such as meat and dairy products (D'Odorico et al., 2018; Tilman et al., 2011). We estimated that if the blue water use was influenced only by the affluence effect, blue water exploitation would be quadrupled over the period considered. Also demographic changes had considerable accelerating effects on blue water use trends (in particular in the MENA region and in South Asia), nevertheless these effects were still five times lower than the ones given by the affluence growth. The affluence and the demographic impacts were globally partially offset by remarkable improvements in the blue water efficiency and, to a lesser extent, by changes in production technology (i.e., the production recipe effect), the latter mainly driven by the final consumers of the USA and China.

Our results show a significant imbalance in the origin of the blue water increasingly consumed by developed and developing countries. On average, the citizens living in developed countries tend to increase their affluence by intensifying mainly the use of foreign water resources, conversely, the affluence growth in developing regions mostly relies on the use of local water resources.

Chapter 5

Conclusion

The present thesis contributes to the literature of freshwater use sustainability and the globalization of water resources in different ways.
The first part of this Thesis provides an easy-to-apply tool - named the Environmental Cost index - to quantify the environmental impact of a water withdrawal on riverine systems. The index is referred to a potential reference withdrawal that can occur in any river section of the world's hydrographic network. Being referred to a unitary reference withdrawal that can occur in any river section, it can be used to analyse any scenario of surface water consumption. The Environmental Cost index aims to describe, with a feasible level of complexity, the multiple interactions between water consumption and its effects on fluvial ecosystems. To this aim, it quantifies (i) the environmental relevance of the impacted riverine ecosystem and (ii) the downstream river network affected by the reference withdrawal. In order to design a parsimonious indicator, we adopted only one parameter and kept at a minimum the number of variables employed; namely, the river discharge and the river network, since they are the main factors that influence the river ecosystem equilibrium. Thanks to the limited amount of data required, the index can be consistently applied at the global scale. Moreover, as the proposed approach is general, it can be applied at any spatial or temporal resolution depending on the available data and the study target. Through the definition of the Environmental Cost index, this Thesis introduced a novel tool to support water management strategies; in fact, the index allows one to easily identify on the hydrographic network the most impacting water consumption patterns. In addition, since the index sys-

tematically accounts for the downstream propagation effect of an hydrological stressor, it can support decision-making in transboundary river basins as well. Building on the approach defined in the first part of the Thesis, in Chapter 3 we quantified the impact of food consumption on local and foreign river environments by adopting an indicator of the environmental value of the riverine water (EVRW) embedded in food and agricultural commodities. We showed that globalization determines an international trade of riverine resources and that (local) rivers are threaten by the food demands across the globe. Over the years, international trade has led to a growing disconnection between food consumers and the riverine resources employed to produce their food. In particular, from 1986 to 2013, food consumers have more than doubled their impact on foreign riverine environments. In Chapter 3, we also studied each trade link under two different scenarios: a business as usual scenario and a self-reliant scenario, where all food is produced and consumed locally. Through these two categories, we quantified the global efficiency of the international food trade network under the perspective of the health of riverine environments. Globally, we found an average annual global saving of impact on world's rivers of 11%. Nevertheless, a large number of trade flows is still largely inefficient and several countries rely on vulnerable fluvial ecosystems locally or abroad. Our results enlighten a new facet of the food-water nexus and depict a picture where country responsibilities on withdrawal-induced degradation of river environments are very heterogeneous in space and time. This Thesis can help policy makers and water planners to quantify the complex linkages between the global food system and environmental sustainability.

In Chapter 3, we pointed out that in 28 years food consumers have more than doubled their impact on foreign riverine environments. In order to quantify the socio-economic determinants behind the growing use of foreign (and domestic) freshwater resources, in Chapter 4, we identified the major socio-economic factors that drove global blue water use trends. To this aim, we decomposed changes in the blue water consumed worldwide both structurally and geographically adopting a Multi-Regional Input-Output framework. The main mechanisms governing the exploitation of domestic and foreign freshwater resources were quantified by undertaking a structural decomposition analysis (SDA) over the 1994 - 2010 period in 186 individual countries. Globally, the affluence growth was the main driver of increasing blue water use trends followed

by the effect of the growing world's population (in particular in the MENA region and in South Asia). The affluence and the demographic impacts were globally partially offset by remarkable improvements in the blue water efficiency of producers and, to a lesser extent, by changes in production technology. In Chapter 4, results showed a significant imbalance in the origin of the blue water increasingly consumed by developed and developing countries. Consumers in developed countries tend to increase their affluence by intensifying the use of foreign water resources; conversely, the affluence growth in developing regions mostly relies on the use of local water resources, revealing a significant imbalance among economies. Moreover, although technological improvements and alternative production patterns offer considerable potential to reduce freshwater exploitation growth, significant achievements would derived from shifts in the affluence effects, thus decreasing the per capita demand of water-intensive products and services.

Limitations and future outlook.

In this Thesis some assumptions were necessary in order to overcome issues related to the lack of a number of historical data. A potential source of uncertainty concerns the fixed subdivision among the blue and green water components. As detailed in Section 3.1.1, for each food item we assessed the country-specific blue share as the ratio of the blue virtual water content (VWC) to the overall VWC, both values averaged over the period 1996-2005. Then, we applied this fixed share to the time-varying overall VWC, which was calculated through the fast track approach (Tuninetti et al., 2017a). This is a negligible approximation for all the countries that have not significantly changed their water supply systems (which can range from fully irrigated to fully rain-fed) after (or before) the 1996 - 2005 period. To overcome this approximation, the blue VWC should be computed modelling the daily evapotranspiration of each crop, which is computationally extremely demanding when long time period and numerous crops are considered. The second shortcoming about virtual water data concerns the adoption of the time averaged country-specific VWC for each animal-derived product. This limitation will be overcome only when reliable data on the country-specific feed composition of each animal category will be available throughout the considered time period. Future analyses should also consider fish products, which were omitted in our work due to a lack of data concerning their blue VWC at the country-scale. In Chapter 3, since the

blue water component includes both groundwater and surface water resources, we adopt the percentage of the area equipped for irrigation served by surface water resources (Rs) given by Siebert et al. (2013) in order to assess the surface water contribution. In a given country, thus, the Rs percentage is fixed over time and is not product-specific. This is a quite rough approximation that should be addressed in future works when reliable data on the use of groundwater and surface water at the product scale will be available. Currently, this approximation does not appear to affect the main findings of the work. Indeed, our results show that even extremely different values of Rs do not substantially affect the global efficiency of the EVRW network (see Fig.3.8). In Chapter 3, a further limitation concerns the geography of the actual water withdrawals. In fact, although the environmental cost is known at 0.5° spatial resolution, we employed country-specific environmental cost values as the amount of the volume of water withdrawn from each river section in the world's hydrographic network is currently unidentified. Therefore, in light of the fact that water is generally withdrawn where it is more abundant, we computed the country-specific $EC_{w,c}$ as the weighted average of the EC_w values of the cells within the considered country, using the river discharge as the weight. Since the Environmental Cost Index can be applied at any spatial (and temporal) scale, more refined results will be achieved when the global distribution of surface water supply systems will be determined. Moreover - as discussed in Chapter 2 - the Environmental Cost index systematically considers the impact on the whole downstream hydrographic network, therefore the country-specific $EC_{w,c}$ value implicitly accounts for the downstream countries impacted. In order to provide an instrument to enhance international water cooperation – especially in transboundary river basins - future works could explicitly and systematically decouple the shares of the country-specific $EC_{w,c}$ value that depends on the impacts within the considered country, c, and the shares that concerns the neighbouring countries (e.g., see Section 2.2.3). In Chapter 3, we highlight hotspots of food-related river-environment degradation to target priority agricultural patterns that put at risk surface water systems. In order to support policy-makers, these initial results need to be further supported by local surveys, which should employ more case-specific data and incorporate additional socio-economic, cultural and environmental aspects. In Chapter 4, a source of uncertainty concerns the assessment of the virtual water flows within

the world's economy based on the monetary transactions between sectors. In this context, each dollar sold by a given sector to every other sector (or to the final consumers) corresponds to a fixed volume of blue water (where the latter volume coincides with the water intensity of the considered sector). This leads to unavoidable simplifications: (i) in a given sector, products with the same economic value have the same water footprint and (ii) in a given sector and year, each good or service is sold at the same price to all the other sectors. These assumptions could be fully overcome only by using Input-Output tables in physical units (e.g., in tonnes) and at the product scale; however these tables are currently unavailable at the global scale. Despite the limitations and in light of the encouraging outcomes, we are confident that the present Thesis provides a general and consistent framework for supporting researchers and water planners in the analysis of the complex linkages between the global food system and environmental sustainability.

Appendix A

A.1 Further considerations on the variability of EC_w with α

Section 2.2 presented the EC_w geography employing $\alpha = 0.5$, however, it is possible to use different α values based on the study target as explained in Section 2.1.2. Therefore, this section provide more detailed information about the variability of EC_w with α.
Fig.A.1, Fig.A.2, Fig.A.3, and Fig.A.4 report the overall impact (EC_w) values normalized by EC_{world} and obtained with $W = 1\ \mathrm{m^3\,s^{-1}}$ and $\alpha = 0$, $\alpha = 0.25$, $\alpha = 0.75$, and $\alpha = 1$, respectively. Comparing these figures it is evident that the ranges between the minimum and maximum impact values decrease with α, as mentioned in Section 2.1.2. Overall, also the global mean environmental cost value ($\overline{EC}_w$) decreases with α, as also detailed in Fig.A.5d.

In Fig.A.3 and Fig.A.4 one can notice some cells characterized by low EC_w values (blue cells) localized close to areas with high EC_w values (yellow areas). Some of these cells can be noticed in Fig.A.3 and Fig.A.4: for example in Iran, in the Australian Outback, in south-west Mongolia, and in north-western China. In these cells, in spite of the high ec_w values, the overall impact (EC_w) is apparently small because is assessed along ephermal streams characterized by short river networks. It follows that these cells have low EC_w values because when $\alpha > 0.75$, the undisturbed river discharge has a very limited (or null) effect on ec_w (see Eq.(2.5)); as a consequence, the length of the downstream river network turns out to be the main factor that influences the environmental cost of a surface water withdrawal when an high value of α is chosen (see Eq.(2.10)).

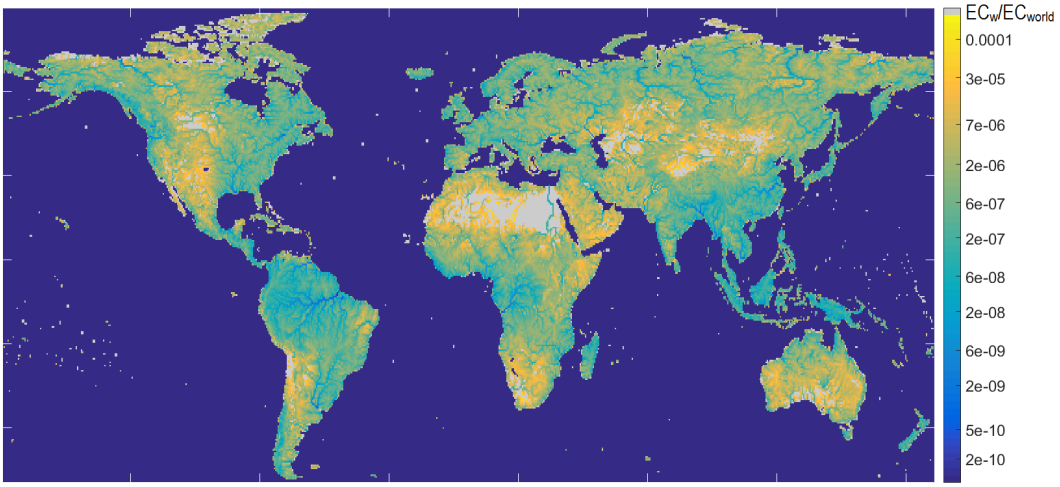

Fig. A.1 The overall environmental cost (EC_w) normalized by EC_{world} and estimated with $\alpha = 0$ and $W = 1$ m^3 s^{-1} in cells of 30 x 30 arc min. Grey areas have $Q < 1$ m^3 s^{-1}, therefore in those areas the environmental cost is not computed. The colour bars is in log scale.

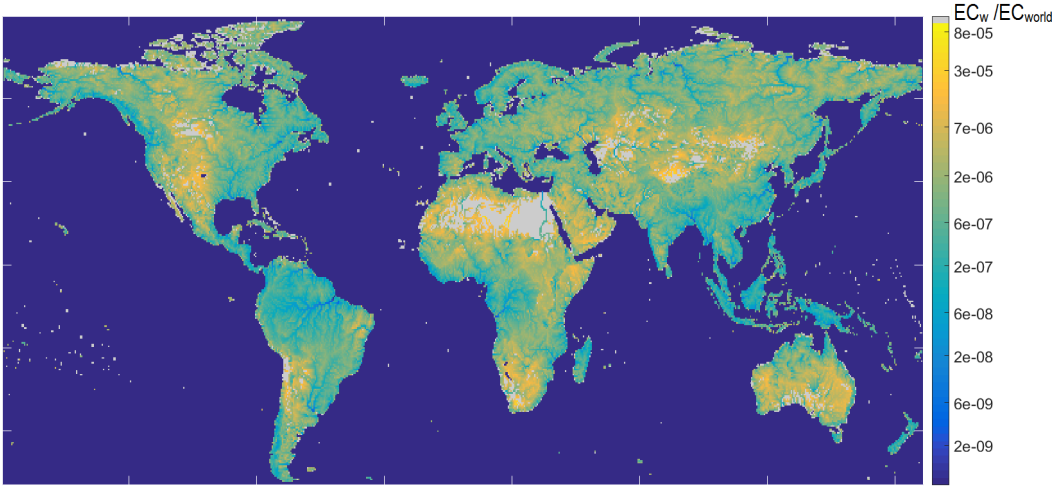

Fig. A.2 (The overall environmental cost (EC_w) normalized by EC_{world} and estimated with $\alpha = 0.25$ and $W = 1$ m^3 s^{-1} in cells of 30 x 30 arc min. Grey areas have $Q < 1$ m^3 s^{-1}, therefore in those areas the environmental cost is not computed. The colour bars is in log scale.

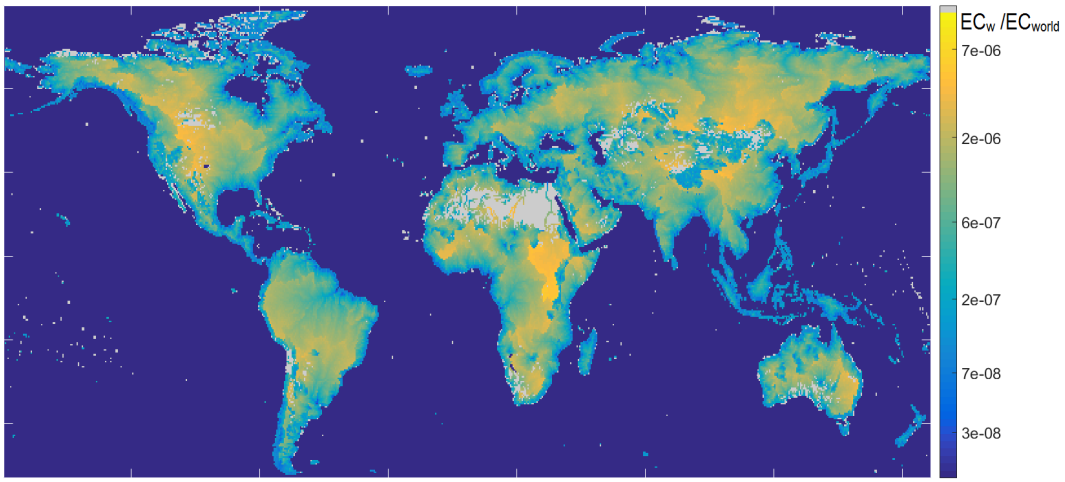

Fig. A.3 The overall environmental cost (EC_w) normalized by EC_{world} and estimated with $\alpha = 0.75$ and $W = 1$ m^3 s^{-1} in cells of 30 x 30 arc min. Grey areas have $Q < 1$ m^3 s^{-1}, therefore in those areas the environmental cost is not computed. The colour bars is in log scale.

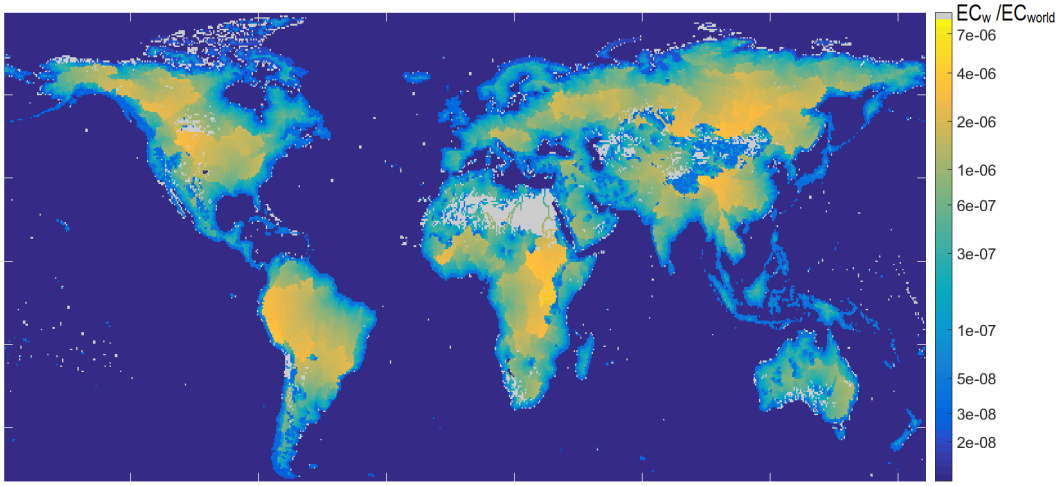

Fig. A.4 The overall environmental cost (EC_w) normalized by EC_{world} and estimated with $\alpha = 1$ and $W = 1$ m^3 s^{-1} in cells of 30 x 30 arc min. In this case the value of ec_w/EC_{world} is constant and equal to $8 \cdot 10^{-13}$. Grey areas have $Q < 1$ m^3 s^{-1}, therefore in those areas the environmental cost is not computed. The colour bar is in log scale.

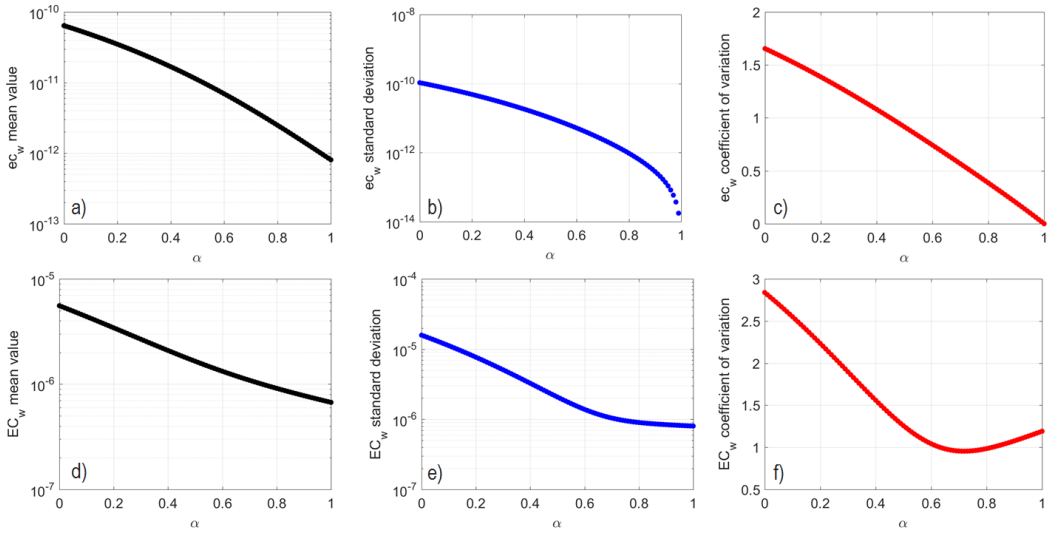

Fig. A.5 (a) Global average value of ec_w as a function of α; b) global standard deviation of ec_w as a function of α; (c) global coefficient of variation of ec_w as a function of α; (d) global average value of EC_w as a function of α; (e) global standard deviation of EC_w as a function of α; (f) global coefficient of variation of EC_w as a function of α. All values are normalized by EC_{world} and are obtained with $W = 1$ $m^3\,s^{-1}$.

This can be highlighted as well observing Fig.A.4 where the environmental cost of a water withdrawal is completely unrelated to the local amount of Q and depends only on the length of the downstream river network of each section.
The downstream propagation effect considered in EC_w implies that in any cell $ec_w \leq EC_w$, where the equality holds only at the river mouth; as a consequence, the global mean value of EC_w is always considerably greater than the global mean value of ec_w for any α. For example, for $\alpha = 0.5$, $\overline{ec}_w/ec_{world} = 8.32 \cdot 10^{-12}$ and $\overline{EC}_w/EC_{world} = 1.31 \cdot 10^{-6}$, where the overbar indicates the global mean average. Overall, both $\overline{ec}_w$ and $\overline{EC}_w$ decrease with the value of α, as well as the coefficients of variation (CV) of $\overline{ec}_w$ as displayed in Fig.A.5. In the case of EC_w, the variation coefficient reaches a minimum when $\alpha = 0.64$, then (for $\alpha \geq 0.64$) starts to gradually increase with α. Globally, EC_w has an higher variability than ec_w for any α value (see Fig.A.5f): for example, considering the case $\alpha = 0.5$, the CV of all the ec_w values is 0.91 and the CV of all the EC_w values is 1.26.
Instead of focusing on specific α values, a possible choice is to define the environmental cost considering different river characteristics at the same time.

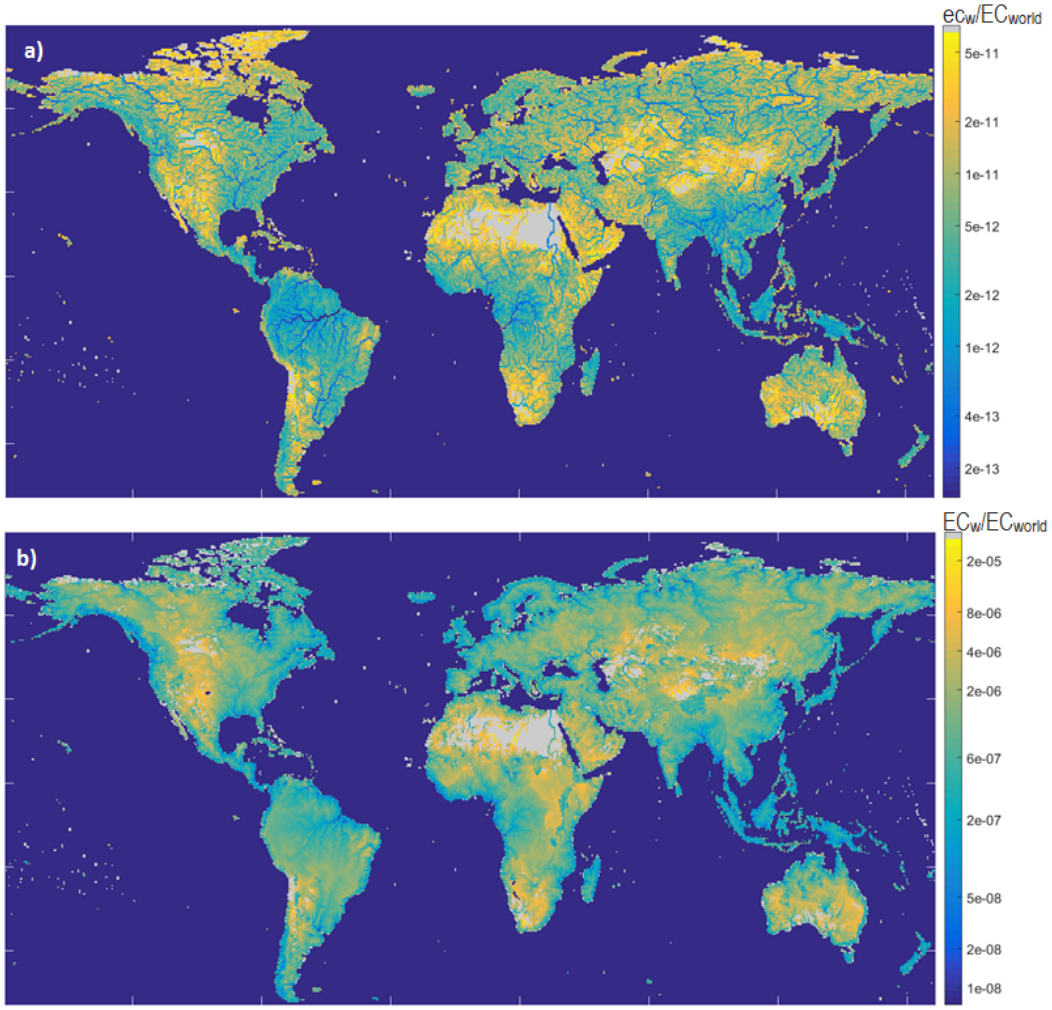

Fig. A.6 (a) The environmental cost per unit length, ec_w; (b) the overall environmental cost, EC_w. Both maps are estimated considering all the α values between 0 and 1 and weighing them with a triangular kernel distribution (see Eq.7 and Eq.9), where the top vertex of the triangular distribution corresponds to $\alpha = 0.5$. The environmental costs are normalized by EC_{world} and assessed with $W = 1\ \mathrm{m^3\,s^{-1}}$ in cells of 30 x 30 arc min. The colour bars are in log scale. Grey areas have $Q < 1\ \mathrm{m^3\,s^{-1}}$, therefore in those areas the environmental cost is not computed.

In this case, all the values of α in the range [0 1] are considered and weighted through a kernel distribution (see Eq.(2.7) and Eq.(2.11)). Fig.A.6 shows ec_w and EC_w obtained using a triangular kernel distribution, where the triangular distribution has the lower limit in $\alpha = 0$, the upper limit in $\alpha = 1$ and the peak in $\alpha = 0.5$.
The environmental cost per unit length values estimated considering different values of α are not shown because they are linked by a power-law relation, as discussed in Section 2.1.2 (see Eq.(2.6)). Therefore, all the maps of ec_w are equivalent to the one in Fig.2.5a (note that the ec_w values are plotted in log-scale), but with the values of ec_w catheterized by different ranges of variation. The range between the minimum and maximum ec_w/EC_{world} values decreases with α; with ec_w values spanning five orders of magnitude for $\alpha = 0$ and assuming a uniform global value when $\alpha = 1$.

A.2 The assessment of the virtual water content of a crop-derived product: a simplified example

Section 3.1.1 presented the data and methods used to assess the global virtual surface water network. In order to provide more detailed information about this topic, this section illustrates an example (the dry pasta) of the estimation of the virtual water content of a crop-derived product.

The VWC of each crop-derived product is assessed based on the VWC of the primary input crop, adjusted with the product fraction and value fraction. The primary input product is the good required to produce the considered crop-derived product. The product fraction, fp, is defined as the weight of a derived product obtained per ton of root product. For example, if with one ton of wheat 0.8 tons of wheat flour are produced, the product fraction is 0.8. The value fraction, fp, is the market value of the crop-derived product divided by the aggregated market value of all crop products resulting from one primary input crop. For example, in a production process from wheat to wheat flour there can be other economically valuable by-products (e.g., wheat germs to feed animals); hence, the value of wheat flour constitutes only a portion (i.e., the

value fraction) of the total value generated by the process. The list of primary input products and the product and value fractions are given by Mekonnen and Hoekstra (2010b).

The alluvial diagram in Fig.A.7 shows the steps to assess the virtual water content of the dry pasta, taking into account that usually a derived product is obtained from both local and imported root products (in this case wheat and wheat flour). For the sake of simplicity, the example in Fig.A.7 describes a very simple network composed by 3 countries: A, B and C. According to Mekonnen and Hoekstra (2010b) the main raw material of dry pasta is wheat flour and the latter derives from the milling process of wheat. Due to different yields and climatic conditions, wheat production in each country is associated to different VWCs; thus, to produce one ton of wheat different amounts of water are needed in country A, B, and C. In the example we assume 2500 m^3, 1000 m^3, and 1500 m^3 of water are used, respectively.

The VWC of the wheat flour produced within, say, country B (see Fig.A.7) is assessed considering that the average amount of wheat used in B comes both from domestic production and imports from A and C. Therefore, the average VWC of the wheat employed in the production process of wheat flour is assessed as the weighted average between the VWC related to domestic production (1000 [m^3/ton]) and the VWC of the imports (2500 [m^3/ton] and 1500 [m^3/ton]), where the weights are the tons of the domestic production minus the exports (1.8 million tons - 1 million tons) and the imports tons of wheat (0.5 million tons from A and 0.5 million tons from C). Finally, the average VWC of the wheat employed in B to produce wheat flour is adjusted applying the value fraction (0.79) and the product fraction (0.80) as follows:

$$\frac{(1000 \cdot 0.8 \cdot 10^6) + (2500 \cdot 0.5 \cdot 10^6) + (1500 \cdot 0.5 \cdot 10^6)}{0.8 \cdot 10^6 + 0.5 \cdot 10^6 + 0.5 \cdot 10^6} \cdot \frac{0.79}{0.80} = \\ = 1540 \quad \left[\frac{m^3}{ton}\right]. \tag{A.1}$$

Similarly, the VWC of the dry pasta produced in B also depends on the wheat flour imported from foreign countries (see Fig.A.7), and thus can be estimated

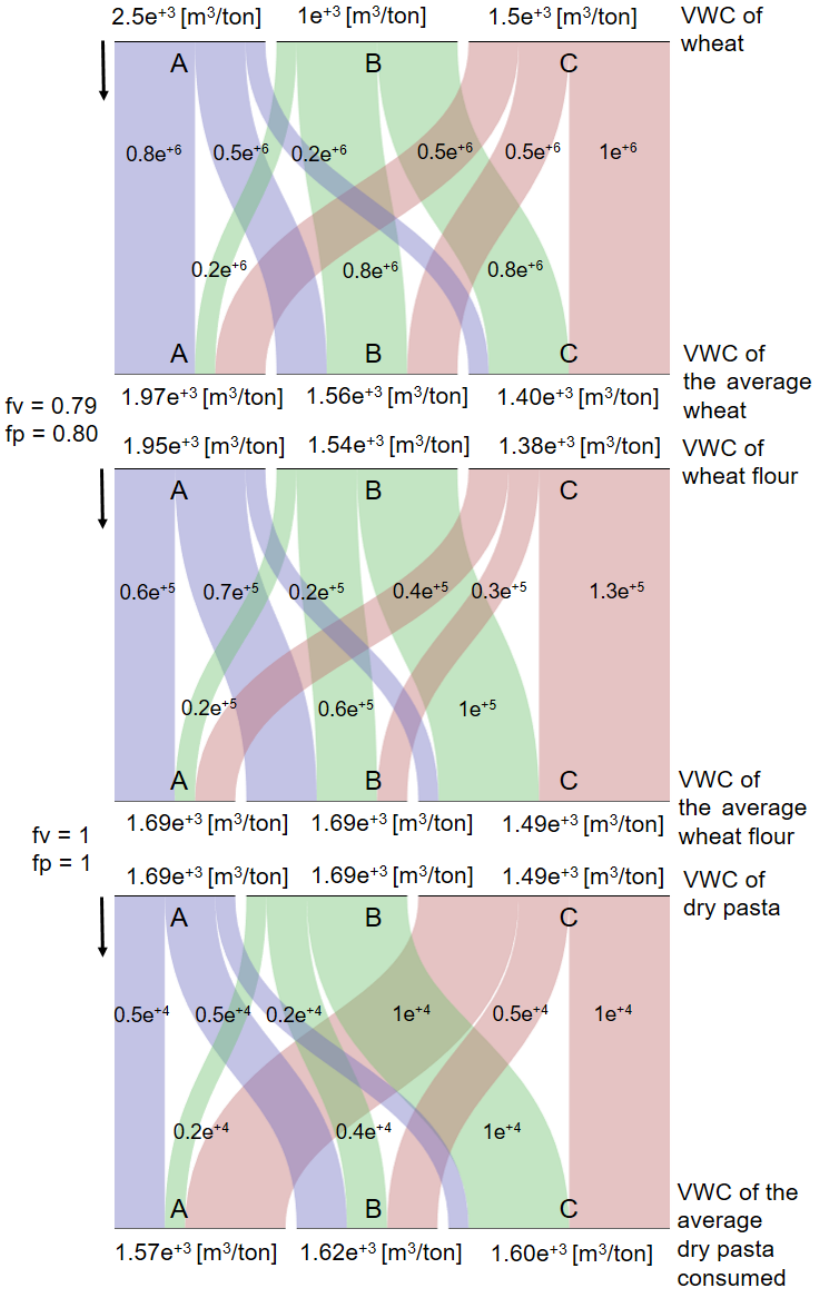

Fig. A.7 Steps to assess the virtual water content (VWC) of the dry pasta considering a simplified trade network composed by 3 countries: A, B and C. Intra-panels numbers refer to the country-specific virtual water contents, while numbers inside panels refer to the tons of product. The graph was built using RAWGraphs (https://rawgraphs.io/).

as:

$$\frac{(1540 \cdot 0.6 \cdot 10^6) + (1950 \cdot 0.7 \cdot 10^6) + (1380 \cdot 0.3 \cdot 10^6)}{0.6 \cdot 10^6 + 0.7 \cdot 10^6 + 0.3 \cdot 10^6} \cdot \frac{1}{1} = 1690 \quad \left[\frac{m^3}{ton}\right]. \tag{A.2}$$

In our work, in order to assess the country-specific VWC of each crop-derived product, this conceptual scheme was applied to all products in the global trade network at the annual scale. Notice that the country-specific VWC of each crop-derived product needs to be reconstructed every year because: (i) in the food trade network, both the active links and the corresponding exchanged flows change; (ii) the VWCs of the primary crops are not constant in time but depend on the yield trends (see Eq.(3.1) in the previous section).

A.3 MRIO-based spatial decomposition at the regional scale

In Section 4.2.2 we decoupled the drivers of domestic and outsourced blue water use trends by splitting the blue water consumed by the final demand of each country into contributions from domestic production and international imports. Since often supply chains are regional instead of global (Rugman et al., 2009) and since the strongest trade relationships are frequently among geographically close countries (Tamea et al., 2014), this section shows the results of a MRIO-based spatial decomposition at the scale of macro-region (the macro region subdivision is detailed in Fig.B.1).

Fig.A.8 schematically describes the approach adopted in this study to perform a MRIO-based spatial decomposition at the regional scale. Similarly to the country-specific example presented in Section 4.1.3, Fig.A.8 displays an economic system constituted by three countries (i.e., A, B, and C) where A and C belong to the same macro-region. In order to decouple between the use of water resources within and out of the considered region, we split the MRIO framework into two mutually exclusive components, which are displayed in Fig.A.8a and Fig.A.8b.

Fig.A.9 and Fig.A.10 identify the major socio-economic factors that drove blue water use trends within (top panels) and out of each macro region (bottom

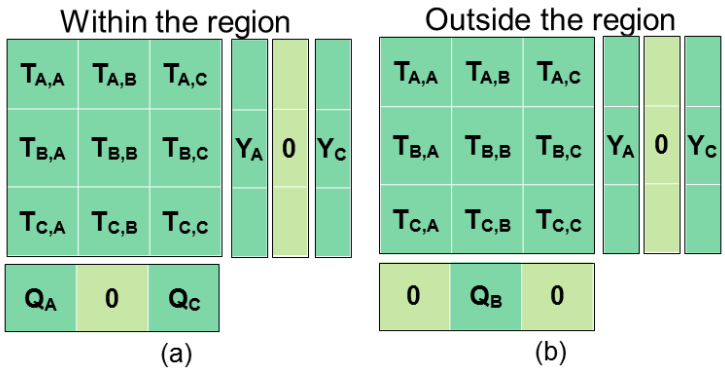

Fig. A.8 MRIO-based spatial decompositions at the regional scale by considering 3 countries (i.e., A,B, and C as in Fig.4.1b). The general structure of a MRIO table is detailed in Fig.4.2. In the example, country A and country C belong to the same macro-region. (a) the "within the region" decomposition takes into account only the water used in the countries that belong to the considered region (i.e., $\mathbf{Q}_A$ and $\mathbf{Q}_C$), while b) the "out of the region" decomposition considers the blue water used in all the countries that do not belong to the considered macro-region.

panels). As expected, most of the macro regions significantly influenced internal water use trends. However, Europe and North America stood out from this global tendency. In particular, European consumers drove slightly more changes in non-European water resources rather than within Europe.

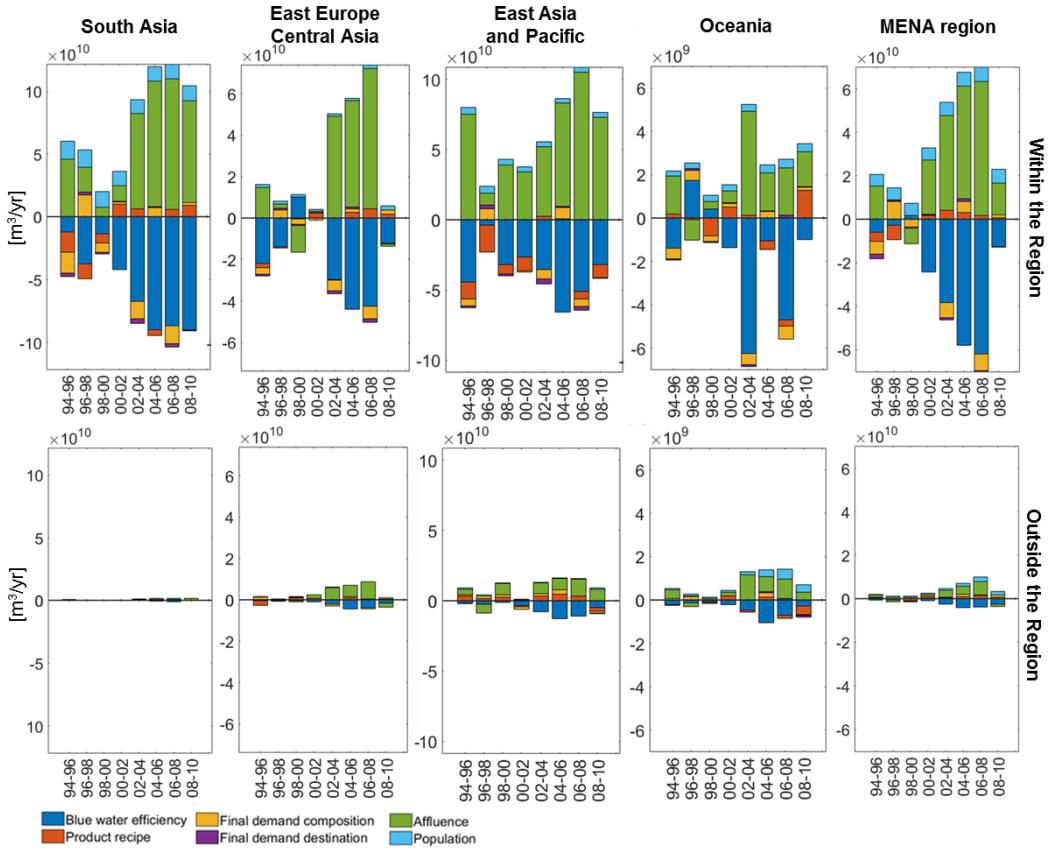

Fig. A.9 Drivers of blue water use (in m^3/yr) within (top panels) and outside (bottom panels) each macro-region from 1994 to 2010 at 2-year time step. The world's macro-region subdivision is mapped in Fig.B.1.

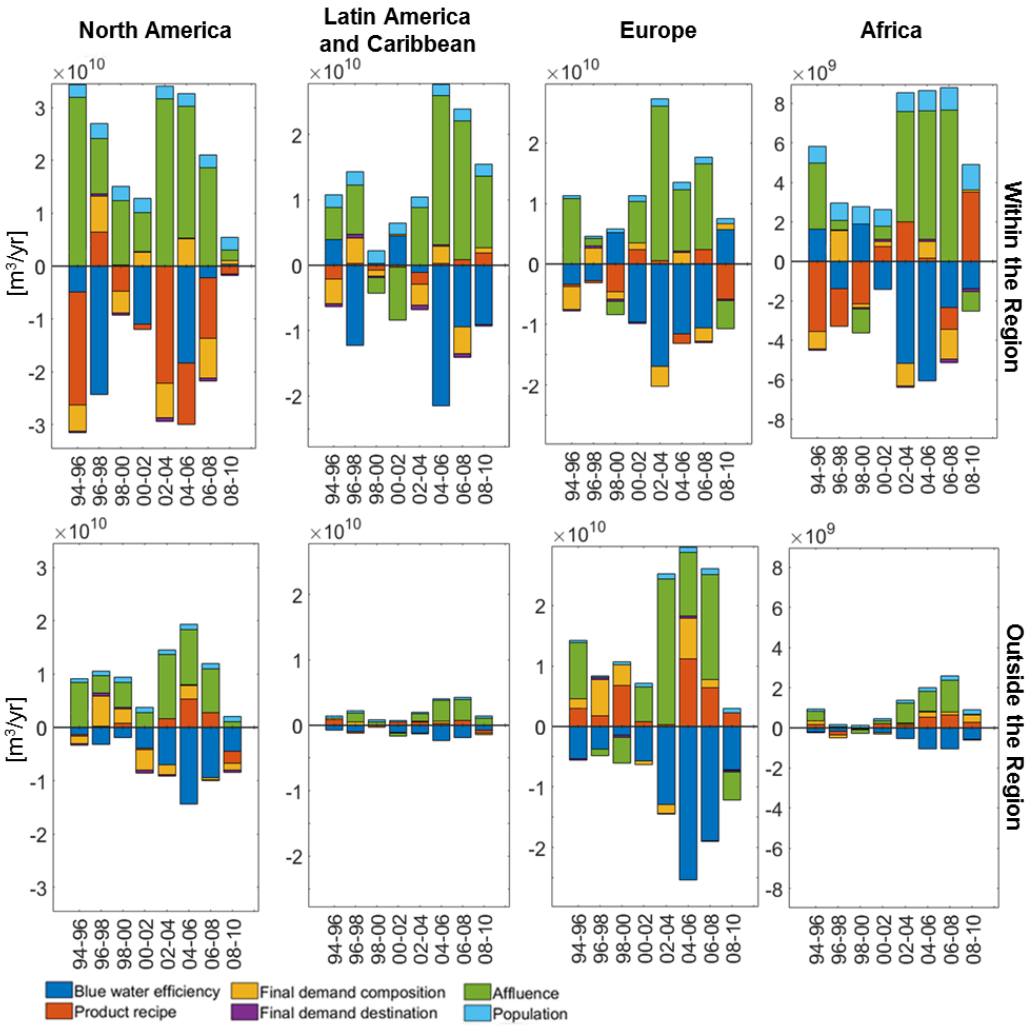

Fig. A.10 Drivers of blue water use (in m^3/yr) within (top panels) and outside (bottom panels) each macro-region, from 1994 to 2010 at 2-year time step. The world's macro-region subdivision is mapped in Fig.B.1.

Appendix B

B.1 Supplementary figures and tables

Table B.1 Commodities considered in the analyses. The first and the second column of the Table denote the name and the code of the item according to the FAO nomenclature. As mentioned in Section 3.1.1, in order to avoid double counting issues the total amount of surface water used for food production was estimated without considering secondary products (e.g., bread) (see the column labelled "in production"). While the trade flows were reconstructed considering all the food commodities (see the column labelled "in trade"). Finally notice that in the FAOSTAT database some items have different codes in the trade data and in the production data (e.g., in trade data there is "Rice-total", while in production data there is "Rice, paddy").

Item Name	**Id FAO**	**in trade**	**in production**
Agave Fibres Nes	800	0	1
Almonds Shelled	231	1	0
Almonds, with shell	221	0	1
Animals live nes	1171	1	0
Anise, badian, fennel, corian.	711	1	1
Apples	515	1	1
Apricots	526	1	1
Arecanuts	226	0	1
Artichokes	366	1	1
Asparagus	367	1	1
Asses	1107	1	0
Avocados	572	1	1
Bacon and Ham	1039	1	0

Bambara beans	203	1	1
Bananas	486	1	1
Barley	44	1	1
Barley Pearled	46	1	0
Beans, dry	176	1	1
Beans, green	414	1	1
Beer of Barley	51	1	0
Berries Nes	558	0	1
Beverages, fermented rice	39	1	0
Blueberries	552	1	1
Brazil nuts, with shell	216	0	1
Bread	20	1	0
Broad beans, horse beans, dry	181	1	1
Buckwheat	89	1	1
Buffaloes	946	1	0
Bulgur	21	1	0
Butter Cow Milk	886	1	0
Butterm.,Curdl,Acid.Milk	893	1	0
Cabbages and other brassicas	358	1	1
Cake of Cottonseed	332	1	0
Cake of Linseed	335	1	0
Cake of Palm Kernel	259	1	0
Cake of Rapeseed	272	1	0
Cake of Soybeans	238	1	0
Cake, copra	253	1	0
Cake, groundnuts	245	1	0
Canary seed	101	1	1
Carobs	461	0	1
Carrots and turnips	426	1	1
Cashew apple	591	1	1
Cashew nuts, with shell	217	1	1
Cassava	125	1	1
Cassava Dried	128	1	0
Cassava leaves	378	0	1
Cassava Starch	129	1	0

Castor oil seed	265	0	1
Cattle	866	1	0
Cattle meat	867	1	1
Cauliflowers and broccoli	393	1	1
Cereal preparations, nes	113	1	0
Cereals, nes	108	0	1
Cheese of Sheep Milk	984	1	0
Cheese of Whole Cow Milk	901	1	0
Cherries	531	1	1
Chestnuts	220	1	1
Chick peas	191	1	1
Chickens	1057	1	0
Chicory roots	459	0	1
Chillies and peppers, dry	689	1	0
Chillies and peppers, green	401	1	1
Chocolate Prsnes	666	1	0
Cinnamon (canella)	693	1	1
Citrus fruit, nes	512	0	1
Citrus juice, single strength	513	1	0
Cloves	698	1	1
Cocoa beans	661	1	1
Cocoa Butter	664	1	0
Cocoa Paste	662	1	0
Cocoapowder and Cake	665	1	0
Coconut (copra) oil	252	1	0
Coconuts	249	1	1
Coffee Roasted	657	1	0
Coffee, green	656	1	1
Copra	251	1	0
Cotton Carded,Combed	768	1	0
Cotton lint	767	1	1
Cotton Linter	770	1	0
Cotton Waste	769	1	0
Cottonseed	329	1	1
Cow milk, whole, fresh	882	1	1

Cow peas, dry	195	0	1
Cranberries	554	1	1
Cream fresh	885	1	0
Cucumbers and gherkins	397	1	1
Currants	550	1	1
Dates	577	1	1
Dry Apricots	527	1	0
Duck meat	1069	1	1
Ducks	1068	1	0
Eggplant-baseds (aubergines)	399	1	1
Eggs Dried	1064	1	0
Eggs Liquid	1063	1	0
Fat of Pigs	1037	1	0
Fat, cattle	869	1	0
Fat, liver prepared (foie gras)	1060	1	0
Fibre Crops Nes	821	0	1
Figs	569	1	1
Flax fibre and tow	773	1	1
Flax Tow Waste	774	1	0
Flour of Maize	58	1	0
Flour of Pulses	212	1	0
Flour of Roots and Tubers	150	1	0
Flour of Wheat	16	1	0
Flour, cereals	111	1	0
Fonio	94	0	1
Food Prep Nes	1232	1	0
Frozen Potatoes	118	1	0
Fruit Fresh Nes	619	1	1
Fruit Juice Nes	622	1	0
Fruit, dried nes	620	1	0
Fruit, pome nes	542	0	1
Fruit, tropical fresh nes	603	1	1
Garlic	406	1	1
Germ, maize	57	1	0
Ghee, of buffalo milk	953	1	0

Ginger	720	1	1
Glucose and Dextrose	172	1	0
Goat meat	1017	1	1
Goats	1016	1	0
Goose and guinea fowl meat	1073	1	1
Gooseberries	549	1	1
Grape Juice	562	1	0
Grapefruit (inc. pomelos)	507	1	1
Grapes	560	1	1
Groundnut oil	244	1	0
Groundnuts Shelled	243	1	0
Groundnuts, with shell	242	0	1
Hazelnuts Shelled	233	1	0
Hazelnuts, with shell	225	0	1
Hemp Tow Waste	777	0	1
Hempseed	336	0	1
Hen eggs, in shell	1062	1	1
Hops	677	1	1
Horse meat	1097	1	1
Horses	1096	1	0
Ice cream and edible ice	910	1	0
Jojoba seed	277	0	1
Juice of Grapefruit	509	1	0
Juice of Pineapples	576	1	0
Juice of Tomatoes	390	1	0
Jute	780	1	1
Kapok fruit	310	0	1
Karite Nuts (Sheanuts)	263	0	1
Kiwi fruit	592	1	1
Kolanuts	224	1	1
Lard	1043	1	0
Leeks, other alliaceous vegetables	407	1	1
Lemons and limes	497	1	1
Lentils	201	1	1
Lettuce and chicory	372	1	1

Linseed	333	1	1
Linseed oil	334	1	0
Lupins	210	0	1
Macaroni	18	1	0
Maize	56	1	1
Maize oil	60	1	0
Maize, green	446	1	1
Malt	49	1	0
Mangoes, mangosteens, guavas	571	1	1
Manila Fibre (Abaca)	809	1	1
Maple Sugar and Syrups	160	1	0
Mate	671	1	1
Meal, meat	1173	1	0
Meat indigenous, ass	1122	0	1
Meat indigenous, bird nes	1084	0	1
Meat indigenous, buffalo	972	0	1
Meat indigenous, cattle	944	0	1
Meat indigenous, chicken	1094	0	1
Meat indigenous, duck	1070	0	1
Meat indigenous, geese	1077	0	1
Meat indigenous, goat	1032	0	1
Meat indigenous, horse	1120	0	1
Meat indigenous, mule	1124	0	1
Meat indigenous, pig	1055	0	1
Meat indigenous, sheep	1012	0	1
Meat indigenous, turkey	1087	0	1
Meat, ass	1108	1	1
Meat, beef, preparations	875	1	0
Meat, bird nes	1089	0	1
Meat, buffalo	947	0	1
Meat, chicken	1058	1	1
Meat, chicken, canned	1061	1	0
Meat, dried nes	1164	1	0
Meat, game	1163	1	1
Meat, mule	1111	0	1

Meat, nes	1166	1	1
Meat, pork	1038	1	0
Meat-Cattle, boneless	870	1	0
Melonseed	299	0	1
Milk Skimmed Dry	898	1	0
Milk Skm of Cows	888	1	0
Milk Whole Cond	889	1	0
Milk Whole Dried	897	1	0
Milk, whole evaporated	894	1	0
Milk, whole fresh buffalo	951	0	1
Milk, whole fresh goat	1020	0	1
Milk, whole fresh sheep	982	1	1
Millet	79	1	1
Mixed grain	103	1	1
Molasses	165	1	0
Mules	1110	1	0
Mushrooms and truffles	449	1	1
Mustard seed	292	1	1
Natural rubber	836	1	1
Nutmeg, mace and cardamoms	702	1	1
Nuts, nes	234	1	1
Oats	75	1	1
Oats Rolled	76	1	0
Offals of cattle, edible	868	1	0
Offals of Goats, Edible	1018	1	0
Offals of Pigs, Edible	1036	1	0
Offals of Sheep,Edible	978	1	0
Offals, liver chicken	1059	1	0
Offals, liver duck	1075	1	0
Offals, liver geese	1074	1	0
Offals, nes	1167	0	1
Oil of Castor Beans	266	1	0
Oil, palm fruit	254	0	1
Oils, fats of animal nes	1168	1	0
Oilseeds, Nes	339	1	1

Okra	430	0	1
Olives	260	1	1
Olives Preserved	262	1	0
Onions (inc. shallots), green	402	1	1
Onions, dry	403	1	0
Orange juice, single strength	491	1	0
Oranges	490	1	1
Other Bastfibres	782	0	1
Other bird eggs,in shell	1091	1	1
Other Fructose and Syrup	166	1	0
Other melons (inc.cantaloupes)	568	1	1
Palm kernel oil	258	1	0
Palm kernels	256	0	1
Palm oil	257	1	1
Papayas	600	1	1
Paste of Tomatoes	391	1	0
Peaches and nectarines	534	1	1
Pears	521	1	1
Peas, dry	187	1	1
Peas, green	417	1	1
Pepper (Piper spp.)	687	1	1
Peppermint	748	1	1
Persimmons	587	1	1
Pig meat	1035	1	1
Pigeon peas	197	0	1
Pigs	1034	1	0
Pineapples	574	1	1
Pistachios	223	1	1
Plantains	489	1	1
Plums and sloes	536	1	1
Plums Dried (Prunes)	537	1	0
Poppy seed	296	1	1
Potatoes	116	1	1
Potatoes Flour	117	1	0
Prep of Pig Meat	1042	1	0

Processed Cheese	907	1	0
Prod.of Nat.Milk Constit	909	1	0
Pulses, nes	211	0	1
Pumpkins, squash and gourds	394	1	1
Quinces	523	1	1
Quinoa	92	0	1
Raisins	561	1	0
Ramie	788	0	1
Rapeseed	270	1	1
Rapeseed oil	271	1	0
Raspberries	547	0	1
Rice, paddy	27	1	1
Roots and Tubers, nes	149	1	1
Rye	71	1	1
Safflower seed	280	0	1
Sausage Beef and Veal	874	1	0
Sausages of Pig Meat	1041	1	0
Seed cotton	328	0	1
Sesame oil	290	1	0
Sesame seed	289	1	1
Sheep	976	1	0
Sheep meat	977	1	1
Sisal	789	0	1
Sorghum	83	1	1
Sour cherries	530	1	1
Soya Paste	240	1	0
Soya Sauce	239	1	0
Soybean oil	237	1	0
Soybeans	236	1	1
Spices, nes	723	1	1
Spinach	373	1	1
Stone fruit, nes	541	0	1
Strawberries	544	1	1
String beans	423	0	1
Sugar beet	157	1	1

Sugar cane	156	0	1
Sugar crops, nes	161	1	1
Sugar flavoured	171	1	0
Sugar Refined	164	1	0
Sugar, nes	167	1	0
Sunflower Cake	269	1	0
Sunflower oil	268	1	0
Sunflower seed	267	1	1
Sweet Corn Frozen	447	1	0
Sweet potatoes	122	1	1
Tallow	1225	1	0
Tallowtree seed	305	0	1
Tangerines, mandarins, clem.	495	1	1
Taro (cocoyam)	136	0	1
Tea	667	1	1
Tobacco, unmanufactured	826	1	1
Tomato Peeled	392	1	0
Tomatoes	388	1	1
Triticale	97	1	1
Tung nuts	275	0	1
Turkey meat	1080	1	1
Turkeys	1079	1	0
Vanilla	692	1	1
Veg.Prod.Fresh Or Dried	460	1	0
Vegetable Frozen	473	1	0
Vegetables fresh nes	463	1	1
Vegetables Preserved Nes	472	1	0
Vegetables, dried nes	464	1	0
Vegetables, leguminous nes	420	0	1
Vermouths and Similar	565	1	0
Vetches	205	1	1
Walnuts Shelled	232	1	0
Walnuts, with shell	222	1	1
Watermelons	567	1	1
Wheat	15	1	1

Whey Condensed	890	1	0
Whey, dry	900	1	0
Wine	564	1	0
Yams	137	0	1
Yautia (cocoyam)	135	0	1
Yoghurt, concentrated or not	892	1	0

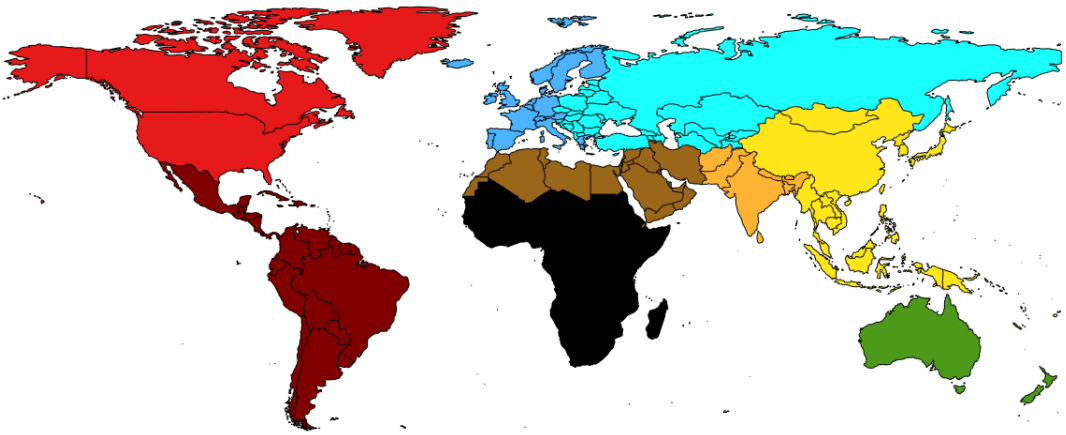

Fig. B.1 The geographical division into the nine macro-region analysed in Fig.3.5 and Fig.4.5; i.e., North America,Latin America and the Caribbean, Europe, Africa, North Africa and the Middle East, East Europe and Central Asia, South Asia, East Asia, and Oceania.

References

Michael C Acreman and Michael J Dunbar. Defining environmental river flow requirements? a review. *Hydrology and Earth System Sciences Discussions*, 8(5):861–876, 2004.

J. Alcamo, M. Flörke, and M. Märker. Future long-term changes in global water resources driven by socio-economic and climatic changes. *Hydrological Sciences Journal*, 52(2):247–275, 2007.

A. Alizadeh and A. Keshavarz. Status of agricultural water use in iran, water conservation, reuse and recycling. *The National Academies Press*, 2005.

J.A. Allan. *'Virtual water': a long term solution for water short Middle Eastern economies?* School of Oriental and African Studies, University of London London, 1997.

J.D. Allan and M.M. Castillo. *Stream ecology: structure and function of running waters*. Springer Science & Business Media, 2007.

N.W. Arnell. Climate change and global water resources. *Global environmental change*, 9:S31–S49, 1999.

I. Arto and E. Dietzenbacher. Drivers of the growth in global greenhouse gas emissions. *Environmental science & technology*, 48(10):5388–5394, 2014.

Millennium Ecosystem Assessment. *Ecosystems and Human Well-being: Synthesis*. Island Press, Washington, DC, 2005.

M. Berger and M. Finkbeiner. Methodological challenges in volumetric and impact-oriented water footprints. *Journal of Industrial Ecology*, 17(1):79–89, 2013.

C. Camporeale, P. Perona, and L. Ridolfi. Hydrological and geomorphological significance of riparian vegetation in drylands. In *Dryland ecohydrology*, pages 161–179. Springer, 2006.

J. Carnicer, M. Coll, M. Ninyerola, X. Pons, G. Sanchez, and J. Penuelas. Widespread crown condition decline, food web disruption, and amplified tree mortality with increased climate change-type drought. *Proceedings of the National Academy of Sciences*, 2011.

S.R. Carpenter, E.H. Stanley, and M.J. Vander Zanden. State of the world's freshwater ecosystems: physical, chemical, and biological changes. *Annual review of Environment and Resources*, 36:75–99, 2011.

J. A. Carr, P. D'Odorico, F. Laio, and L. Ridolfi. Recent history and geography of virtual water trade. *PloS one*, 8(2):e55825, 2013.

I. Cazcarro, R. Duarte, and J. Sánchez-Chóliz. Economic growth and the evolution of water consumption in spain: A structural decomposition analysis. *Ecological Economics*, 96:51–61, 2013.

C. Dalin and I. Rodríguez-Iturbe. Environmental impacts of food trade via resource use and greenhouse gas emissions. *Environmental Research Letters*, 11(3):035012, 2016.

C. Dalin, M. Konar, N. Hanasaki, A. Rinaldo, and I. Rodriguez-Iturbe. Evolution of the global virtual water trade network. *Proceedings of the National Academy of Sciences*, 109(16):5989–5994, 2012.

C. Dalin, Y. Wada, T. Kastner, and M. J. Puma. Groundwater depletion embedded in international food trade. *Nature*, 543(7647):700–704, 2017.

P.L. Daniels, M. Lenzen, and S.J. Kenway. The ins and outs of water use–a review of multi-region input–output analysis and water footprints for regional sustainability analysis and policy. *Economic Systems Research*, 23(4):353–370, 2011.

E. Dietzenbacher and B. Los. Structural decomposition techniques: sense and sensitivity. *Economic Systems Research*, 10(4):307–324, 1998a.

E. Dietzenbacher and B. Los. Structural decomposition techniques: sense and sensitivity. *Economic Systems Research*, 10(4):307–324, 1998b.

T. Distefano, G. Chiarotti, F. Laio, and L. Ridolfi. Spatial distribution of the international food prices: unexpected randomness and heterogeneity. Technical report, SEEDS, Sustainability Environmental Economics and Dynamics Studies, 2018a.

T. Distefano, M. Riccaboni, and G. Marin. Systemic risk in the global water input-output network. *Water Resources and Economics*, 2018b.

P. D'odorico and M.C. Rulli. The fourth food revolution. *Nature Geoscience*, 6 (6):417, 2013.

P. D'Odorico, F. Laio, and L. Ridolfi. Does globalization of water reduce societal resilience to drought? *Geophysical Research Letters*, 37(13), 2010.

P. D'Odorico, J.A. Carr, and L.and Vandoni S. Laio, F.and Ridolfi. Feeding humanity through global food trade. *Earth's Future*, 2(9):458–469, 2014.

P. D'Odorico, K.F. Davis, L. Rosa, J.A. Carr, D. Chiarelli, J. Dell'Angelo, J. Gephart, G.K. MacDonald, D.A. Seekell, S. Suweis, et al. The global food-energy-water nexus. *Reviews of Geophysics*, (2018), 2018.

P. Döll and B. Lehner. Validation of a new global 30-min drainage direction map. *Journal of Hydrology*, 258(1):214–231, 2002.

P. Döll, H. Hoffmann-Dobrev, F.T. Portmann, S. Siebert, A. Eicker, M. Rodell, G. Strassberg, and B. Scanlon. Impact of water withdrawals from groundwater and surface water on continental water storage variations. *Journal of Geodynamics*, 59:143–156, 2012.

P. Döll, H. Mueller Schmied, C. Schuh, F.T. Portmann, and A. Eicker. Global-scale assessment of groundwater depletion and related groundwater abstractions: Combining hydrological modeling with information from well observations and grace satellites. *Water Resources Research*, 50(7):5698–5720, 2014.

B. Doulatyari, S. Basso, M. Schirmer, and G. Botter. River flow regimes and vegetation dynamics along a river transect. *Advances in Water Resources*, 73:30–43, 2014.

D. Dudgeon, A.H. Arthington, M.O. Gessner, Z. Kawabata, Duncan J Knowler, C. Lévêque, R.J. Naiman, A. Prieur-Richard, D. Soto, M. Stiassny, et al. Freshwater biodiversity: importance, threats, status and conservation challenges. *Biological reviews*, 81(2):163–182, 2006.

M. Fader, D. Gerten, M. Krause, W. Lucht, and W. Cramer. Spatial decoupling of agricultural production and consumption: quantifying dependences of countries on food imports due to domestic land and water constraints. *Environmental Research Letters*, 8(1):014046, 2013.

M. Falkenmark. The massive water scarcity now threatening africa: why isn't it being addressed? *Ambio*, pages 112–118, 1989.

M. Falkenmark and J. Rockström. *Balancing water for humans and nature: the new approach in ecohydrology*. Earthscan, 2004.

M. Falkenmark and J. Rockström. The new blue and green water paradigm: Breaking new ground for water resources planning and management, 2006.

FAO. *The State of Food Insecurity in the World. Economic Crises-Impacts and Lessons Learned*. Food and Agricultural Organization of the United Nations Rome, 2009.

FAO. *The state of the world's land and water resources for food and agriculture: managing systems at risk*. Food and Agriculture Organization of the United Nations, Rome and Earthscan, London, 2011.

FAO. *Drought Characteristics and Management in Central Asia and Turkey*, volume 44. FAO, Water for Food Institute, University of Nebraska-Lincoln, USA, 2017.

B.M. Fekete, C.J. Vörösmarty, and W. Grabs. High-resolution fields of global runoff combining observed river discharge and simulated water balances. *Global Biogeochemical Cycles*, 16(3), 2002.

K. Feng, A. Chapagain, S. Suh, S. Pfister, and K. Hubacek. Comparison of bottom-up and top-down approaches to calculating the water footprints of nations. *Economic Systems Research*, 23(4):371–385, 2011.

J. A. Foley, N. Ramankutty, K.A. Brauman, E.S. Cassidy, J.S. Gerber, M. Johnston, N.D. Mueller, C. O'Connell, D. K. Ray, P.C. West, et al. Solutions for a cultivated planet. *Nature*, 478(7369):337–342, 2011.

Food and Agriculture Organization of the United Nations. Aquastat main database, last accessed 10/01/2017, 2017. URL http://www.fao.org/nr/water/aquastat/main/index.stm.

Andrea Fracasso, Martina Sartori, and Stefano Schiavo. Determinants of virtual water flows in the mediterranean. *Science of the Total Environment*, 543: 1054–1062, 2015.

R. Fremdling, H. De Jong, and M.P. Timmer. British and german manufacturing productivity compared: a new benchmark for 1935/36 based on double deflated value added. *The Journal of Economic History*, 67(2):350–378, 2007.

Kevin P. Gallagher. *Handbook on Trade and the Environment*. 2008.

P.H. Gleick. A look at twenty-first century water resources development. *Water International*, 25(1):127–138, 2000.

I. Haddeland, J. Heinke, H. Biemans, S. Eisner, N. Flörke, M.and Hanasaki, M. Konzmann, F. Ludwig, Y. Masaki, J. Schewe, et al. Global water resources affected by human interventions and climate change. *Proceedings of the National Academy of Sciences*, 111(9):3251–3256, 2014.

N. Hanasaki, T. Inuzuka, S. Kanae, and T. Oki. An estimation of global virtual water flow and sources of water withdrawal for major crops and livestock products using a global hydrological model. *Journal of Hydrology*, 384(3): 232–244, 2010.

N. Hanasaki, S. Fujimori, T. Yamamoto, S. Yoshikawa, Y. Masaki, Y. Hijioka, M. Kainuma, Y. Kanamori, T. Masui, K. Takahashi, et al. A global water scarcity assessment under shared socio-economic pathways. *Hydrology and Earth System Sciences*, 17(7):2393, 2013.

A.Y. Hoekstra and A.K. Chapagain. *Globalization of Water: Sharing the Planet's Freshwater Resources*. Blackwell Publishing Ltd, 2008.

A.Y. Hoekstra and P.Q. Hung. Virtual water trade: A quantification of virtual water flows between nations in relation to international crop trade. *Value of Water Research Report Series*, 11:166, 2002.

A.Y. Hoekstra and M.M. Mekonnen. The water footprint of humanity. *Proceedings of the national academy of sciences*, 109(9):3232–3237, 2012.

A.Y. Hoekstra, M.M. Mekonnen, A.K. Chapagain, R. E Mathews, and B.D. Richter. Global monthly water scarcity: blue water footprints versus blue water availability. *PLoS One*, 7(2):e32688, 2012.

IPCC. *Global Warming of 1.5 °C*. 2018.

J. Jägermeyr, D. Gerten, S. Schaphoff, J. Heinke, W. Lucht, and J. Rockström. Integrated crop water management might sustainably halve the global food gap. *Environmental Research Letters*, 11(2):025002, 2016.

P.Y. Julien and J. Wargadalam. Alluvial channel geometry: theory and applications. *Journal of Hydraulic Engineering*, 121(4):312–325, 1995.

M. Konar, C. Dalin, N. Hanasaki, A. Rinaldo, and I. Rodriguez-Iturbe. Temporal dynamics of blue and green virtual water trade networks. *Water Resources Research*, 48(7), 2012.

P. Kristensen. Eea core set of indicators. *European Environment Agency*, 2003.

M. Kummu, J. Guillaume, H. de Moel, S. Eisner, M. Flörke, M. Porkka, S. Siebert, T. Veldkamp, and P.J. Ward. The world's road to water scarcity: Shortage and stress in the 20th century and pathways towards sustainability. *Scientific reports*, 6:38495, 2016.

J. Lan, A. Malik, M. Lenzen, D. McBain, and K. Kanemoto. A structural decomposition analysis of global energy footprints. *Applied Energy*, 163: 436–451, 2016.

M. Lenzen, D. Moran, K. Kanemoto, B. Foran, L. Lobefaro, and A. Geschke. International trade drives biodiversity threats in developing nations. *Nature*, 486(7401):109–112, 2012.

M. Lenzen, D. Moran, K. Kanemoto, and A. Geschke. Building eora: a global multi-region input–output database at high country and sector resolution. *Economic Systems Research*, 25(1):20–49, 2013a.

M. Lenzen, D.l Moran, A. Bhaduri, K. Kanemoto, M. Bekchanov, A. Geschke, and B. Foran. International trade of scarce water. *Ecological Economics*, 94: 78–85, 2013b.

Manfred Lenzen. Decomposition analysis and the mean-rate-of-change index. *Applied Energy*, 83(3):185–198, 2006.

J. Liu and H. Yang. Spatially explicit assessment of global consumptive water uses in cropland: Green and blue water. *Journal of Hydrology*, 384(3): 187–197, 2010.

A. Malik and J. Lan. The role of outsourcing in driving global carbon emissions. *Economic Systems Research*, 28(2):168–182, 2016.

L. Marston, M. Konar, X. Cai, and T. Troy. Virtual groundwater transfers from overexploited aquifers in the united states. *Proceedings of the National Academy of Sciences*, 112(28):8561–8566, 2015.

M.M. Mekonnen and A.Y. Hoekstra. *The green, blue and grey water footprint of farm animals and animal products*, volume 1. UNESCO-IHE Institute for water Education Delft, 2010a.

M.M. Mekonnen and A.Y. Hoekstra. The green, blue and grey water footprint of crops and derived crop products. In *Value of Water Research Report Series No.48*. UNESCO-IHE Institute for Water Education, 2010b.

M.M. Mekonnen and A.Y. Hoekstra. National water footprint accounts: the green, blue and grey water footprint of production and consumption. In *Value of Water Research Report Series No.50*. UNESCO-IHE Institute for Water Education, 2011.

M.M. Mekonnen and A.Y. Hoekstra. Four billion people facing severe water scarcity. *Science advances*, 2(2):e1500323, 2016.

E. Meyer-Peter and R. Müller. Formulas for bed-load transport. IAHR, 1948.

R. Miller and P.D. Blair. *Input-output analysis: foundations and extensions*. Cambridge University Press, 2009.

D. Molden. *Water for Food Water for Life: A Comprehensive Assessment of Water Management in Agriculture*. Routledge, 2007.

H. Müller Schmied. *Evaluation, modification and application of a global hydrological model*. PhD thesis, Johann Wolfgang Goethe-Universität, 2017.

H. Müller Schmied, S. Eisner, D. Franz, M. Wattenbach, F.T. Portmann, M. Flörke, and P. Döll. Sensitivity of simulated global-scale freshwater fluxes and storages to input data, hydrological model structure, human water use and calibration. *Hydrology and Earth System Sciences*, 18(9):3511–3538, 2014.

H. Müller Schmied, L. Adam, S Eisner, G. Fink, M. Flörke, H. Kim, T. Oki, Felix T. P., C. Reinecke, R.and Riedel, et al. Variations of global and continental water balance components as impacted by climate forcing uncertainty and human water use. *Hydrology and Earth System Sciences*, 20(7):2877–2898, 2016.

R.J. Naiman, H. Decamps, and M. Pollock. The role of riparian corridors in maintaining regional biodiversity. *Ecological applications*, 3(2):209–212, 1993.

R.J. Naiman, H. Decamps, and M.E. McClain. *Riparia: ecology, conservation, and management of streamside communities*. Elsevier, 2010.

T. Oberdoff, J. Guégan, and B. Hugueny. Global scale patterns of fish species richness in rivers. *Ecography*, 18(4):345–352, 1995.

OCHA. *United Nations Technical Mission on the Drought Situation in the Islamic Republic of Iran*. 2000.

T. Oki and S. Kanae. Virtual water trade and world water resources. *Water Science and Technology*, 49(7):203–209, 2004.

T. Oki, Y. Agata, S. Kanae, T. Saruhashi, D. Yang, and K. Musiake. Global assessment of current water resources using total runoff integrating pathways. *Hydrological Sciences Journal*, 46(6):983–995, 2001.

N. Poff, P. Angermeier, S.D. Cooper, P.S. Lake, K. Fausch, K.O. Winemiller, L.AK. Mertes, M.W. Oswood, J. Reynolds, and F.J. Rahel. Fish diversity in streams and rivers. In *Global Biodiversity in a Changing Environment*, pages 315–349. Springer, 2001.

P. Raskin, P. Gleick, P. Kirshen, G. Pontius, and K. Strzepek. *Water futures: assessment of long-range patterns and problems. Comprehensive assessment of the freshwater resources of the world*. SEI, 1997.

B. Richter. *Chasing water: a guide for moving from scarcity to sustainability*. Island Press, 2014.

B.G. Ridoutt and S. Pfister. A revised approach to water footprinting to make transparent the impacts of consumption and production on global freshwater scarcity. *Global Environmental Change*, 20(1):113–120, 2009.

P. Rørmose and T. Olsen. Structural decomposition analysis of air emissions in denmark 1980-2002. 2005.

S. Rost, A. Gerten, D.and Bondeau, W. Lucht, J. Rohwer, and S. Schaphoff. Agricultural green and blue water consumption and its influence on the global water system. volume 44 of *9*. Wiley Online Library, 2008.

Alan M Rugman, Jing Li, and Chang Hoon Oh. Are supply chains global or regional? *International Marketing Review*, 26(4/5):384–395, 2009.

S. Sabater and K. Tockner. Effects of hydrologic alterations on the ecological quality of river ecosystems. In *Water scarcity in the Mediterranean*, pages 15–39. Springer, 2009.

W.J. Sacks, B.I. Cook, N. Buenning, S. Levis, and J.H. Helkowski. Effects of global irrigation on the near-surface climate. *Climate Dynamics*, 33(2-3): 159–175, 2009.

J.F. Schyns, A.Y. Hoekstra, and M. Booij. Review and classification of indicators of green water availability and scarcity. *Hydrology and earth system sciences*, 19(11):4581–4608, 2015.

S. Seibel. Decomposition analysis of carbon dioxide emission changes in germany-conceptual framework and empirical results. *Luxembourg: Office for Official Publications of the European Communities, European Communities*, 2003.

P.B. Shafroth, J.C. Stromberg, and D.T. Patten. Riparian vegetation response to altered disturbance and stress regimes. *Ecological Applications*, 12(1): 107–123, 2002.

S. Siebert and P. Döll. Quantifying blue and green virtual water contents in global crop production as well as potential production losses without irrigation. *Journal of Hydrology*, 384(3):198–217, 2010.

S. Siebert, V. Henrich, K. Frenken, and J. Burke. Update of the digital global map of irrigation areas to version 5. *Rheinische Friedrich-Wilhelms-Universität, Bonn, Germany and Food and Agriculture Organization of the United Nations, Rome, Italy*, 2013.

I. Soligno, L. Ridolfi, and F. Laio. The environmental cost of a reference withdrawal from surface waters: Definition and geography. *Advances in Water Resources*, 110:228–237, 2017.

I. Soligno, L. Ridolfi, and F. Laio. The globalization of riverine environmental resources through the food trade. *Environmental Research Letters*, 2018.

I. Soligno, A. Malik, and M. Lenzen. Socio-economic drivers of global blue water use. *Water Resources Research*, UNDER REVIEW, 2019.

S. Tamea, J.A. Carr, F. Laio, and L. Ridolfi. Drivers of the virtual water trade. *Water Resources Research*, 50(1):17–28, 2014.

D. Tilman, C. Balzer, J. Hill, and B. L. Befort. Global food demand and the sustainable intensification of agriculture. *Proceedings of the National Academy of Sciences*, 108(50):20260–20264, 2011.

M. Tuninetti, S. Tamea, P. D'Odorico, F. Laio, and L. Ridolfi. Global sensitivity of high-resolution estimates of crop water footprint. *Water Resources Research*, 51(10):8257–8272, 2015.

M. Tuninetti, S. Tamea, F. Laio, and L. Ridolfi. A fast track approach to deal with the temporal dimension of crop water footprint. *Environmental Research Letters*, 12(7):074010, 2017a.

M. Tuninetti, S. Tamea, F. Laio, and L. Ridolfi. To trade or not to trade: link prediction in the virtual water network. *Advances in Water Resources*, 110: 528–537, 2017b.

UN-DESA. *World Population Prospects: The 2017 Revision, Key Findings and Advance Tables*. 2017.

UN-Water. *Comprehensive assessment of the freshwater resources of the world*, volume 1. UNESCO Publishing, 1997.

UN-Water. *The United Nations World Water Development Report 2015: water for a sustainable world*, volume 1. UNESCO Publishing, 2015.

D. Vanham, A.Y. Hoekstra, Y. Wada, F. Bouraoui, A. de Roo, M.M. Mekonnen, W.J. Van De Bund, O. Batelaan, P. Pavelic, W. Bastiaanssen, et al. Physical water scarcity metrics for monitoring progress towards sdg target 6.4: An evaluation of indicator 6.4. 2 "level of water stress". *Science of the total environment*, 613:218–232, 2018.

C.J. Vörösmarty, B.M. Fekete, M. Meybeck, and R.B. Lammers. Global system of rivers: Its role in organizing continental land mass and defining land-to-ocean linkages. *Global Biogeochemical Cycles*, 14(2):599–621, 2000a.

C.J. Vörösmarty, P. Green, J. Salisbury, and R.B. Lammers. Global water resources: vulnerability from climate change and population growth. *science*, 289(5477):284–288, 2000b.

C.J. Vörösmarty, P.B. McIntyre, M.O. Gessner, D. Dudgeon, A. Prusevich, P. Green, S. Glidden, S.E. Bunn, C.A. Sullivan, C.R. Liermann, et al. Global threats to human water security and river biodiversity. *Nature*, 467(7315): 555–561, 2010.

Y. Wada and M. Bierkens. Sustainability of global water use: past reconstruction and future projections. *Environmental Research Letters*, 9(10):104003, 2014.

Y. Wada, L. Van Beek, and M. Bierkens. Modelling global water stress of the recent past: on the relative importance of trends in water demand and climate variability. *Hydrology and Earth System Sciences*, 15(12):3785–3808, 2011.

Y. Wada, L. Van Beek, N. Wanders, and M. Bierkens. Human water consumption intensifies hydrological drought worldwide. *Environmental Research Letters*, 8(3):034036, 2013.

L. Wan, W. Cai, Y. Jiang, and C. Wang. Impacts on quality-induced water scarcity: drivers of nitrogen-related water pollution transfer under globalization from 1995 to 2009. *Environmental Research Letters*, 11(7):074017, 2016.

H. Wang and D. Small, M.and Dzombak. Factors governing change in water withdrawals for us industrial sectors from 1997 to 2002. *Environmental science & technology*, 48(6):3420–3429, 2014.

R. Wang and J. Zimmerman. Hybrid analysis of blue water consumption and water scarcity implications at the global, national, and basin levels in an increasingly globalized world. *Environmental science & technology*, 50(10): 5143–5153, 2016.

W.A. Wurtsbaugh, C. Miller, S.E. Null, R.J. DeRose, P. Wilcock, M. Hahnenberger, F. Howe, and J. Moore. Decline of the world's saline lakes. *Nature Geoscience*, 10(11):816, 2017.

D. Xenopoulos, M.and Lodge. Going with the flow: using species–discharge relationships to forecast losses in fish biodiversity. *Ecology*, 87(8):1907–1914, 2006.

M. Xenopoulos, D. Lodge, J. Alcamo, M. Märker, K. Schulze, and D. Van Vuuren. Scenarios of freshwater fish extinctions from climate change and water withdrawal. *Global Change Biology*, 11(10):1557–1564, 2005.

A. Yang, H.and Zehnder. Globalization of water resources through virtual water trade. *Water for Food in a Changing World*, page 117, 2008.

Z. Yang, H. Liu, X. Xu, and T. Yang. Applying the water footprint and dynamic structural decomposition analysis on the growing water use in china during 1997–2007. *Ecological indicators*, 60:634–643, 2016.

S. Yano, N. Hanasaki, N. Itsubo, and T. Oki. Water scarcity footprints by considering the differences in water sources. *Sustainability*, 7(8):9753–9772, 2015.

S. Yano, N. Hanasaki, N. Itsubo, and T. Oki. Potential impacts of food production on freshwater availability considering water sources. *Water*, 8(4): 163, 2016.

M.and Yang H. Zhang, Z.and Shi. Understanding beijing's water challenge: A decomposition analysis of changes in beijing's water footprint between 1997 and 2007. *Environmental science & technology*, 46(22):12373–12380, 2012.

Y. Zhi, Z.F. Yang, and X.A. Yin. Decomposition analysis of water footprint changes in a water-limited river basin: a case study of the haihe river basin, china. *Hydrology and Earth System Sciences*, 18(5):1549, 2014.